TECHNICAL AND VOCATIONAL TRAINING INSTITUTE (TVTI)

School of Graduate Studies

FACULTY OF ELECTRICAL AND ELECTRONICS TECHNOLOGY AND INFORMATION AND COMMUNICATION TECHNOLOGY (DEPARTMENT OF ELECTRICAL AND ELECTRONICS TECHNOLOGY)

Design and Performance Enhancement of Massive MIMO PIFA Arrays for 5G Wireless Communication Systems

A Thesis Proposal for the Partial Fulfillment of Master of Science (MSc) in Electronics and Communication Technology Management

By:

MESFIN BERHANU (TTMR/159/16)

Supervisor:

Dr. HABIB MOHAMMED

March 14, 2026

Addis Ababa, Ethiopia

Design and Performance Enhancement of Massive MIMO PIFA Arrays for 5G Wireless Communication Systems

A Thesis proposal submitted to

TECHNICAL AND VOCATIONAL TRAINING INSTITUTE (TVTI)

FACULTY OF ELECTRICAL AND ELECTRONICS TECHNOLOGY AND INFORMATION AND COMMUNICATION TECHNOLOGY

(DEPARTMENT OF ELECTRICAL AND ELECTRONICS TECHNOLOGY)

In partial fulfillment for the Degree

MASTER OF SCIENCE *in* ELECTRICAL AUTOMATION AND CONTROL TECHNOLOGY MANAGEMENT

By:

Mesfin Berhanu (TTMR/159/16)

Supervisor:

Dr. Habib Mohammed

Faculty of Electrical & Electronics Technology and Information & Communication Technology (Dept. of Electrical and Electronics Technology)

Thesis Proposal on

Design and Performance Enhancement of Massive MIMO PIFA Arrays for 5G Wireless Communication Systems

By:

Mesfin Berhanu (TTMR/159/16)

APPROVED BY THESIS ADVISORY COMMITTEE

Name of the Advisor	Signature	Date
Dr. Habib Mohammed		
Name of the Examiner, Internal	Signature	Date
Name of the Examiner, External	Signature	Date
Name of the Chairperson	Signature	Date

DECLARATIONS

I hereby declare that the work, which is being presented in this thesis proposal, entitled ***"Design & Performance Enhancement of Massive MIMO PIFA Arrays for 5G Wireless Communication Systems"*** is the original work of my own, has not been presented for a degree in this or other universities, and all sources of materials used for this thesis work have been fully acknowledged.

Name: **Mesfin Berhanu (TTMR/159/16)**

Signature: ____________________

Place: Addis Ababa, Ethiopia

Date of submission: ________________________

This thesis proposal has been submitted for examination with my approval as a TVTI advisor.

Advisor Name:	**Signature**	**Date**
Dr. Habib Mohammed	__________________	_____________

ACKNOWLEDGEMENTS

First of all, I want to praise, honor, and thank Almighty God, who gave me life and saved me from all my lifetime sins through his precious gospel of water and the Spirit and gave me wisdom, strength, and perseverance and supported me in my academic life and in achieving this thesis.

Secondly, I would like to thank my respected advisor, Dr. Habib Mohammed, who supported me through all the hardships of the research process, constantly encouraging me, giving me insightful ideas, valuable recommendations, and constructive feedback. He was very knowledgeable in electrical and communication engineering, patient supervision, and professional mentorship, which contributed a lot to the quality of this work. His enthusiasm for achieving academic excellence and devotion to helping me with my research have contributed greatly to my knowledge on the implementation of advanced technology in antenna systems and wireless communication technologies of tomorrow. I really owe him a debt of gratitude regarding the time, effort, and expertise that he applied in overseeing this thesis.

I would also want to express my sincere gratitude to the faculty and staff members of FTVTI (Federal Technical and Vocational Training Institute), specifically the Department of Electrical and Electronics Technology, who have given me a healthy academic environment, technical facilities, and institutional resources that are needed to be in place to help me complete this research. The academic background that I acquired in the institute has been crucial in my professional and academic growth.

Lastly, I wish to give my utmost gratitude to my family, who have been praying, supporting me unconditionally, encouraging me, and being patient with me to succeed in my studies. They have always believed in me, and it is the best motivation and strength that I have.

ABSTRACT

The rapid deployment of fifth-generation (5G) wireless communication systems has increased the demand for small-size, high-gain, and high-directivity antennas that can operate efficiently at millimeter wave frequencies. This thesis presents the design, simulation, and performance of single and massive MIMO Planar Inverted-F Antenna (PIFA) configurations with a resonant frequency of 28 GHz by using High Frequency Structural Simulator (ANSYS HFSS) software. Starting from a single PIFA element, the work systematically explores 1x2, 4x4, and 4x5 PIFA MIMO arrays in order to quantify the effect of array scaling on impedance matching, bandwidth, gain, directivity, and radiation behavior.

According to the obtained simulation, the single PIFA element has a reflection coefficient of around -24.93 dB, VSWR 1.1 Db, gain 6.8 dBi, directivity 6.9i dB, bandwidth 4.56 GHz, and efficiency of 99.56% at the operating frequency of 28 GHz, and by the array configuration, 1×2 reflection coefficient -20.7 dB, VSWR 1.6 dB, gain 10.47 dBi, directivity 10.25 dBi, bandwidth 2.3 GHz, and MIMO metrics ECC 0.0016, DG 9.9999, and TARC -12.66 dB; 4×4 reflection coefficient -22.7 dB, VSWR 1.2 dB, gain 17.89 dBi, directivity 17.48 dBi, bandwidth 1.3 GHz, MIMO metrics ECC 0.0012, DG 9.9999, TARC -24.5 dB, and CCL 0.060 bits/s/Hz; and 4×5 reflection coefficient -18.3457 dB, VSWR 2 dB, gain 20.4 dBi, directivity 20.2 dBi, bandwidth 3.4 GHz, MIMO metrics ECC 0.003134, DG 9.9999, TARC -21.65 dB, and CCL 0.0441 bits/s/Hz. Gain and directivity are much enhanced in the performance by extending to array configurations, and MIMO metric results low values of ECC and high values of diversity gain, which prove good isolation and proper spatial diversity of antenna elements.

A comparative analysis of existing millimeter-wave frequency design confirms that the proposed 4x5 massive MIMO PIFA array offers high gain, directivity, and sufficient bandwidth while maintaining a small size and excellent matching characteristics. The results make massive MIMO PIFA arrays a scalable solution and viable for high-rate, energy-efficient 5G millimeter-wave communication systems.

Key Words: *PIFA array, 5G wireless communication systems, mm-Wave, massive MIMO, ECC*

TABLE OF CONTENTS

LIST OF TABLES

LIST OF FIGURES

LIST OF ABBREVIATIONS AND ACRONYMS

5G	Fifth Generation
AAS	Active Antenna System
CST	Computer Simulation Technology
dB	Decibel
dBi	Decibel Isotropic
ECC	Envelope Correlation Coefficient
FD-MIMO	Full Dimension Multiple Input Multiple Output
GHz	Gigahertz
HFSS	High Frequency Structure Simulator
LTE	Long-Term Evolution
MIMO	Multiple Input Multiple Output
mm-Wave	Millimeter Wave
m-MIMO	Massive Multiple Input Multiple Output
PCB	Printed Circuit Board
PIFA	Planar Inverted-F Antenna
RA	Reflect-Array
RF	Radio Frequency
S11	Scattering Parameter (Reflection Coefficient)
SAR	Specific Absorption Rate
TA	Transmit-Array
VSWR	Voltage Standing Wave Ratio

CHAPTER ONE

INRODUCTIONS

1.1.Background of the Study

MIMO system has become the focus as a result of the rapid development of wireless communication technologies, particularly the implementation of fifth-generation (5G) communication network. Massive MIMO exploits the large number of antenna elements in the base station to offer services to a large number of users at the same time, improving spectral efficiency, throughput and reliability. Planar Inverted-F Antenna (PIFA) is one of the most promising antenna structures that can be integrated in compact MIMO systems due to the fact that it has a low-profile, compact size, and can be used in multiple bands. Nevertheless, massive MIMO PIFA array design to use in 5G has a number of challenges, especially in ensuring high element isolation, wide band, and small size without compromising on its performance. Recent literature has been dedicated to the improvement of the performance of PIFA-based MIMO antennas through new design methods. Wakrim et al.[1] used genetic algorithms with a non-uniform overlapping approach to design a dual-band PIFA MIMO antenna, which has better isolation and bandwidth. In the same manner, Abbasi et al.[2][3] suggested a pattern reconfigurable PIFA-based MIMO antenna, which can be dynamically steered to the changing communication environment. Khan et al.[4] developed an array of millimeter wave MIMO antennas for 5G communication terminals, which is another key development, and seeks to obtain the maximum gain and the lowest mutual coupling under higher frequencies.

In addition, surface enhancement methods have also been proposed using metamaterials and frequency-selective methods to enhance isolation and radiation properties in dense array arrangements [5][6][7]. Didi et al.[8] Illustrated that these structures could be integrated in a high-performance millimeter-wave PIFA array to improve the performance of the array in terms of directivity and efficiency. In mobile applications, Padmanabhan et al.[9] proposed a compact multiband reconfigurable MIMO antenna optimized for sub-6 GHz 5G terminals, which overcomes the issues of element separation and high isolation in small sizes and form factors. It is these more recent developments that give a good platform to continue the research into the design and performance improvement of massive MIMO PIFA arrays with the help of the advanced methodologies that can be used with next-generation wireless systems.

1.2. Statement of Problems

The high rate of development of 5G wireless networks demands high standards of antenna systems, especially in the millimeter-wave range, where high path loss, poor coverage, and vulnerability to interference are obstacles to effective communication. Traditional single-element antennas and early designs of MIMO antennas tend to have low gain, narrow bandwidth, weak impedance matching, and low directivity, preventing them from being able to support high-data-rate, low-latency 5G services. Moreover, array integration, mutual coupling, and non-optimal beamforming decrease the system efficiency and spectral use. The above difficulties underscore the critical necessity of methodically developed, miniature, and HFSS-enhanced massive MIMO PIFA arrays that obtain high gain, enhanced directivity, broadband functionality, and steady characteristics of impedance, hence enabling powerful, energy-efficient, and high-capacity 5G wireless communication.

1.3. Objectives

1.3.1. General Objectives

Design and performance enhancement of massive MIMO PIFA arrays using HFSS software for 5G wireless communication systems.

1.3.2. Specific Objective

- To review the existing research on the massive MIMO PIFA arrays for 5G wireless communication systems.
- To enhance key antenna parameters such as gain, directivity, and bandwidth.
- To compare the performance of the proposed designs with respect to gain, directivity, reflection coefficient, VSWR, and bandwidth.
- To evaluate the performance of single, 1x 2, 4 x 4, and 4 x 5 PIFA MIMO antenna arrays in terms of gain, directivity, and bandwidth.
- To identify the most suitable antenna configuration for compact and high-capacity 5G millimeter wave applications.

1.4. Thesis Motivations

The growing need for high-capacity wireless services has put an extraordinary performance compression on antenna subsystems in fifth-generation (5G) communication networks. The use of technologies like ultra-dense connectivity, mobile broadband with high gain, and low-latency communication cannot be reliably supported without antenna architectures that offer simultaneously high gain and wide band with strong spatial diversity. Massive MIMO systems have then become essential to the existence of current wireless infrastructure, but their actual implementation is heavily limited by the limitations of antenna design. The Planar Inverted-F Antenna (PIFA) has a number of unique characteristics: it has mechanical strength, a low profile, and can be used with integrated radio platforms. But in dense MIMO arrays of PIFA elements (and in particular sub-6 GHz and millimeter-wave 5G applications), high levels of mutual coupling, bandwidth compression, impedance match, and radiation efficiency are common factors that cause poor performance. All these effects fundamentally restrict the accuracy of beamforming, the capability of spatial multiplexing, and the system throughput. So that traditional PIFA designs cannot be used to realize large-scale MIMO systems. However, with recent research suggesting reconfigurable designs, optimization methods, and isolation-enhancement solutions, most of the available literature deals with isolated antenna elements or smaller arrays and lacks scalable massive MIMO designs. In addition, there are limited comparative studies between the various array geometries in a stable electromagnetic modeling environment. The study will improve the key antenna parameters such as gain, directivity, bandwidth, impedance matching, radiation patterns, and the isolation between the antenna elements by studying single-element, small-scale, and large-scale designs of the antenna array in the same designing framework. The findings would present effective design considerations and proven antenna designs that facilitate effective beamforming and high spectral performance for modern wireless applications.

1.5. Significance of Thesis

Design and performance enhancement of massive MIMO PIFA arrays using HFSS software for 5G wireless communication systems. "It is substantial because it addresses one of the core technological enablers in the future of wireless networks, which is the efficient deployment of massive MIMO systems. Massive MIMO is essential for 5G, as it dramatically increases capacity, coverage, and spectral efficiency by using large numbers of antennas at the base station. This research is focused specifically on optimizing Planar Inverted-F Antenna (PIFA) arrays, which are favored in mobile and small systems due to their low profile and easy integration. By improving the design, design arrangement, and performance parameters (gain, directivity, bandwidth, mutual coupling, etc.) of these PIFA arrays, the thesis has contributed to more reliable, efficient, and scalable 5G communication systems. The result is improved beamforming, less interference, and higher energy efficiency, all of which are strictly important to meet the high demands of modern wireless applications.

1.6. The Scope of Thesis

The scope of the thesis 'Design and performance enhancement of massive MIMO PIFA arrays using HFSS software for 5G wireless communication systems' includes the study, design, simulation, and optimization of Planar Inverted-F Antenna (PIFA) arrays designed for massive MIMO architectures in a 5G environment. This research involves the analysis of the electromagnetic behavior of PIFA element parameters in an array arrangement, the study of mutual coupling effects, and the improvement of parameters, such as gain, directivity, bandwidth, return loss, and radiation pattern. It also addresses the integration of these arrays in a compact platform for mobile or base station applications focused on minimizing size and maximizing performance. Using an electromagnetic simulation tool, namely HFSS, the study investigates the array geometry, spacing, and excitation techniques to aid beamforming and spatial multiplexing. The work is limited to sub-6 GHz and physical fabrication.

1.7. Limitations

In this work, the limitations are that the performance of the antenna is entirely based on simulations using Ansys HFSS software without the physical fabrication or experimental validation of the proposed antenna. Consequently, realistic considerations like fabrication tolerances, connector losses, material defects, and environmental factors are not taken into consideration. Also, electromagnetic performance metrics like reflection coefficient, gain, bandwidth, and MIMO metrics are considered as the primary subject of analysis, whereas the effects of real-world wireless propagation and the issue of hardware integration are not examined.

1.8. Methodology

The study is based on a systematic electromagnetic design and optimization of a 28 GHz Massive MIMO Planar Inverted-F Antenna for 5G millimeter-wave applications. The size of a single PIFA component is calculated by the application of analytical transmission line and cavity model concepts, considering fringing field effects and calculation of an effective dielectric constant to attain an effective resonance at 28 GHz. The antenna structure, consisting of the radiating patch, shorting plate, feed probe, substrate, and ground plane, is a model whose full-wave simulation is done in Ansys HFSS. To provide good impedance and radiation analysis accuracy, a lumped port excitation and a vacuum radiation boundary at least a quarter that of the antenna are utilized, with numerically convergent and stable S-parameter results being achieved by adaptive mesh refinement.

Once the single element is optimized, the design is expanded to be a multi-element MIMO array with proper inter-element separation to minimize mutual coupling as well as maximize beamforming. The optimization of the parametric encounters adjusts the main geometric parameters to provide S_{11} of less than -10 dB, higher bandwidth, high radiation efficiency, and high gain. The general performance of the antenna is analyzed in terms of S parameter analysis, radiation patterns, gain, directivity, total efficiency, and MIMO parameters like ECC, DG, TARC, and CCL. Steering of beam capability is checked through the analysis of the array factor, and the ultimate findings are compared with the existing literature to prove the effectiveness and dependability of the proposed 28 GHz Massive MIMO PIFA array in the 5G wireless communication networks.

1.9. Thesis Outlines

This thesis is composed of five chapters, and the overview of each chapter is as follows:

Chapter 1: The introduction, problem statement, objective, significance of the study, scope of the study, and layout of the thesis on the planar inverted-F antenna are discussed in this chapter.

This chapter presents the literature review; the key findings and gaps are reviewed.

Chapter 3: This chapter discusses the antenna theories, types of antennas, and analysis.

Chapter 4: Design of antennas from single-element to massive MIMO antenna arrays of the planar inverted-F antenna (PIFA) is discussed and compared in this chapter.

Chapter Five: The simulation results obtained on both single element and array antennas of the planar inverted-F antenna are discussed and compared in this chapter.

Chapter 6: The conclusion of the thesis, recommendations, and suggestions for future work are presented in this final chapter.

CHAPTER TWO

LITERATURE REVIEWS

2.1. Introductions to Reviews of Related Works

This chapter presents reviews of related massive MIMO PIFA arrays for 5G wireless communication systems, which include methods, designs, simulations, and results of previous related works.

2.1.1. Reviews of Related Works

The proposal is a triangular-shaped massive MIMO antenna system with 72 ports (ding 288 antennas) to be used in the fifth generation (5G) base stations. It consists of an antenna system that has three layers on each side and a total size of 44.4 x 29.6 x 0.1524 cm^3 and 24 ports. Every port (subarray) incorporates 2 x 2 patches placed on the upper layer, and the corresponding feeding network (utilizing a set of predefined phases) is placed on the lower layer, and the ground plane is placed in the middle layer. The ports are excited in a way that allows a tilt in the beam direction of the ports relative to the others and, thus, the attainment of uncorrelated individual radiation patterns. The system is peculiar in that it provides two modes of operation, namely simultaneous port-individual operation (i.e., 72-port MIMO) and m-MIMO array operation (i.e., beam switching). The bandwidth achieved is 100 megahertz, which is 3.45 to 3.55 gigahertz. The single-port gain is 9.41 dBi. The envelope correlation coefficient is held to not more than 0.1198. It presents a beam steering method, whereby the 24-port side of the beam can be steered to different spatial locations, depending on non-uniform patterns of the ports, unlike most other historical methods. It reaches thirteen switched beams and has a central elevation of up to angles of 34 degrees and a peak gain of 19.5 dBi[10].

The presented paper is aimed to introduce a carefully designed multiband planar inverted-F antenna (PIFA), which will be optimized to work under LTE/5G systems and below 6 GHz as well as support Vehicle-to-Everything (V2X) communications. The PIFA antenna has a large band frequency response with a resonance between 950 MHz and 6 GHz. The given design of the PIFA antenna is divided into three parts, the upper, frontal, and rear parts, and ends with a unique and effective antenna layout. The substrate used for making the antenna is FR-4 material (FR-4 dielectric constant = 4.4). The total size of the antenna is 54x38x25 mm^3. The proposed PIFA antenna has been empirically tested and has proven that it has a voltage standing wave ratio (VSWR) of less than 2 across the entire frequency range of 950 MHz to 6 GHz. Moreover, the antenna will have the greatest gain of 7.08 dBi at 5.5 GHz, 6.81 dBi at 5.2 GHz, and 6.65 dBi at 5.9 GHz. Other gains of a receiver at 3.8 GHz and 1.7 GHz are a gain of 6.67 dBi and a gain of 3.31 dBi, respectively. To conclude, this paper explains an effective and rational multiband PIFA antenna that is most appropriate to use in the automobile industry. An antenna with the ability to cover a wide band and ensure high gain makes it a very viable option to be implemented as part of the LTE/5G systems, as well as in V2X communications[11].

Hybrid analog-digital design is often considered an enticing way of implementing millimeter-wave (mm-Wave) massive multiple-input multiple-output (MIMO) systems, mainly due to the significant reduction of the count of costly radio-frequency (RF) chains through the abacus of signal-processing tasks to the analog domain. However, the analog feed network (RF dividers, combiners, phase shifters, and interconnecting lines) is confronted with the problem of scalability because of its disproportionately high-power consumption when employed with a large number of transmitting antennas. In order to deal with this impediment, the current paper explores novel massive MIMO configurations, namely reflect-array (RA) and transmit-array (TA) antennas. It is shown that precoders to be used in RA and TA schemes have different constraints than those needed by traditional MIMO constructions. Considering these limitations and leveraging the natural scarcity of mm-Wave channels, we design an efficient precoder of RA and TA systems via the orthogonal matching pursuit algorithm. In addition, to be able to make a fair performance comparison of RA and TA antennas with the conventional fully digital and hybrid MIMO schemes, we construct a full-fledged power-consumption model. The obtained results of the simulation indicate that compared to conventional MIMO structures, RA and TA antennas are higher in energy efficiency and scalability to a greater number of transmitting antennas. This paper presents new massive MIMO designs—that is, reflect-array (RA) and transmit-array (TA) antennas—that are able to overcome scalability and energy-efficiency issues of mm-Wave systems. The authors prove the effectiveness of RA and TA architecture over conventional MIMO systems by creating efficient precoders with the use of the orthogonal matching pursuit algorithm and creating a single power-consumption model[12].

This paper is an in-depth research of full-dimension multiple-input multiple-output (FD-MIMO) technology, which has currently become the intersection point of scholarly research and commercial standardization, and the ultimate goal is to drive Fifth Generation (5G) cellular networks to the next level. FD-MIMO is based on an active antenna system (AAS) that includes a two-dimensional planar array format, the use of which allows a high density of antenna elements to be packed into realistic dimensions for a base station (BS) and allows adaptive electronic beamforming in three-dimensional space. Nevertheless, due to the characteristics of large-scale planar arrays, the small size of planar arrays is contributing to the issue of spatial correlation in FD-MIMO systems. In order to explain the consequences of this phenomenon, we obtain the generalized spatial correlation functions of the two individual element channels as well as the composite antenna ports of the AAS. For instance, we are proposing fractional programming to maximize the minimal signal-to-interference ratio in the multi-user multiple-input single-output (MISO) channel by the use of the quasi-static channel covariance matrix of user data. Application of semi-definite relaxation and an algorithm by Dinkelbach gives a quasi-optimal solution. We eventually get a user group-specific elevation beamforming plan, which improves the performance of the system drastically, as confirmed by running huge simulations. These lessons have a direct implementation in the measuring and implementation of 5G FD-MIMO infrastructures. The literature shows a detailed analysis of the FD-MIMO technology, overcoming the challenges present currently and providing solid solutions to improve the performance of the 5G cellular network[13].

A high performance multiple-input multiple-output (MIMO) antenna design to be used in the 28 GHz band is presented in this literature. With 1 x 8 series fed arrays at each port, the configuration of the 4-port MIMO antenna has demonstrated peak gains of 15.5 dBi with a 2 GHz bandwidth. A decoupling scheme with appropriately designed metamaterial cells and carefully controlled antenna element spacing helps reduce the interference between these antenna elements, resulting in this improved performance of the antenna. The system has demonstrated an exceedingly low mutual coupling and has been demonstrated to be almost -40 dB under the frequency spectrum under consideration having ECC of 0.00010, DG of nearly 10 dB and channel loss capacity of 0.11-bit/s/Hz. This has been tested by experiment and the design can be a candidate, applicable to numerous millimeter-wave communication systems. An advanced MIMO antenna design with a four-port configuration and 1 * 8 series-fed arrays per port is presented in this literature for 28 GHz frequency band. The design makes use of metamaterial based decoupling techniques and optimized spacing to attain peak gains of 15.5 dBi and bandwidths of 2 GHz. Little mutual coupling exists in the system[14].

An 18-element antenna system operating with fourth and fifth generation (4G/5G) handsets, with large scale multiple input multiple output (MIMO) and diversity support is presented in this work. The design of the antennas is for operation on the sub-6 GHz LTE bands 42 (3.4-3.6 GHz) and 43 (3.6-3.8 GHz). The radiating element is a simple slot antenna using open-ended slots to allow miniaturization. Furthermore, these slots act as decouplers so as to enhance the isolation between different radiators. With the size of 150mm * 80mm * 1.6mm, the proposed antenna elements are built on a low-cost FR4 substrate for 6-inch smartphones. It is found that the measured and simulated gain of antenna are beyond 5.3dBi. The simulated and experimental results for the antenna gain are obtained to be higher than 5.3 dBi. The simulation and measurement results of the proposed design reveal a good impedance matching (reflection coefficient > 20dB), port isolation (> 20dB), overall efficiency (> 87%) and envelope correlation coefficient (< 0.01) over the operating frequency. MIMO antenna performance metrics are checked by computing the ergodic channel capacity with the help of the Kronecker channel model[15].

5G applications are expected to support 1GHz bandwidth, and will operate in the 28, 37, 60 and 73GHz frequency bands. A planar inverted F antenna with 28 GHz operation is introduced in this paper; it has achieved a gain of 9.30dB and return loss of -17.46dB. Moreover, by the addition of an L slot in the patch the design has been modified for dual band operation at 28 and 37GHz. Remarkable return losses of 32.54dB and -18.57dB and gain of 8.62dB have been observed. Furthermore, the improved design has proved to have an improved bandwidth of 1.3GHz for both of the frequency bands, whereas the original design only achieved a bandwidth of 1.02GHz. The original design has been modified to a MIMO with two antenna elements (2x1) to improve the gain and data rate performance, and the corresponding performance parameters have been tested[16].

Planar inverted F antenna (PIFA) is primarily used in the mobile devices. PIFA can cover extensive wireless services and so they are suitable in dual-band frequencies. This aspect renders them a suitable option to design mobile devices. The size of the ground plane and the position of PIFA with respect to the ground plane affect the performance of the PIFA. As an example, a PIFA placed close to the ground plane corner exhibits an outstanding radiation pattern. The biggest demand of 5G is to boost the amount of data required by all consumers while accommodating the number of mobile subscribers and the emergence of new technologies. Luckily, these requirements could be fulfilled using sophisticated antenna array technologies. Despite PIFA antennas popularization in designing mobile phones due to their light weight, cost effectiveness, and enhanced directivity, PIFA antenna array has performed well as a pillar in future mobile communication systems of 5G. They have greater gain compared to a single PIFA antenna in the same frequency range. This paper will provide a close examination of the role of PIFAs and PIFA arrays in the infrastructure of future mobile technologies that can be used in the future in 5G communication. The significance of Planar Inverted F Antennas (PIFA) and PIFA arrays in offering support to the future mobile technologies befitting the 5G communication is keenly discussed in this literature[17].

In this development, patch antennas have played a critical role, and this is a crucial part of the modern wireless communication system. Specifically, compared to conventional microwave antennas, microstrip antennas are lighter, smaller, simpler to manufacture, cheaper, and easier to incorporate into cellular networks. When paired with the proper base station antenna layout, the mm-Wave MIMO antenna arrays with beamforming will greatly enhance network coverage and capacity and decrease the cellular communication interference, enhancing the overall user experience. In the case of MIMO cellular radio communication, the Planar Inverted F-Antenna (PIFA) Microstrip Antenna Array at the mm-Wave with an appropriate bandwidth increment at the V-band frequency is designed in this thesis. MIMO PIFA antenna array topology, as illustrated by the antenna array design, can be applied to the mm-Wave cellular radio communication system to achieve the required effective gain of the antenna and increase the channel capacity. The various PIFA antenna designs have been modeled at various such design parameter levels in the course of this thesis. To apply in the current and future cellular communication technologies, single element, 1x4, and 4x4 PIFA elements have been built, modeled, and proposed. The parameters of the antenna, which are considered and modeled in the case of the PIFA antenna array at V-band (60 GHz), include gain, directivity, return loss, polarization, beam width, bandwidth, and radiation patterns. This thesis aims at reducing the mutual coupling by designing a planar multilayer substrate and defining a ground plane with spacing between the elements of an infinity ground plane probe-fed PIFA antenna in FEKO. Then, make wire probes between the patches and the ground plane. Gain of 6.25 dBi, 6.67 dBi, and 12.14 dBi; directivity of 10.34 dBi, 12.51 dBi, and 15.12 dBi; VSWR of 1.01, 1.03, and 1.18; bandwidth of S11 ≤ -10 dB are 3.81 GHz, 3.22 GHz, and 2.69 GHz; and return loss was -46.1 dB and -48 dB. When comparing the proposed alternative PIFA designs, the 4X4 PIFA antenna array had an advantage over the single and 1X4 PIFA antennas in most performance factors. The directivity of the PIFA antenna array can be enhanced slightly by adding more PIFA elements and by varying the steering angles at constant substrate thickness to enhance the bandwidth efficiency. Each of the PIFA-designed antennas, which had been discussed, was a tough competition for mm-Wave 5G wireless communications and other applications[18].

Future 4G/5G-wide backplane MIMO smartphone technologies are presented with a reconfigurable antenna array. The antenna design consists of two modules of the 2 x 2 MIMO

4G antenna, which has frequency and other circular polarization diversities, and a 6 x 6 MIMO 5G antenna, which has pattern diversity. All the elements in the 4G and 5G modules are excited through a microstrip line with a tuning slot as a conductor on the ground plane, including a spiral patch and a short-ended C-shaped stub as a parasitic element on the non-conductive structure. The space area of each element is 22 x 9.3 mm^2 on the ground plane. These antenna elements use techniques of spatial diversity and polarization to reduce the effects of coupling and enhance isolation. The 4G antenna module has the ability to operate in two operating bands, i.e., LTE-2500 and 5G band, with the combination of a PIN diode into the antenna element structure, while the 5G antenna module operates at a range of the 3.4-3.6 GHz spectrum that meets the requirements of future 5G applications. The suggested MIMO antenna array has been manufactured, and the tests done. The antenna isolation value is measured to be over 15.2 dBi under the ON and OFF condition of the PIN diodes without having any decoupling structures. Also, the article confirms the determined antenna efficiency, radiation pattern, envelope correlation coefficient, and ergodic channel capacity throughout the range of bands. This paper introduces a novel reconfigurable MIMO antenna array to be used in 4G and 5G smartphone operation, which has frequency agility, polarization diversity, and pattern diversity to enhance its performance in the LTE-2500 and 3.4-3.6 GHz[19].

In this paper, an inquiry and a setup that involves the use of two antennas known as microstrip patch antennas are discussed. These antennas are designed in a 2x1 pattern. The antenna is designed in an easy way by feeding it on a microstrip line. Such a feeding of the antenna is good since it provides us with the bandwidth that we can easily understand and less radiation that we may not want is prevented. The space between the feed line and the antenna patch is adjustable such that it is brought to equal the characteristics of the antenna impedance. This is important for the antenna to work properly with the 5G system. This setup includes the microstrip patch antennas, and they considerably contribute to the effectiveness of the 5G wireless communication setup. It was the array of antennas we are discussing. Experimented upon with the help of a special computer program known as high-frequency structure simulator software. This software helped us view the efficiency of the antenna array in 28 GHz, the frequency of 5G. There is a special material under the antenna array, and it is referred to as Rogers RT/duroid 5880. Some of the properties of this material include a relative permittivity of 2.2. It is also very thin, 0.5 mm thick, and it loses very little energy with a loss tangent of 0.0009. The antenna array and the Rogers RT/duroid 5880 material are important for making the 5G antenna work properly. The results of this paper demonstrate the following regarding the antenna array: reflection coefficient -35.91 dB, standing wave ratio 1.032, bandwidth 1.43 GHz, gain 9.42 dB, directivity 9.47 dB, radiated power 29.94 dBm, accepted power 29.99 dBm, radiation efficiency 29.95, and overall efficiency 99.83%[20].

This paper presents a new hybrid technique to supply printed PIFA antennas with dual-frequency operation at 29 GHz and 32 GHz, the optimum bands for 5G mobile communications. The proposed prototype is a 2-element rectangular PIFA with an inset feed around the 29 GHz and 32 GHz. To make the second program symmetric, two-element dual-band two-element slotted rectangular patches with PIFA inset-fed lines are used. Primary inverted I-shaped inverted patches at slots could be used to produce a dual-band response. The applications in 5G portable are using hybrid algorithms. These two methods can be used in 5G wireless applications, which are the genetic algorithm and the Bayesian convolution. The third prototype is an inverted I-shaped slotted perpendicular patch on the inverted I-shaped PIFA antenna used in dual service. The partly rectangular ground plane is installed in the slot-shaped DGS. The substrate is 52074 mm^2 in width, making it simpler to fit within the handset devices with the looming 5G mobile communications, given that the embedded antennas have extremely small planar designs and occupy minimal spaces. There is a decrease in bandwidth and a decrease in demand. PIFA undergoes less mutual coupling with no additional constructions. Besides anticipated reflections and interactive application features, the directivity, gain, and effective values of the antenna systems are suitable for 5G mobile applications due to the two algorithms[21].

PIFA antennas are suggested for 5G communication networks, which include LTE Advanced mobile communication services. The proposed antenna structure consists of the substrate, ground plane, shorting plate, and feeding post connected to the ground plane. This antenna with a relative permittivity of 4.3 has a volume of 1.5 mm^3, based on an FR-4. The experimental findings of the Planar Inverted F Antenna (PIFA) measured at 3 to 4 GHz at the frequencies measured as 510 MHz indicated that the values of the return loss, bandwidth, VSWR, and impedance were -41.15 dB, 510 MHz, 1.04, and 48.414 Ω, respectively, at resonant frequency 3.5 GHz[22].

2.2. Literature Summary

Table 2.1. Literature Summary

Ref	Year for Publications	Authors	Focused Area	Frequency	Bandwidth	Gain	Observed Gap
[10]	2018	M. A. Al-Tarifi, M. S. Sharawi, A. Shamim	72-port triangular mMIMO for 5G Base Stations	3.45–3.55 GHz	100 MHz	9.41dBi (port), 19.5 dBi (array/max)	Novel dual-mode (port/array) operation with beam steering, but very narrow bandwidth or limited to 100 MHz bandwidth; sub-6 GHz only; large physical size unsuitable for compact mm-Wave systems
[11]	2023	Nikam, A.A & Patil, R.B	Multiband & PIFA for vehicular LTE/5G (Sub-6 GHz) & V2X communications	Sub 6 GHz	2.4-2.48GHz, 5.2-5.8 GHz	3.2 – 5.6 dBi	Limited gain, single element not MIMO and mm-Wave
[12]	2019*	V. Jamali, A. M. Tulino, G. Fischer, R. Müller, R. Schober	Reflect-Array (RA) & Transmit-Array (TA) mm-Wave MIMO architectures, energy-efficient design	mm-Wave	Not specified	Not specified	Focus on Energy efficiency and architecture lacks specific measurement results for fabrication

[13]	2018	Q.-U.-A. Nadeem, A. Kammoun, M.-S. Alouini, M. Debbah	FD-MIMO and 3D beamforming using 2D planar arrays	mm-Wave	Not specified	Not specified	Focus on algorithmic optimization (fractional programming); lacks physical antenna design
[14]	2025	N. Alsaab et al.	Series-Fed Array MIMO Antenna at 28 GHz	28 GHz	2 GHz	15.5 dBi	Uses a 1 x 8 linear array; effective but lower gain than 2D, limited to 4 ports.
[15]	2021	C. C. By	18-Element Massive MIMO for 5G Smartphones	3.4–3.8 GHz	Sub-6 Ghz (3.4-3.8 GHz)	<5.3 dBi	Operation is sub-6 GHz (not mm-Wave); low gain (<5.3 dBi) due to mobile constraints.
[16]	2017	A. Rachakonda et al.	Dual-band PIFA (28 & 37 GHz) for MIMO	28 & 37 GHz	1.3 GHz	8.62 dBi (Dual) / 9.30 dBi (single)	Limited to 2x1 MIMO configuration; moderate gain and bandwidth compared to massive arrays.
[17]	2021	K. Kunda et al.	PIFA & PIFA Array for Mobile 5G	Sub-6 GHz	Not Specified	Not Specified	Generalized review of PIFA capabilities; lacks specific massive array design data and not mm-Wave
[18]	2022	T. Watro Wate	PIFA Microstrip Array for V-band(60GHz)	60 GHz	2.69 – 3.81 GHz	12.14 dBi (4x4 array)	Operating Frequency is V-band (60 GHz), not the 28 GHz 5G standard

[19]	2021	M. M Fakharian	Switchable MIMO Frame Antenna (4G/5G)	LTE + sub-6 GHz	Not Specified	15.2 dB	Smartphone application; but not used high-gain beamforming, not PIFA and mm-Wave
[20]	2023	S. E. Didi et al.	2x1 Microstrip Patch Array at 28 GHz	28 GHz	1.43 GHz	9.42 dBi	Small array size 2x10 limits the total gain and directivity compared to massive MIMO.
[21]	2021	Padmapriya, T & Manikanthan SV	Dual-band PIFA for 5G mobile applications(mmWave) using ML optimization	29 and 32 GHz	700 MHz & 2.6 GHz	3.5 dBi	Design complexity, which is inefficient for high-frequency mm-Wave 5G antennas (29/32 GHz) Narrow bandwidth and impedance matching challenges at dual frequencies
[22]	2023	Taban et al. I.N., A.H., & Naser, A.A.	Single-band PIFA for 5G & wireless applications at 3.5 GHz	3.5GHz	510 MHz	Note specified	Narrow bandwidth, single antenna no MIMO configuration, not mm-Wave

2.3. Literature Review Overview

The literature on the fifth-generation (5G) wireless communication systems indicates that there has been an increasing requirement of higher data rate, better spectral efficiency, lower latency, and network capacity. To meet these needs, frequency bands in the millimeter-wave (mm-Wave) frequency ranges and especially in the 28 GHz range have been extensively explored owing to the vast bandwidth they offer. Nonetheless, the high frequencies of operation (mm-Wave) present serious issues, including more path loss, attenuation of the signal, and propagation sensitivity. To combat these shortcomings, researchers have paid much attention to the Massive MIMO technology and high antenna arrays that can beamform and spatial multiplex. Several studies have explored 5G systems with the application of microstrip-based antennas since they have a small profile, are easily manufactured, and can be integrated into a system.

The Planar Inverted-F Antenna (PIFA) has stood out as one of them because of its small size, lower Specific Absorption Rate (SAR) and better impedance matching properties. Previous reports have demonstrated several PIFA designs that would be applicable at sub-6 GHz and discrete mm-Wave frequencies; these designs have been demonstrated to possess several limitations such as limited bandwidth, low gain, and high mutual coupling in MIMO designs, and beam steering.

Also, some of the MIMO antenna arrays reported in 5G mm-Wave developments are mainly concerned with bandwidth improvement and not extensive assessment of diversity performance indices, including ECC, DG, TARC, CCL, and Mean Effective Gain.

According to the literature review, there is a research gap in terms of the integrated design and the performance improvement of high-efficiency, low-coupling Massive MIMO PIFA arrays, which are specifically 28 GHz with a systematic analysis of the beamforming capability and diversity performance. Consequently, this thesis produces value by developing and optimizing a 28 GHz Massive MIMO PIFA array with better impedance matching, higher gain, less mutual coupling and validated MIMO performance measurements through full-wave electromagnetic simulation and analytical verification, to overcome the main challenges that were reported in earlier works.

CHAPTER THREE

THEORETICAL BACKGROUND AND ANALYSIS

3.1. Introductions

This chapter presents the theoretical base for designing the Planar Inverted-F Antenna (PIFA) in the design of the Massive MIMO antenna at 28 GHz for 5G mm-wave applications. It describes microstrip patch antennas and PIFA structures' operating principles of quarter-wavelength resonance, effective dielectric constant, and impedance matching. Methods of analysis like the Transmission Line Model and Cavity Model can be mentioned to estimate resonant frequency and radiation behavior before simulation in ANSYS HFSS. Moreover, the important parameters of antenna performance, including reflection coefficient, bandwidth, gain, directivity, radiation efficiency, and VSWR, are addressed, as well as the main concepts of the antenna array and significant MIMO parameters, Envelope Correlation Coefficient (ECC), Diversity Gain (DG), Total Active Reflection Coefficient (TARC), and Channel Capacity Loss (CCL), which were discussed as the basis of analyzing the proposed massive MIMO PIFA array.

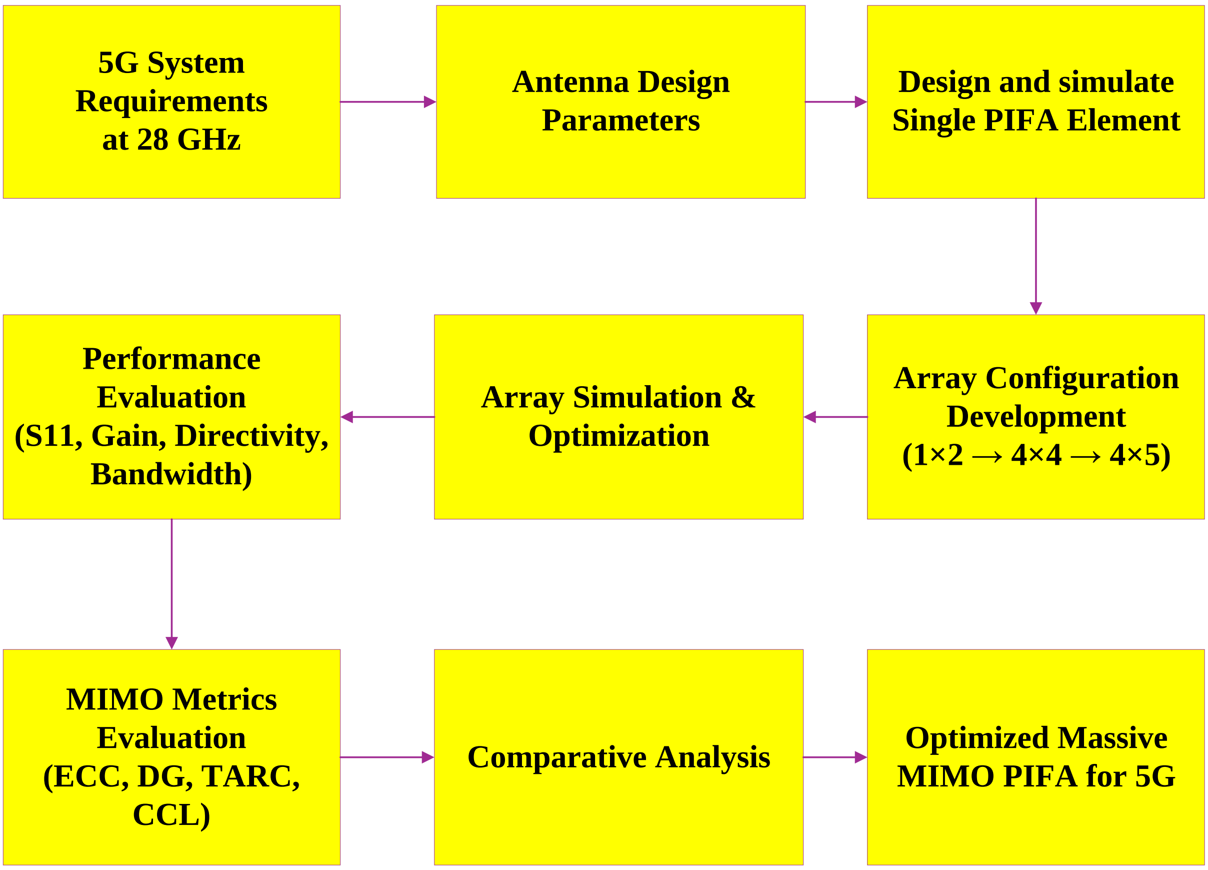

Figure 3.1. block diagram of thesis

3.2. Flow Chart

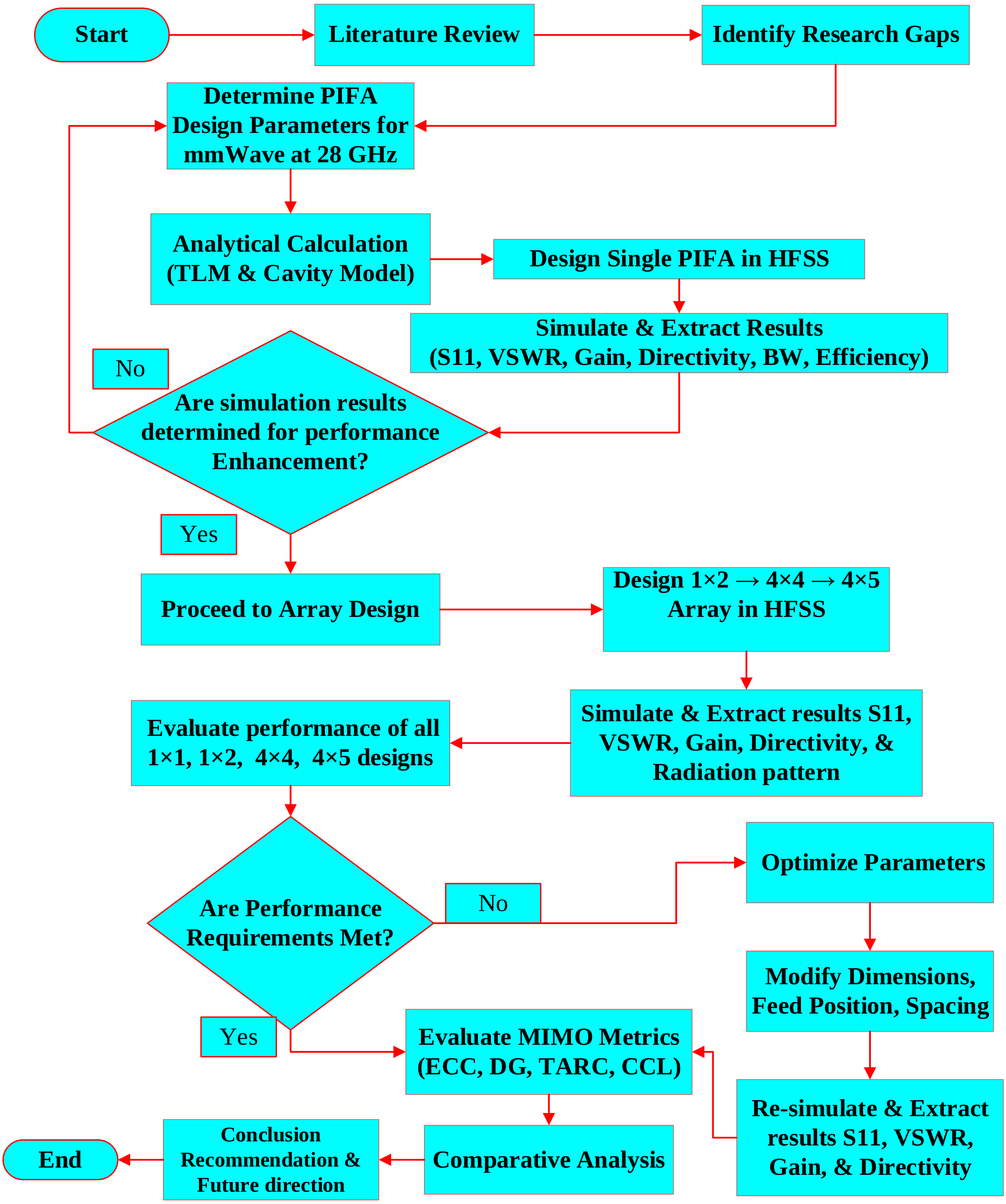

Figure 3.2. Flow Chart of thesis

3.3. Microstrip patch antenna

Microstrip antennas are low-profile antennas and they allow them to be made into curved shapes when their construction using thin substrates since their design allows it. The physical dimensions of a microstrip patch receives approximately half wavelength of operation inside a dielectric medium. This design allows the antennas to be operated optimally at UHF and frequencies into microwave and millimeter wavelength. Its most frequent application in the microwave operations [23][24].

Microstrip antennas offer advantages of their strengths but they have disadvantages of their poor radiation efficiency which is experienced when they are compared to other types of antennas. The efficiency of this process depends on two factors the permittivity and the thickness of the substrate material used. Microstrip antennas have a bandwidth limitation since they have a narrow operating range. According to the design of patch antennas requires a careful selection of feeding methods in order to get their best operational performance [25].

In products such as mobile communication, where weight reduction is very paramount, a careful choice of substrates that would have good dielectric and low density is necessary. A low dielectric constant substrate of greater thickness is usually desired in order to achieve higher performance in radiation efficiency and bandwidth. Nonetheless, this method has also results in a large antenna size [26].

3.3.1. Advantage of Microstrip Patch Antenna [27]

- The product has lightweight materials with low profile and compact size.
- It offers cost-effective manufacturing, simple fabrication processes, and excellent conformability to complex surfaces.
- The technology support dual-band and tri-band operation with good operating efficiencies in all operating frequencies.
- It demonstrates seamless compatibility and is highly integrable with other microstrip-based circuitry, enhancing overall system compactness and performance.

3.3.2. Disadvantages of the Microstrip Patch Antenna [28]

- The system operates in a limited bandwidth that limits the ability of switching the system over various frequency ranges.
- The system has reduced performance as a result of low gain and low radiation efficiency.
- Surface waves cause unintentional excitation which leads to radiation pattern distortion and increased energy loss.

- The system faces trouble to achieve high polarization purity which results in complex polarization control.
- The system works using limited power capacity which liberates it from being utilized in situations with high power consumption.

3.4. PIFA Antenna

The Planar Inverted-F Antenna (PIFA) has found wide use in many applications because of its simplicity in design, relative ease of fabrication, and flexibility in design. The system gives a low-profile design capable to meet the budget requirement while providing adequate performance to match the demand from contemporary compact systems. Low-profile antennas provide essential function in areas where space and weight and budget limits and aerodynamic constraints and performance requirements form critical constraints. The aerospace systems are aircraft and satellites & spacecraft & missiles and mobile radio & wireless communication devices according [29][30].

The PIFA system has several benefits with respect to its design, which is the reason why its system is preferred in designing conventional antennas. The system provides a compact design with high strength of construction and it supports multiple frequencies bands and reduces the level of production cost and it gives good strength to cope with physical stress. The antenna design permits lower specific absorption rate (SAR) values that helps in minimizing exposure of RF radiation to the user as per the head and body needs of based on portable and wearable devices [31].

The PIFA system comprises of a radiating patch, which is located on one side of a dielectric substrate, and a ground plane is located on the opposite side. The radiating element could be of different shapes due to the fact that designers use copper and gold material for making the element. Designers use standardized shapes in their work because these shapes assist in design analysis and evaluation of performance process [32].

According to the feed line and radiating elements had a structural base and support system that was serving as a dielectric substrate [33]. The PIFA design has basically three parts that consist of radiating patch, a shorting plate, and a ground plane. The radiating patch is made with copper material to form size depending on L1 and L2. The antenna is kept at a certain height above the ground plane to create the best radiation performance as per [34].

3.4.1. Advantages and Disadvantages of PIFA [35].

Table 3.1. Advantages and Disadvantages of PIFA

Advantages of PIFA Antennas	**Disadvantages of PIFA Antennas:**
Small size	Narrow bandwidth
Light weight	Lower power gain
Low-profile	Lower power handling capability
Simple fabrication	Polarization impurity
Relatively low specific absorption rate (SAR) and ϖ provides good efficiency	Surface wave
It can be realized in a very compact form, desirable for personal and mobile communication hand held devices.	Narrow bandwidth
It allows for dual and triple band operations	

3.4.2. Challenges of PIFA and Improvement Techniques.

Several design modifications have been suggested in order determine with the best tradeoff of size, bandwidth, and other electrical properties of the PIFA [18].

i. Bandwidth increase technique

Among the most widespread approaches to raising the bandwidth of PIFA is to raise the height of the shorting plate which has the effect of increasing the antenna volume. Ground plane size is another important factor in performance of bandwidth. The size of the ground plane especially when it is shrunk can be adjusted to greatly expand the antenna bandwidth. Also by cutting slits along the sides of the ground plane, the quality factor (Q-factor) of the structure is lowered and therefore increases bandwidth. The process of improving bandwidth may also be done using a number of sophisticated methods. These are the using of dual-resonance behavior through the addition of auxiliary patch which introduces capacitive load[18], applying high permittivity dielectric material[18], and use chip resistor which is increasing loss.

ii. Dimensions of PIFA

The size of PIFA were minimized throgh shorting the dimentions of antenna. But, has an impact on the impedance at the antenna terminals, tending to add the reactive components to the radiation resistance. The occurrence of this undesired effect can be offset by using capacitive top loading. The result of such loading is a shorter effective resonant length of about λ/4 of the length of the waveguide. However, this miniaturization normally causes an impedance matching and bandwidth performance depreciation. The possible practical implementation of capacitive loading is to lay a metallic plate on the plane parallel to the ground therefore establishing a parallel-plate capacitor as used capacitive load [18].

iii. Resonance frequency of PIFA

The following relations is used to approximate PIFA resonance

$$Lp + Wp - Ws = \frac{\lambda}{4} \tag{3.1}$$

$$if \ \frac{Ws}{Lp} = 1, \ Lp + h = \frac{\lambda}{4}, \ and \ if \ Ws = 0, \ Lp + Wp + h = \frac{\lambda}{4} \tag{3.2}$$

$$f_r = \frac{c}{4(L_P + W_p - Ws - h)\sqrt{\in_{eff}}} \tag{3.3}$$

In this expression,

- Wp and Lp are length and width of patch,
- Ws is width of shorting plate,
- h is height of substrate,
- c is sped of light in vacuume,
- $\in_{eff}$ effective dielectric, and
- f_r is resonance frequency

By connecting an open slot, the frequency is reduced. This is because currents are flowing at the boundaries of the opened slots; thus, the frequency and the size of the antenna are reduced considerably by a capacitively loaded slot. In the same way, through slotting in the patch, a frequency band operation of two or more may be obtained. Also, modifying the width of the patch has influence on the choice of resonant frequency. The shorting plate width of the PIFA serves as a source of control over its resonant frequency. Decreases the resonant frequency due to a decrease in Ws plate width. PIFA is made of a quarter wavelength compared to a microstrip. Conventionally, microstrip antennas are formed of half-wavelength resonances by bandwidth analysis. and resonant frequency, which are properties of the antenna, can be readily optimized by finding out. the location where feed point[18] will be located, where the reflection coefficient will be minimized.The inverted F antenna has turned the horizontal component to a plate made of a wire in the so-called planar inverted-F antenna (PIFA). It is self-resonant and has a structure. ohmic load impedance of the frequency of operation. PIFA is an antenna that is small as well as wide-bandwidth and efficient. Rome, distance, and variation of length. and the position of the feed and shorting point, the height of the radiator, etc. are the factors affecting the electrical performance of these antenna structures [18].

PIFA is usually configured as shown in figure 3.4. The antenna is fed by a feeding pin, and the ground plane is connected through the feeding pin to the antenna. A shorting pin permits good impedance matching realized with the patch above the ground plane of size smaller than λ/4 [18]. The resulting PIFA structure is smaller in size than the other conventional patch antennas of λ/2 of the wavelength.

iii. Efficiency of the PIFA design

The efficiency of PIFA is decreased by all the losses through its structure in its environment, such as mismatch losses, ohmic losses, external parasitic resonances, edge power losses, transmission losses, etc. The horizontal element has been modified by the inverted F antenna to a wire to a plate, which gives rise to the PIFA. It has a self-resonating structure having a load impedance of pure resistors at the operating frequency. PIFA is one of these antennas that are not only small but also have a wide bandwidth and high efficiency. Length, distance, and location of the feed and shorting point, radiator height, etc. varied. influences the electrical performance of these antenna structures. A typical configuration of a PIFA is shown in figure 3.3. A feeding pin is used to feed the antenna through the dielectric substrate. The shorting pin permit good contact, impedance matching with patch above ground plane of size below λ/ 4. The PIFA structure resulting is smaller than the traditional λ/2 patch antennas.

3.5. Feeding Techniques

Microstrip patch antennas can be excited by various well-known techniques. The four most popular methods are the microstrip line, coaxial probe, aperture coupling, and proximity coupling methods. These feeding strategies are split into two main categories as usual, contact-based and non-contact-based methods. In contact-based feeding, the radio frequency energy is fed directly to the radiating element by a physical connection usually through a microstrip transmission line or a coaxial probe. On the other hand, the non-contact methods of feeding, on the other hand, utilize the interaction of electromagnetic fields between the feed structure and the radiating patch but do not involve actual electrical contact [36].

3.5.1. Microstrip transmission-line feed

A microstrip antenna is a type of antenna that is made using printed circuit board (PCB) technology using microstrip techniques. Fundamentally, a microstrip patch antenna is made of a conductive patch of radiation above a dielectric substrate that is again above a ground plane. The dielectric substrate has a certain relative permittivity, and this dramatically affects the electromagnetic behavior of the antenna. Typically, the patch is electrically smaller in size as compared to both the substrate and ground plane [37]. The resonant frequency and dielectric constant are the most important parameters that specify the physical dimensions of the patch. Owing to its simplicity, low cost, and ease of integration, the microstrip line feed enjoys wide establishment in practical designs. One particular example of impedance matching is the application of an inset feed where an exact notch is cut into the patch to form an impedance match between the feed line and the element, which is used for radiating. This alignment is precisely regulated by changing the depth of the inset [38].

The feed line is, by nature, narrower than the patch itself, so this is attached directly, and usually the feed line and patch are made of the same conductive material. This feeding method is also suitable for antenna array feeding. However, with this technique, there are some trade-offs. Increasing the thickness of the substrate can be used to improve bandwidth, but this would also result in the formation of surface waves and unnecessary feed radiation, which can impair the overall performance of an antenna. This antenna array feeding is also applicable to using this method of feeding, the substrate's dielectric constant and thickness's care selection are also important to provide a balance between performance and unwanted radiation effects [39].

3.5.2. Coaxial probe feed

In the coaxial probe feeding technique, the inner conductor of the coaxial cable passes through the dielectric substrate and is soldered directly onto the radiating patch, and the outer conductor is connected to the ground plane by a via hole drilled through the substrate. A major advantage of this method is the flexibility of impedance matching, i.e., the feed point can be precisely positioned anywhere on the patch to achieve an optimal impedance matching [40]. However, it does have its faults. The fact that one must drill a hole through the substrate adds a certain level of mechanical complications, and the fact that the connector extends out of the ground plane has an impact on the structural compactness of the antenna itself. Moreover, the technique is defined by its limited bandwidth and can be difficult to model with high fidelity because it is three-dimensional.

3.5.3. Aperture coupling feed

In this type of feeding method, a slot or aperture is identified through the ground plane to allow the transfer of energy between layers. The design uses two separate dielectric substrates with different thickness and permittivity that can be separately optimized to enhance the unique electrical functions of the radiating and feeding structures. The top substrate is usually designed to have a low dielectric constant so that loosely bound fringing fields will increase radiation efficiency. In contrast, the lower substrate is typically chosen with a higher permittivity so as to create tightly confined fields, which maintain low radiation of desire and higher circuit performance But it does have a number of challenges. The requirement of several layers of substrate compounds to a greater thickness of the antennas and contributes to the complexity of the antenna making process. This technique is prone to a comparatively lower operational bandwidth, which restricts the application of this technique to wideband purposes [41][42].

3.5.4. Proximity coupling feed

This feeding technique, which is widely called an electromagnetic coupling configuration, makes use of a dual substrate structure where the feed line is embedded between two dielectric layers with different permittivity values, which are of the order of the dielectric substrate (denoted as epsilon sigma one and two). The radiating patch is placed over the upper dielectric layer through which the indirect coupling is achieved by electromagnetic suspension. A major advantage of this method is due to the possibility to separate the feed and the radiating structure, therefore using two different dielectric materials, each optimized to maximize their relevant performance characteristics. This arrangement supports a broad impedance bandwidth as well as giving the designer more freedom in the choice of substrate. Efficient impedance matching can be obtained by proper adjustment of the feed line length and ratio of patch width to line width [43]. However, this approach is not without drawbacks. The thickness of the overall antenna rises may cause the spurious feed radiation, which can affect the purity of the radiation.

Moreover, the need for high-precision alignment of the two dielectric substrates makes the fabrication process much more complicated and presents challenges in the practical implementation of the process.

3.6. Analyzing Method

Among the various analytical approaches adopted for the evaluation and design of microstrip patch antennas, the most popular models are the Transmission Line Model, the Modified Wolf Model, and Full Wave Electromagnetic Models such as the Integral Equations Model and the Method of Moments (MoM) [44].

The conceptual simplicity and the ease of implementation of the Transmission Line Model (TLM) are well known and recognized. It provides good physical insight by envisioning the patch as a pair of radiating slots separated by a low impedance transmission line, and hence, easy estimation of input impedance, resonant frequency, and other key parameters can be easily done. However, it is somewhat inaccurate, especially with complex geometries, thick substrates, or higher-order modes, because a number of simplifying assumptions are made. The Modified Wolf Model makes some refinements to better approximate the performance characteristics in more realistic conditions, whereas the Full-Wave Models, though computationally expensive, offer high-fidelity analysis of Maxwell equations in a numerical form, e.g., using the Method of Moments, which is highly desirable in terms of providing high-fidelity simulations and more advanced designs [45].

The Transmission Line Model is selected as the primary design tool in the framework of this study due to the reason that the design model is computationally effective and is comparatively simple to conduct; consequently, the design model is applicable in the context of preliminary prototyping and parametric exploration of the patch structure. Additionally, the cavity model methods have been used to study the radiation behavior of microstrip patch antennas, both in their far-field patterns and array factor behavior. The cavity model provides more insight into the resonant modes and field distribution, particularly in the extension to an antenna array where mutual coupling and element spacing become important.

3.6.1. Transmission Line Modeling

The microstrip patch antenna can be well considered a resonant line structure in which the transverse field components are minimal and in which the electromagnetic fields are mostly varying along its longitudinal axis. This length is usually to be made about half the effective wavelength (λ/2) in the dielectric substrate. Such a structure does not produce radiation that is evenly distributed on the surface but concentrates instead on the fringing fields at the open-circuit edges of the patch, where it is the sharp discontinuity between the conductor and the surrounding medium that causes the stored energy to radiate into free space. Fringing fields are significant to the radiation characteristics of the antenna. Analytical models In simpler models, the microstrip patch is often analyzed as a pair of equivalent radiating slots with a distance L of the patch equal to the physical length of the patch in the X-Y plane. These slots are believed to be the major sources of radiation, and their characteristics can be studied to determine the important antenna characteristics, which include input impedance, radiation pattern, and gain [46]. This simplistic model gives good understanding of the resonant behavior and field distribution of microstrip antennas, particularly when operating in quasi-TEM mode, and this is used to build further modeling methods, including the transmission line model and cavity model.

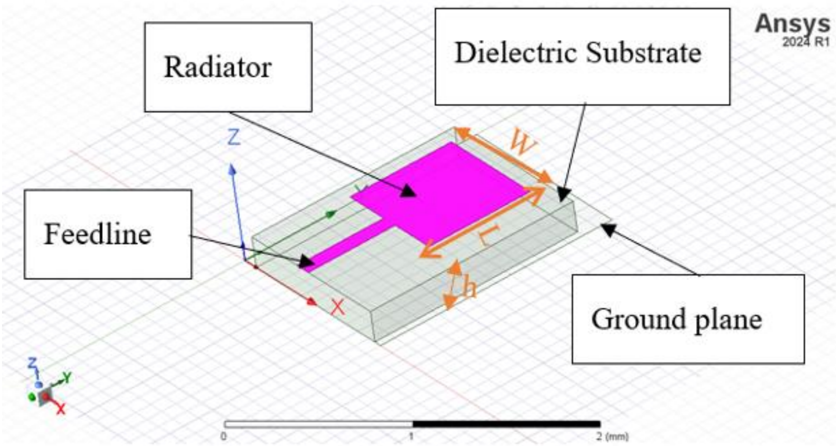

Figure 3.3. Microstrip Patch antenna[47]

The actual antenna length is not the same as the effective antenna length due to the fringing fields this is calculated by:

$$L = L_{eff} - 2\Delta L \tag{3.4}$$

In which ΔL (Delta L) is the added length whose value is a function of substrate height and dielectric constant. The parameter L in a rectangular patch antenna made of microstrip refers to the physical length of the patch, which is closely related to the effective wavelength (L eff) in the dielectric material. This convenient wavelength is based on electromagnetic characteristics of the substrate, and in particular, relative permittivity (εr) defines the resonant characteristics of the antenna. In the extension of the patch when open-circuit conditions apply (such as those at the edges), the voltage distribution lengthways has quite a different character: the amplitude of the voltage is greatest at the open-circuit edges and decreases toward the patch center. In the meantime, the change in electric field at the edges is not large, as the open-circuit terminations place constraints on the boundaries [48].

The fringing fields at the edges play a critical role in the radiation mechanism. Since the electric fields on opposite edges are anti-phase, the normal (perpendicular) field components would tend to cancel in the broadside direction—i.e., along the axis perpendicular to the patch surface. Nevertheless, the patch edges have tangential (horizontal) field components that are in coherence, and hence constructive interference creates a radiation orthogonal to the patch surface. The Planar Inverted-F Antenna (PIFA) is extensively utilized in the current wireless systems owing to the small size, low profile, and desirable impedance characteristics. Electromagnetically, the PIFA may be considered to be a quarter-wavelength resonant structure of the microstrip patch antenna, a patch antenna in which one side of the radiating element is shorted to the ground plane. This shorting effect is useful in reducing the resonant length of the antenna, and this enables the antenna to be miniaturized without loss of the radiation efficiency. The resonant frequency of the PIFA is largely determined by the effective electrical length of the radiating patch. It is also unlike ideal transmission lines in that the relative electric field at the edges of a microstrip structure propagates partially into the surrounding air, and the antenna therefore has a longer electrical length than its physical length. This effect is known as the fringing effect, and it has to be taken into consideration in proper antenna modeling. These radiating edges are well modeled as slots that are high-impedance terminations at transmission line extremities. The arrangement ensures that the structure becomes highly resonant, and the resonance condition is largely dependent on the length of the patch. An important aspect to point out is that depending on the fringing fields, the electromagnetic length of the patch (also called the effective length (Leff)) is a little longer than its physical length (L). This bond is crucial in the correct determination of the resonant frequency and maximization of the radiation properties of the antenna.

$$L_{eff} = \frac{c}{4 f_0 \sqrt{\epsilon_{eff}}} \tag{3.5}$$

where L_{eff} is the effective length of the antenna, ΔL is given by:

$$\Delta L = 0.412h \frac{(\in_{eff} + 0.3)(\frac{W}{h} + 0.264)}{\in_{eff} - 0.258)(\frac{W}{h} + 0.8)} \tag{3.6}$$

With reference to the design of the microstrip patch antenna, there are a few important geometrical and material parameters that determine the performance of the antenna. Of these, the effective dielectric constant of the substrate is denoted by εeff, the height (or thickness) of dielectric layer between the patch and the ground plane is denoted by h and the width of the rectangular-shaped radiating patch is denoted by W. One should know that the length of the patch is not the main contributor to radiation as it may be thought. Rather, the radiation is predominantly oriented within the width of the patch, i.e. along the two open-ended edges in perpendicular direction with the length. These edges are the radiating apertures most dominant, with fringing fields the most intense, and these meet the electromagnetic energy successfully into free space [49].

The radiation mechanism is caused because the tangential components of the electric field along the patch width are in-phase and cause constructive interference in the broadside direction (that is, normal to the patch surface). The width (w) becomes a very important parameter in defining the radiated power and directivity of the antenna. The equation of the radiated field element or the related design parameter in terms of patch width can be expressed as:

$$W = \frac{c}{2 f_0 \frac{\sqrt{\varepsilon r + 1}}{2}} \tag{3.7}$$

Where:

- W is the optimal patch width for efficient radiation,
- c is the speed of light in vacuum,
- f0 is the resonant frequenc, and
- εr is the relative permittivity of the substrate.

A patch width is described in this equation as the dominating factor in the behavior of the antenna, such as the impedance, bandwidth, and radiation efficiency, and it should be chosen with care in the design process to achieve the best antenna performance. An important parameter in the analysis and design of the patch antenna made of microstrip is the effective dielectric constant (denoted εeff). It is the perceived permittivity of the electromagnetic wave as it passes through the microstrip structure, comprising the dielectric substrate material as well as the surrounding air [50].

Because of the existence of the fringing fields, the electromagnetic fields are outside the physical confines of the dielectric and the surrounding air, and the wave is no longer solely contained in the substrate. As a result, a part of the field spreads via air, the relative permittivity (εr) is 1. The effective dielectric constant thus always has a lesser value than the actual relative permittivity of the substrate, since the wave passes effectively through a composite matter of air and dielectric. This diffusion of dielectric environments decreases the average permittivity felt by the wave, and the effective dielectric constant is empirically obtained as follows:

$$\epsilon_{eff} = \frac{\varepsilon r+1}{2} + \frac{\varepsilon r-1}{2}[1+\frac{12W}{h}]^{(-\frac{1}{2})} .... for \frac{W}{h} \geq 1 \tag{3.8}$$

Where:

- ϵ_{eff} is the effective dielectric constant,
- εr is the relative permittivity of the substrate material,
- h is the height (thickness) of the dielectric substrate, and
- W is the width of microstrip patch.

It is a mathematical expression of great essence since it represents the distribution of electromagnetic fields within the dielectric substrate and within the air interface. This kind of interaction between fields within a field takes place since the lines of the electric field are not completely contained within the dielectric medium but extend to the surrounding air and create fringing fields. Consequently, the effective dielectric constant (ε) is a weighted average, which is on account of the electromagnetic behavior of this hybrid medium [51].

This useful dielectric constant is vital in the correct rating of some essential performance parameters of microstrip antennas and transmission lines such as the phase velocity of propagation, the guided wavelength (λg), and the resonant frequency. These are the main parameters in the design and optimization of high-frequency circuits and radiating structures. Considering the effect that substrate geometry and dielectric properties have on signal propagation, the effects they have on the characteristic impedance (Zo) of microstrip transmission lines are also necessary. The impedance is another crucial parameter, and it should be paired with the source as well as the load to allow optimum power transfer as well as minimum reflection [52]. A typical impedance of a microstrip line that is based on a derivation of εeff, substrate size, and patch width is usually expressed as:

$$Z_0 = \frac{\frac{120\pi}{\sqrt{\epsilon_{eff}}}}{\frac{W}{h}1.393 + 0.667\ln\left(\frac{W}{h} + 1.444\right)} \dots\dots\dots\dots\dots for\ \frac{W}{h} \geq 1 \tag{3.9}$$

These models provide good modeling of impedance properties, which enables engineers to get the best performance out of microwave circuits, RF modules, and antenna feeding networks. The second case occurs when relative to the height of the substrate (h), the ratio of patch width (W) and substrate height (h) is below or equal to one (i.e. W/h 1). The condition normally arises in the microstrip designs when the patch is narrow and/or the substrate is relatively thick. In this situation, the electromagnetic distribution differs dramatically from situations where the width is significantly larger than the height, and thus the fringing effect and air-dielectric interaction play a more important role. In such a structure, the effective dielectric constant that defines the behavior of propagating waves on the substrate-air interface has to be calculated with the help of a certain empirical formula that takes into consideration the increased extension of the field to the surrounding air. The value is important in the determination of the guided wavelength, velocity of phase, and resonant frequency of the antenna system with precision [53]. The effective dielectric constant here is determined by use of the formula below:

$$\epsilon_{eff} = \frac{\varepsilon r + 1}{2} + \frac{\varepsilon r - 1}{2}\left[1 + \frac{12W}{h}\right]^{\frac{-1}{2}} + \frac{1}{25(1 - \frac{W}{h})} \dots\dots\dots\dots\dots\dots for\ \frac{W}{h} \leq 1 \tag{3.10}$$

Where:

- εeff is the effective dielectric constant,
- εr is the relative permittivity of the substrate,
- h is the height (thickness) of the dielectric substrate, and
- W is the width of the microstrip patch.

This is a proper description of the electromagnetic environment in the antenna structure, particularly in structures where the aspect ratio (W/h) is in this range. It allows accurate modeling and optimization of microstrip components of high frequency, such as transmission lines, filters, and radiating components. After having established the effective dielectric constant (εeff) of the dielectric substrate and the surrounding air on the propagation properties, the next parameter of significance that is to be considered is the characteristic impedance (Z_0) of the microstrip transmission line. It is an impedance that determines the dependence of voltage and current along the transmission line and is a key to the effective transfer of power, impedance matching, and minimal signal reflection between communicating RF and microwave devices [54]. How the electric field spreads both in and above the substrate is the effective dielectric constant, which directly affects the propagation velocity and mechanisms of impedance behavior of the line. The characteristic impedance can be determined using εff and customized equations that take into account the aspect ratio (W/h) of the patch and substrate, where W is the width of the microstrip conductor and h is the height of the substrate. In the situation in which the ratio W/h < 1, the characteristic impedance can be established in the form of an empirical expression:

$$Z_0 = \frac{60}{\sqrt{\in_{eff}}} \ln\left[\frac{8h}{W} + 0.25\frac{W}{h}\right] \ldots\ldots\ldots\ldots\ldots \mathit{for}\ \frac{W}{h} \le 1 \tag{3.11}$$

This is a formula that is accurate in estimating the transmission line impedance by taking into consideration both the geometry of the microstrip and the effective electromagnetic environment formed by the substrate-air interface. These types of calculations play an important role in the design of the high-performance RF systems where loss reduction and maximized efficiency of the bandwidth with respect to the impedance control are crucial. The actual physical length of a rectangular microstrip patch antenna is a basic design parameter that directly affects the resonant frequency and general performance of the patch antenna. This wavelength governs the resonance condition of the half wavelength of the antenna at which the antenna radiates electromagnetic energy most effectively [55][52].

But, due to the existence of fringing fields in which the electromagnetic waves are somewhat beyond the physical edges of the patch, the effective electrical length of the antenna is a little longer than its physical counterpart. This means the fringing effect has to be added to the length (L) so that the actual length (L) is obtained. So, the actual length of the rectangular patch is based on the formula of equation 3.4. This equation is used to have the correct dimensions of the patch to support the dominant mode of TMMN, which is the most used mode in rectangular microstrip antennas. Making this calculation is crucial to the exact engineering of small, high-performance microstrip radiators, as the antenna can be programmed to work in a given frequency by thoughtfully choosing L [56].

Although the transmission line model of microstrip patch antennas is mathematically calculated based on the assumption that the ground plane is infinitely large, the ideal condition in this context is impossible to achieve in practice when making the antenna. In real-world applications, because of physical and production limitations, designers have to deal with ground planes of finite extent. However, in order to have the radiation properties of the antenna, as well as impedance behavior and field distribution, be closer to those produced by the infinity ground assumption, certain rules should be observed in the determination of the ground plane size. It is well known that the dimensions of the ground plane must be larger than the patch by a factor of at least six times the dielectric substrate thickness (6h) all around. This extra margin will ensure the reduction of edge diffraction effects, the avoidance of surface wave excitation, and that the radiation patterns remain constant. With this rule of thumb, the finite ground plane will be able to perform well in the simulation, as the electromagnetic environment of an infinite plane can be effectively simulated, which implies a consistency in the accuracy of the simulation and the performance of the model in the real world.

The ground plane area is critical in the radiation efficiency, band of operation, bandwidth, and front-to-back ratio of PIFA. The large size of the ground plane improves radiation stability as well as minimizes losses to surface waves, but a small size of the ground plane can cause distortion of the radiation pattern and impedance mismatch. It depends on the geometry of the antenna and the substrate, which has an impact on the characteristic impedance Zo of the feeding structure and can be estimated by the microstrip transmission line theory. Impedance matching is necessary to reduce the return loss and have a Voltage Standing Wave Ratio (VSWR) of near unity throughout the desired operating band. Based on that, the ground plane length (Lg) can be determined by the following expression:

$$L_g = 6h + L \quad (3.12)$$

Where:

- Lg is the total length of the ground plane,
- L is the physical length of the patch, and
- h is the thickness (height) of the dielectric substrate.

This is a formula that accommodates adequate ground plane extension to maintain correct wave propagation, impedance equality, and radioactivity that are extremely important in the correct operation of microstrip antennas during application. As a part of the design principles that make a microstrip antenna act as theoretically predicted, the width of the ground plane should be considered as well. Similarly to the extension of the ground plane beyond the patch needed to reduce the effect of the edges and retain the radiation characteristics, the width needs to be similarly considered. In order to adequately model the conditions of an infinite ground plane as in the case of the transmission line model, it is advisable that the ground plane be extended beyond the patch width by a distance that will absorb and dampen both spurious surface waves and unwanted edge radiation. It has been empirically indicated, and practical design experience indicates, that an extension of the ground plane on either side by about 6 times the substrate thickness (6h) yields an optimum of performance and size [57]. Therefore, the width of the ground plane (Wg) can be determined using the following expression:

$$W_g = 6h + W \tag{3.13}$$

Where:

- Wg is the area width of ground plane,
- W is the width of the patch which is a rectangle, and
- h is the thickness of the dielectric substrate.

This design rule will ensure that the ground plane is sufficiently large to reduce electromagnetic interference, to maintain uniform field distribution, and to care for effective radiation, which will enable the antenna to work in a way that is closer to the theoretical predictions and simulation results.

3.5.2. Cavity Modeling

The area surrounding the radiating patch of the antenna and the ground plane is conceptually represented in the cavity model method of the analysis of rectangular patch antennas of microstrip as a resonant cavity. This theoretical approach is more rigorous in the electromagnetic behavior of the antenna structure and especially effective in the prediction of the radiation patterns, the resonant frequencies, and quality factors [58][59]. The fact that patch antennas are often studied in terms of cavity model theory, the proposed PIFA structure is considered based on the standard rectangular patch approximations that can be applied to this geometry. Through this description, the upper and bottom surfaces of the cavity are characterized by perfect electric conductors (PEC), the patch on the upper surface, and the ground plane on the bottom surface. In the meantime, the sides of the cavity, which are exposed to the surrounding medium, are modeled as perfect magnetic walls (PMCs). These are also magnetic walls, which are used to model the fringing field-based boundary conditions, which are out of the physical boundaries of the patch. Consequently, the cavity will be virtually closed on the electric boundaries on the top and bottom and the magnetic boundaries on the sides.Because the antenna is etched in a thin dielectric substrate and the substrate height (h) is significantly smaller than the guided wavelength (λg) of the cavity, the electromagnetic fields are typically uniform in the Z-axis (vertical) direction. This is why the assumption of a quasi-TMmn mode can be used when the field variations are mainly in the horizontal (X-Y) plane and the dependence in the vertical direction can be disregarded. This is a simplified but effective modeling procedure that enables designers to estimate the resonant modes, the most significant ones being the TMmn mode, and understand the performance of the antenna, including such parameters as input impedance, radiated power, and bandwidth.

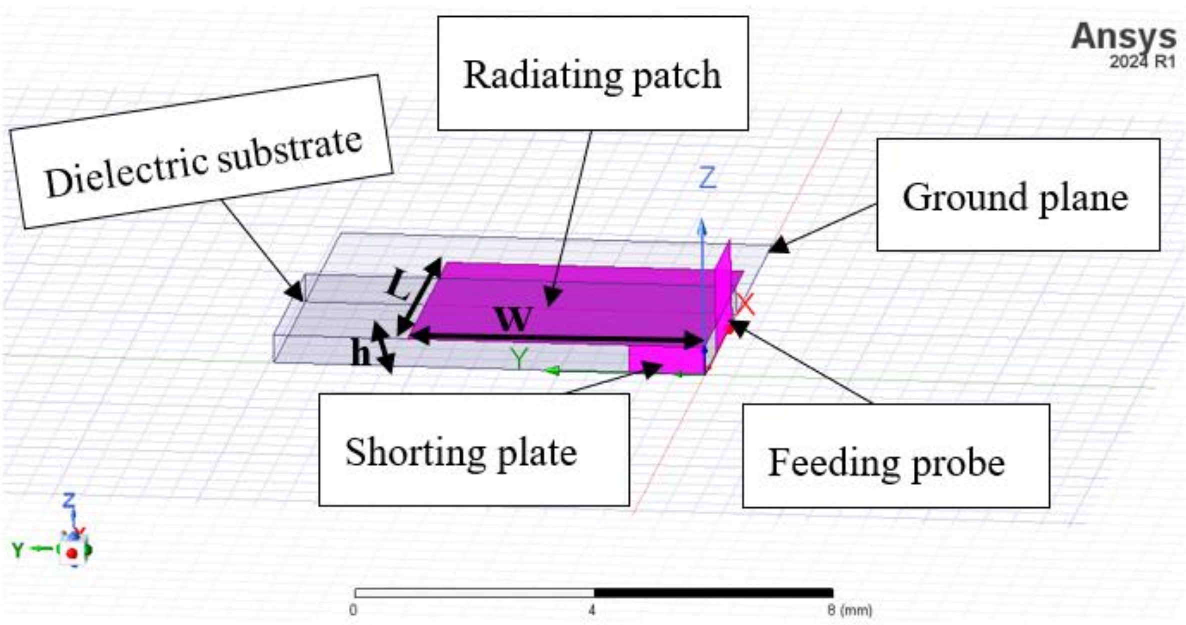

Figure 3.4 PIFA antenna structure

In the vertical dimension, the influence of the dielectric substrate on the propagation of the electromagnetic wave is insignificant when the height of the dielectric substrate is much less than the operating wavelength. Consequently, the distribution of fields is mostly independent of the height of the substrate. In such a case, the electromagnetic action is mostly restricted in the plane of the substrate. Thus, there are only three field components of importance: the component of the electric field oriented along the Z-axis and the components of the magnetic field oriented along the X-axis and Y-axis. The given field arrangement exemplifies the quasi-TMmn characteristics of the wave propagation in these microstrip constructions, the changes in vertical fields of which are small because of the thinness of the dielectric layer [60].

$$H_z = 0 \tag{3.14}$$

$$E_x = 0 \tag{3.15}$$

$$E_y = 0 \tag{3.16}$$

The Z-direction electric field that describes the vertical distribution of the electric potential in the system can be analytically described by the following expression:

$$Ez = E_0 \cos(\frac{m\pi x}{L}) \cos(\frac{n\pi y}{W}) \tag{3.17}$$

Where Ez electric field is in the Z-direction and the dominant PIFA mode (TM_{10}):

$$E_{z(x,y)} = E_0 \cos(\frac{\pi x}{L_{eff}}) \tag{3.18}$$

Corresponding magnetic field components

$$H_x = (\frac{-j}{\omega\mu} \frac{\partial Ez}{\partial y}) \tag{3.19}$$

And magnetic fields across Y-directions expressed as:

$$H_y = (\frac{-j}{\omega\mu} \frac{\partial Ez}{\partial x}) \tag{3.20}$$

3.6.2. Array Factor

The total radiation pattern produced by an antenna array can be well calculated as the product of two basic components: the element factor, which represents the radiation pattern of a single radiating element, and the array factor, which describes the effect of the spatial geometry, relative amplitude, and phase of all the elements in the array. This multiplicative relationship gives a strong structure in the analysis and synthesis of the overall radiation behavior of the antenna array [61].

$$\frac{e^{-jkr}}{4\pi r} \tag{3.21}$$

Thus, the amount of radiation produced in such a situation is the same in all directions, implying an isotropic radiation pattern. The radiating element, in this instance, is not biased towards a given direction; hence, the power distribution throughout the spatial domain is even. The unnormalized array factor of such a configuration can therefore be written mathematically as:

$$AF = 1 \tag{3.22}$$

We shall now consider the linear array setup, which is intended to accept an incident plane wave bouncing off an angle θ of the plane of the array, with respect to the array normal. Although all the antenna elements in the array are excited in a uniform manner with a unity amplitude, the propagation paths of the elements are different, which establishes a difference in the phases of the elements as they have varying angular incidences. The reason why such phase shifts occur is that the wavefront arrives to each element at a slightly different time. Consequently, the array factor, which describes the aggregate radiation or reception shape of the array, may be expressed to the effect that:

$$AF = e^{j\varepsilon 0} + e^{j\varepsilon 1} + e^{j\varepsilon 2} + \ldots\ldots\ldots\ldots\ldots\ldots e^{j\varepsilon N-1} \tag{3.23}$$

3.7. Parameters that Measure the Performance of Antenna

Parameters used to measure the performance of the antenna. There are numerous critical parameters that are used to test and prove the performance of the designed antenna system. These performance metrics are: Return Loss (efficiency of power transmission between the source and the antenna), Bandwidth (maximum and minimum frequencies over which the antenna can successfully operate), Gain (capability of the antenna to direct energy in one direction), Directivity (relationship of how well the radiated energy is concentrated around one direction to that of an isotropic source), and Beamwidth (angular width of the main lobe of the radiation pattern). The combination of these parameters is a full picture of the efficiency of the functioning of the antenna, the characteristic of its radiation, and its efficiency in the field.

3.7.1. Return Loss

Return Loss (RL) is a fundamental and highly significant parameter in the evaluation and testing of antenna performance. It is an important measure of matching impedance between the antenna and its transmission line and directly proportional to the Maximum Power Transfer Theorem, which states that the best power transfer is where the load impedance is equal to that of the source. Return loss basically measures the efficiency of the antenna in the usage of power provided by the source without being reflected by the antenna. A large return loss means that the impedance matching is good and the power is reflected in small quantities, hence showing that the transmitter is delivering power to the antenna efficiently. Return loss Mathematically, return loss is given by the logarithmic ratio of the power incident on the antenna input side to the reflected power. It is normally measured in decibels (dB), where bigger negative units reflect high performance [62].

3.7.2. S-parameters

In microwave engineering S-parameters (scattering parameters) are important in characterization and analysis of the behavior of high-frequency electrical networks. Such parameters are used to characterize radio frequency (RF) signal propagation within a multi-port network and are important to characterize important performance parameters that include Voltage Standing Wave Ratio (VSWR), Return Loss, Gain, Isolation, and others [63][47].

S-parameters are important parameters that fundamentally define the relationship between the input and output of different ports in a network and enable engineers to gain a better understanding of the extent to which the input signal is sent to, reflected by, or lost by a port. Amongst them, S_{11} and S_{22} are the input and output reflection coefficients, respectively, which is the power reflected by each port due to impedance mismatch. S_{21} is usually used to represent the forward transmission coefficient, which is the value of power or gain passing between port 1 and port 2. On the other hand, S_{12} is the reverse transmission coefficient, which is a measure of isolation, or the power passing in the opposite direction from port 2 to port 1. In particular, S11 is also called return loss, which is a key measure of the efficiency of power delivery to a device or an antenna. It measures the ratio of the reflected incident power to the incident power to the source. An S11 value of 0 dB would mean that 100% of the power is reflected, that is, no power is passed through the antenna, which is an indication of a full impedance mismatch. The greatest amount of negative S11 should preferably be as negative as possible (e.g., -10 dB or less), which represents efficient transfer of power and minimal reflected power.

3.7.3. Bandwidth

Bandwidth of antenna is the frequency range within which the antenna can perform satisfactorily in terms of particular electrical and radiation properties. In this operating frequency range, gain, radiation pattern, and Voltage Standing Wave Ratio (VSWR) will be maintained within acceptable and pre-determined limits, making sure that electromagnetic signals in terms of transmission and reception will occur successfully. [64].

This bandwidth is what determines the frequency range in which the antenna is efficient in conducting power in and out of the transmission line to free space where there is a minimum amount of reflection and maximum radiation efficiency. The bandwidth (BW) is calculated mathematically by the difference between upper cutoff frequency (FH) and lower cutoff frequency (FL) as presented in the following equation:

$$BW = FH - FL \tag{3.24}$$

A bigger bandwidth means that the antenna can be useful with a wider range of frequencies and stay with similar operation, which is an attractive quality in wideband communication system and multiband communication system.

3.7.4. **Gain** [65], [66]

The gain of an antenna is a basic parameter that measures the capacity of an antenna to radiate power to a preferred direction over an ideal isotropic radiator that radiates the same amount of power in all directions. In particular, it is the ratio between the power emitted (or received) by the antenna in the direction where it emits (or receives) the highest radiation and that which an isotropic source would emit (or receive) with the same input level of power. Antenna gain, in a word, captures the effectiveness of an antenna concerned with directing energy. Mathematically

$$G = \eta D \tag{3.25}$$

Where: η = efficiency D = Directivity. In terms of power:

$$G(\theta,\phi) = \frac{4\pi U(\theta,\phi)}{P_{input}} \tag{3.26}$$

Where: U = radiation intensity, Pinput = input power. Unit: dBi

In comparison to directivity, which only indicates the concentration of the radiation with no consideration of losses, gain takes into consideration the efficiency of the antenna, hence coming up with a more realistic description of the performance of the antenna. This is why gain is more often used in the specifications of an antenna, as it is a measure of not only the directional properties of a given system but also the dielectric, conduction, and impedance losses that are intrinsic to a particular system [67].

For instance, the gain of an antenna of 3 dB actually radiates twice the power in a specific direction as a hypothetical lossless isotropic antenna fed with the same amount of power. In this context, the lossless term means that the antenna is 100% efficient (or 0 dB loss), or all the power input is converted to radiated power. Likewise, an equivalent gain of 3 dB, directional antenna would receive twice as much power as an equivalent, lossless, isotropic antenna at the same point in the air. This increased reception ability puts antenna gain as an important parameter in the transmission and reception both in long-range wireless communication and radar systems.

3.7.5. Directivity

Directivity refers to the ability of a given antenna to focus radiated electromagnetic energy in a specific direction as compared to an isotropic radiator. The ratio of the radiation intensity in a given direction to the average radiation intensity in all directions in space is called directivity. Where U (θ, ϕ) is the intensity of the radiation and Prad is the total radiated energy, then the directivity function can be represented as:

$$D(\theta,\phi) = \frac{4\pi U(\theta,\phi)}{P_{rad}} \tag{3.27}$$

In which the value of 4π is the solid angle sum of three-dimensional space. The peak directivity D_0 is in the direction of the maximum radiation intensity U_{max} and it is denoted by:

$$D_0 = \frac{4\pi U_{mx}}{\mathrm{P}_{rad}} \tag{3.28}$$

Alternatively, directivity may also be expressed in terms of beam solid angle Ω_A as:

$$D_0 = \frac{4\pi}{Q_A} \tag{3.29}$$

Where narrower beams (smaller ΩA) result in greater directivity. For millimeter-wave massive MIMO arrays at 28 GHz, more radiating elements decrease beamwidth and therefore increase directivity, which is required in 5G systems to do spatial filtering and interference suppression.

3.7.6. Radiation efficiency

Productive capability or effectiveness is called efficiency. In an antenna system, radiation efficiency lists the ability of the accepted input power to be changed into radiated electromagnetic power. Conductor losses, losses as a result of dielectric, and loss as a result of surface waves are such that not all the power supplied is radiated. In the event that Prad is accepted input power and Prad is the radiated power, then the radiation efficiency is:

$$\eta = \frac{P_{rad}}{P_{input}} \tag{3.30}$$

At 28 GHz, the skin effect becomes a significant conductor loss, and the loss tangent of dielectrics is important, and therefore optimization of efficiency is vital in PIFA-based massive MIMO arrays. Maximum efficiency means that the gain realized is very close to the theoretical directivity.

3.7.7. Radiation Pattern

A radiation Pattern is a spatial distribution, and it is the angular variation of an antenna with respect to the power of the emitted electromagnetic field or radiated power. The electric field of an antenna in the far-field region can be given as:

$$F(\theta,\phi) = \frac{E(\theta,\phi)}{E_{\max}} e^{-jkr} \tag{3.31}$$

measures the angular dependence of the field, and k is the wave number. The normalized field pattern is usually used to represent the radiation pattern.

$$F(\theta,\phi) = \frac{E(\theta,\phi)}{E_{\max}} \tag{3.32}$$

By the pattern of power $P(\theta,\phi) = |F(\theta,\phi)|^2$ which gives the allocation of power in space. Radiation patterns can be displayed in three dimensional or in two major cuts including E-plane and H-plane. The radiation pattern of massive MIMO PIFA arrays at 28 GHz becomes more directional with the size of the array and it develops narrow beams that can be used in beamforming and spatial multiplexing in 5G wireless communication networks.

3.8. Polarizations

The polarization of the emitted electromagnetic wave of the antenna is referred to as antenna polarization. A better way of putting it is that it defines the position and time character of the electric field vector of the emitted wave at a point of space. The transmitting antenna polarization and the receiving antenna polarization should be the same in order to be efficient in regards to energy transfer in the wireless systems [67] [68].

Polarization is in essence an attribute of the electromagnetic wave and is how the intensity and direction of the electric field vector vary. In simpler terms, it means the direction and signal of the electric field at a particular point of the wave path. According to this behavior, polarization is divided into 3 broad categories, namely, linear, circular, and elliptical polarization. The electric field vector in the linear polarization is limited to a plane of propagation. When the field is perpendicular to the earth's surface, the antenna is vertically polarized; when the field is parallel to the earth, it is horizontally polarized. This form of polarization is normally applied in radio communication systems on earth. Circular polarization, on the other hand, is characterized by a rotation in the direction of wave propagation of the electric field vector in a circular manner. This implies that the wave disperses power in every direction of the wave's vertical, horizontal, and intermediate planes [69].

Within one wave period, the electric field rotates 360º, and circular polarization is especially beneficial in situations where the antenna relative orientation between transmitters and receivers can change, such as in satellite and mobile communications. Lastly, more general is elliptical polarization, where the electric field vector traces an elliptical path, a linear and circular polarization combination. The type of polarization that is selected in an antenna system is indeed a decisive factor in how that antenna system may perform, as well as suit and conduct itself in different wireless conditions.

3.9. MIMO Metrics [70]

MIMO performance metrics are quantitative parameters that are used to assess how effective multiple antenna elements operating as a system in a MIMO communication system are compared to traditional single antenna performance metrics, such as return loss or gain. MIMO systems employ spatial diversity and parallel paths of data to enhance their reliability and spectral efficiency and, therefore, require special measures to investigate inter-element correlation, diversity performance, impedance interaction, and capacity preservation.

3.9.1. Envelop Correlation coefficient (ECC)

ECC is a basic MIMO performance measure that determines the level of correlation between the radiation patterns of various antenna components and hence depicts how independently the antenna ports can be utilized in a multipath scenario. The low value of ECC suggests uncorrelated fading channels, and this is what is needed to get high diversity performance and channel capacity. ECC is best expressed in the far-field radiation patterns, and this is:

$$ECC_{ij} = \frac{\left| \iint \overrightarrow{F_i}(\theta,\phi).\overrightarrow{F_j}(\theta,\phi) d\Omega \right|^2}{\left(\iint |\overrightarrow{F_i}|^2 \, d\Omega \right)\left(\iint |\overrightarrow{F_j}|^2 \, d\Omega \right)}, \tag{3.33}$$

Where $\overrightarrow{F_i}$ and $\overrightarrow{F_j}$ represent the far-field radiation vectors the i^{th} , and j^{th} of the and antenna elements, respectively. As a practical approximation, ECC has been approximated in a two-port system in S-parameters as:

$$ECC = \frac{\left| S^*_{11} + S^*_{12} + S^*_{21} S_{22} \right|^2}{(1 - |S_{11}|^2 - |S_{21}|^2)(1 - |S_{22}|^2 - |S_{12}|^2)} . \tag{3.34}$$

Ideally, ECC tends to zero, which implies the existence of highly independent radiation properties, low mutual coupling and high diversity capability of MIMO antenna systems.

3.9.2. Diversity Gain (DG)

DG is the signal reliability, which can be improved through the use of several antenna elements, which reduce the multipath fading in wireless communication systems. It measures the efficiency of the spatial diversity in terms of increasing the link robustness over the single-antenna setup. Diversity gain is dependent on ECC and is usually given as:

$$DG = 10\sqrt{1-(ECC)^2} \quad (3.35)$$

According to this equation, the greater the correlation between the elements in the antenna, the less diversity gain there is. ECC approaches zero, meaning that DG approaches its theoretical maximum of 10 dB, which is ideal diversity performance. Thus, DG is a useful measure of the effectiveness of MIMO antenna systems to fight against fading and to sustain stable communication channels in the conditions of multipath propagation.

3.9.3. Channel capacity loss (CCL)

Channel capacity loss is a measure of the degradation of theoretical MIMO channel capacity by correlation and mutual coupling of antenna elements. The main goal of MIMO technology is to enhance spectral performance by parallel spatial data streams; hence, any correlation between ports decreases the attainable Shannon capacity. The CCL is then computed by taking the determinant of the S-parameter correlation matrix, and this is given by:

$$CCL = -\log_2(\det(\Psi)), \quad (3.36)$$

where Ψ is the correlation matrix defined for a two-port system as:

$$\Psi = \begin{bmatrix} 1-|S_{11}|^2 - |S_{21}|^2 & -(S^*_{11}S_{12} + S^*_{12} + S^*_{21}S_{22} \\ -(S^*_{22}S_{21} + S^*_{12}S_{11}) & 1-|S_{22}|^2 - |S_{12}|^2 \end{bmatrix} \quad (3.37)$$

Lower CCL values demonstrate that there is little capacity degradation and spectral efficiency is preserved better. CCL is generally kept below 0.4 bits/s/Hz in high-performance MIMO systems in order to achieve effective transmission of multi-streams.

3.9.4. Total Active Reflection Coefficient (TARC)

The total active reflection coefficient (TARC) is a MIMO-specific quantity, and it can be used to assess the maximum performance of a multi-port antenna system with respect to the reflection of an antenna during simultaneous excitation of all the ports with arbitrary phase shifts. TARC takes into account mutual coupling and inter-port interaction of realistic multi-port operation, unlike the more traditional method of return loss (S11) that only considers a single active port at a time. The general expression for an N-port system is:

$$TARC = \sqrt{\frac{\sum_{i=1}^{N} |b_i|^2}{\sum_{i=1}^{N} |a_i|^2}}, \tag{3.38}$$

Where a_i and b_i represent the incident and reflected waves at the i^{th} port, respectively. In logarithmic form, and is expressed as:

$$TARC_{dB} = 20\log_{10}(TARC) \tag{3.39}$$

A lower TARC value corresponds to efficient multi-port impedance matching with minimal reflected power during simultaneous excitation which is an important parameter to assess the practical MIMO antenna performance in high-capacity wireless systems.[71]

CHAPTER FOUR

ANTENNA DESIGN

4.1. Introductions

This chapter presents the design and development of the proposed Planar Inverted-F Antenna (PIFA) array at the resonance frequency of the 28 GHz mm-wave 5G wireless communication system. The design technique, structural arrangement, and optimization of parameters of the antenna elements as adopted in the realization of the desired radiation properties to suit the next generation of wireless networks are described in the chapter. The antenna is designed based on a Duroid dielectric substrate with a relative permittivity of 2.2 that is chosen because of low dielectric loss and applicability to high-frequency millimeter-wave operations. The radiating patch in the proposed structure is placed between the dielectric substrate and the ground plain to achieve the PIFA structure. The chapter also details the design process that involves the step-by-step development of the single PIFA element, then the development of antenna array forms, which include 1×2, 4×4, and 4×5 massive MIMO arrays, in order to improve the performance of the radiation.

Table 4.1. Common specifications for Smart patch antenna setup

Items	Specification	Amount
Frequency	Hz	28 GHz
Copper sheet	mm	0.01mm
Impedance	Ohm	50
Duroid(tm)	Permittivity	2.2
	Permeability	1
	Dielectric loss tangent	0.0009
	Magnetic loss tangent	0

4.2. Single Element PIFA Design Specifications and Calculation

In the design of this antenna, design parameters are concerned as derived as given below, some of which, such as frequency of operation, substrate material, and height of substrate used, are affected by choice and need to attain a good level of base performance. In PIFA, current travels from the feed pin across the patch and down, shorting to ground. On the shorting side, voltage is zero, but current is maximum, and at the open edge, voltage is maximum and current is zero. Thus, the effective electrical length is approximately λ/4.

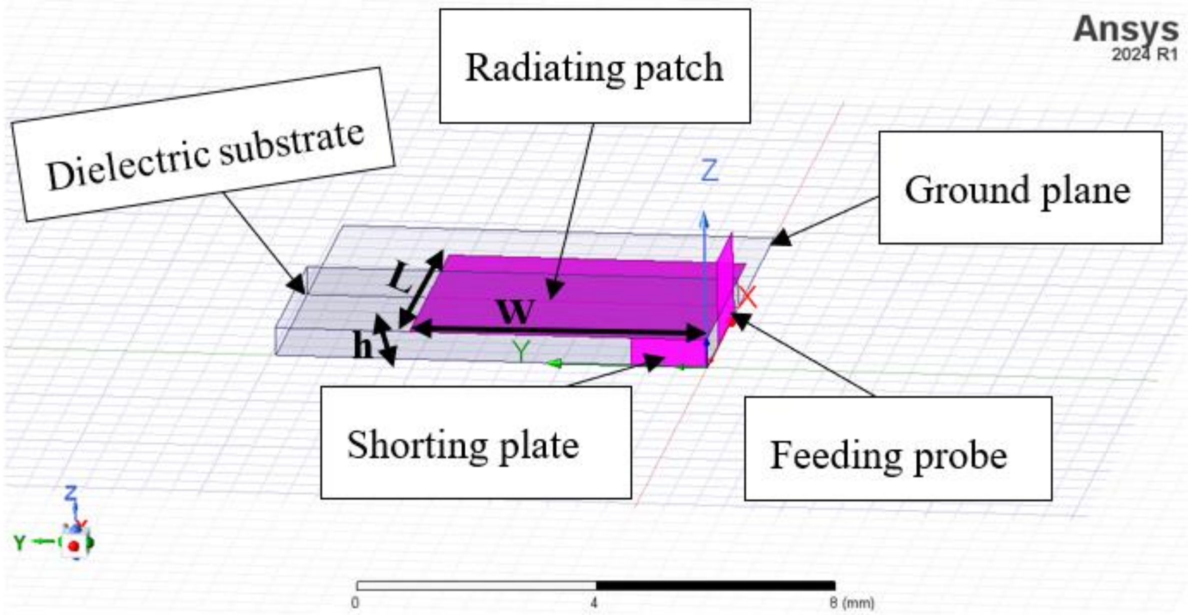

Figure 4.1. Single Element of PIFA structure

4.2.1. Design Procedures

Step 1. Calculation of the wavelength:

$$\lambda = \frac{c}{f} \tag{4.1}$$

$$\lambda = \frac{3\times 10^{8} m/s}{28\times 10^{9}} \qquad \lambda = 10.71mm$$

Step 2: Calculation of the width of Patch: From equation 3.7

$$W = \frac{c}{2f_0\frac{\sqrt{\varepsilon r+1}}{2}} = 0.004235\text{m} \qquad \text{W} = 4.235\text{mm}$$

Step 3: Calculation of the Height:

Where **‘h’** is Height;

The parameter requirements of various antennas might be different; some antennas might want the height of the substrate to get a wide bandwidth. Some antennas might focus on the directivity; in this case, the height or the thickness is better to be less to achieve maximum radiation. This is in consideration of the fringing effect.

$$h = \frac{c}{20 f \sqrt{\varepsilon r - 1}} \tag{4.2}$$

$$h = \frac{3\times10^{8} m/s}{20\times28\times10^{9}\sqrt{2.2-1}} = 0.000489m \qquad h = 0.489mm$$

Step 4: Calculation of effective dielectric constant: from equation 3.8

$$\epsilon_{eff} = \frac{\varepsilon r+1}{2} + \frac{\varepsilon r-1}{2}[1+\frac{12h}{W}]^{-1/2} = 1.0999 \qquad \in_{eff} = 1.0999$$

Step 5: Calculation of the effective length (L_{eff}): from equation 3.5

$$L_{eff} = \frac{c}{4 f_0 \sqrt{\epsilon_{eff}}} = 0.0026786 \qquad L_{eff} = 2.6786mm$$

Due to fringing fields, the additional length from equation 3.6

$$\Delta L = 0.412h \frac{(\in_{eff} + 0.3)(\frac{W}{h} + 0.264)}{(\in_{eff} - 0.258)(\frac{W}{h} + 0.8)} = 0.316\text{mm} \qquad \Delta L = 0.316mm$$

Step 6: Calculation of the actual length of the patch (L): from equation 3.4

$$L = L_{eff} - 2\Delta L = 2.0466 \qquad L = 2.0466mm$$

Step: 7: Calculation of the ground plane dimensions (Lg and Wg):

The transmission line model can be applied only on infinite ground planes. But, when practical value is taken, it is necessary to possess a finite ground plane. Therefore, ground plane dimensions in this design will be provided as follows:

Step 7.1. Length of Ground Plane: from equation 3.12

$L_g = 6h + L = 4.856$ Lg = 4.856

Step 7.2. Width of Ground Plane: from equation 3.13

$W_g = 6h + W = 7.169$ $Wg = 7.169$

Step 8: Calculation for Shorting Pin dimensions:

Step 8.1. Width of shorting Pin: there is no strict formula, but commonly:

$$Ws = 0.005\lambda_0 \ to \ 0.1\lambda_0 \ or \ Ws \approx 0.001 - 3 \ mm \quad \text{for mm-wave designs.} \tag{4.3}$$

$Thus, \ Ws = 0.09$

Step 8.2. Length of shorting pin: length of shorting pin equal to height, because it connects patch to ground.

$$Ls = h \tag{4.4}$$

Where h = 0.489mm thus, Ls = 0.489mm

Step 8.3. Feeding line or feed probe: feed probe dimensions normally selected in terms of realistic coax. Typical rule:

$$r = 0.01\lambda_0 \ to \ 0.15\lambda_0 \tag{4.5}$$

$Thus \ \mathrm{W}f = 1.6mm$

Table 4.1. Single PIFA Antenna design parameters

Antenna design parameters are given in the table below

Antenna Type	Lp	Wp	W_{feed}	Height of Substrate	Ws	Lg	Wg	Substrate Type	f_0
Single PIFA	2.0466 mm	4.235 mm	1.6mm	0.489 mm	1.3 mm	5.4 mm	7.414 mm	Duroid	28 GHz

4.3. Design 1x2 PIFA

Array configuration is associated with element spacing and element coupling, which is important for MIMO performance. This is the element spacing determined by distance (d).

Step 1: Element spacing

$$d = \frac{\lambda}{2} \tag{4.6}$$

$d = \frac{10.71mm}{2}$ $d = 5.355mm$

This spacing is chosen so as to maintain grating lobes at a minimum while keeping the array compact. We know that at the frequency of mm-Wave, the mutual coupling between elements has a significant effect on the radiation pattern and impedance. Advanced decoupling techniques (i.e., deflated ground structures and neutralization lines) are also recommended but are beyond the range of this initial design.

Step 2: Array Geometry

The 1x2 arrangement is used to have two element PIFAs on the X-axis having the same dimensions as the single element but shared from a common ground plane. The 1x2 configuration is where PIFA elements (two elements) of the Y-axis are of the same dimensions but share a common ground plane with the single element.

Table 4.2. 1x2 PIFA Antenna design parameters

Antenna Type	L_P	Wp	W_{feed}	Height of Substrate	Ws	Lg	Wg	Substrat e Type	f_0
1x2 PIFA	2.0466 mm	4.235 mm	1.6mm	0.489 mm	1.3 mm	11.4mm	7.414 mm	Duroid	28 GHz

Step 3: Simulation and optimization

HFSS simulations of the antenna involve adjusting the feedline and ground plane extensions to optimize the return loss of the antenna so that it has a uniform radiation pattern.

4.4. Design 4x4 PIFA Array

The 4*4 array is an expansion of the 1*2 design in order to achieve higher directivity and gain for massive MIMO applications.

Step 1: Element spacing step

$d = \frac{10.71mm}{2}$ $d = 5.355mm$

Step 2: Patch dimensions

The size of each element is that of the single element PIFA to guarantee that it resonates at 28 GHz

Step 3: Ground plane considerations

The long ground plane helps uniform current distribution and reduces edge diffraction which is crucial for high gain performance.

Table 4.3. 4x4 PIFA Antenna design parameters

Antenna Type	L_P	Wp	W_{feed}	Height of Substrate	Ws	Lg	Wg	Substrate Type	f_0
4x4 PIFA	2.0466 mm	4.235 mm	1.6mm	0.489 mm	1.3 mm	23.4 mm	25.5 mm	Duroid	28 GHz

Step 4: Simulation validation

HFSS is utilized to simulate the S parameters, radiation pattern, gain, and bandwidth of the 4*4 array. Special attention is given to mutual coupling, which can be mitigated through the use of inter-element spacing, decoupling effective stubs, or metamaterial-inspired isolation structures.

4.5. Design 4x5 PIFA Array

The 4x5 increases the 4x4 design further to get better directivity and gain for massive MIMO array applications.

Step 1: Element spacing

$$d = \frac{10.71mm}{2} \qquad d = 5.355mm$$

Step 2: Patch dimensions

Each element has the dimensions of a one-element PIFA to guarantee the resonance for 28 GHz.

Table 4.4. 4x5 PIFA Antenna design parameters

Antenna Type	L_P	Wp	W_{feed}	Height of Substrate	Ws	Lg	Wg	Substrate Type	f_0
4x5 PIFA	2.0466 mm	4.235 mm	1.6mm	0.489 mm	1.3 mm	23.4 mm	31.5 mm	Duroid	28 GHz

Step 3: Ground plane considerations

The extended ground plane is used to ensure uniform current distribution and to minimize edge diffraction, which is very important for high gain performance.

Step 4: Simulation validation

The S-parameters, radiation pattern, gain, and bandwidth of the 4 x 5 array are simulated using HFSS. Special attention is given to mutual coupling, which can be overcome with the help of inter-element spacing, decoupling stubs, or metamaterial-inspired isolation structures.

CHAPTER FIVE

RESULTS AND DISCUSSION

5.1. Introduction

This chapter presents the simulation results and performance analysis of the proposed PIFA designs at 28 GHz to be used in the 5G wireless communication applications. The antenna designs of the single element and the array design were developed and simulated with Ansys HFSS. Reflection coefficient (S_{11}), bandwidth, gain, directivity, VSWR, radiation pattern, and MIMO metrics are some of the key performance enhancement parameters that are measured to determine the effectiveness of the proposed designs. The results of the simulation obtained are discussed and presented to show how the array configurations have improved the performance.

5.2. Simulation Results of Single PIFA at 28GHz

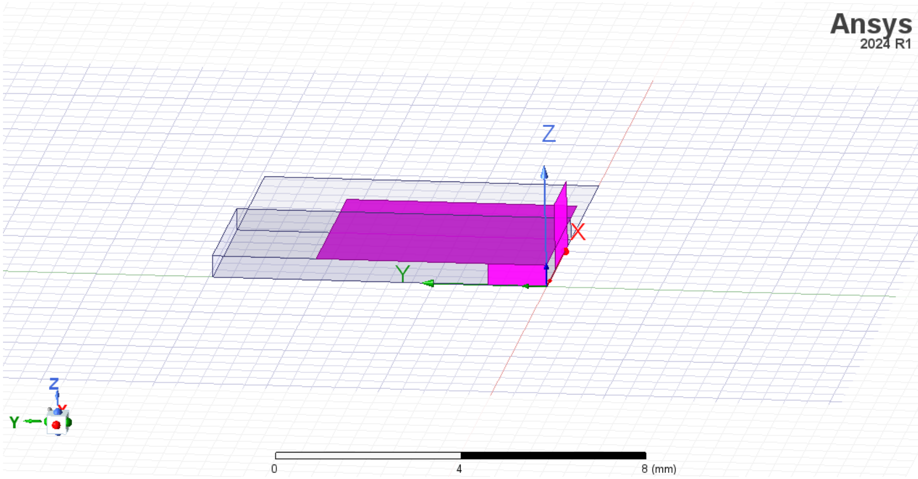

Figure 5.2.1 Single PIFA structure

5.2.1. Reflection Coefficient and Bandwidth of Single PIFA at 28GHz

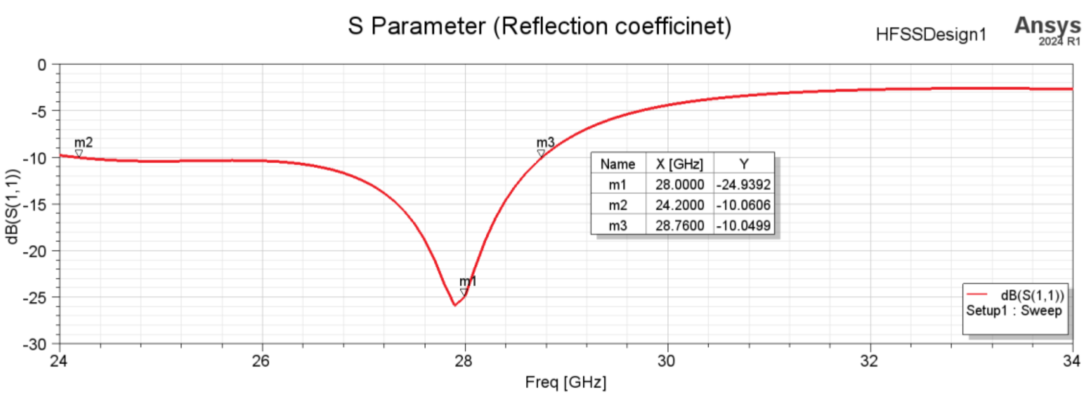

Figure 5.2.2: Reflection Coefficient and BW of Single PIFA at 28GHz

The HFSS result of the proposed single PIFA element is well matched at the designed 28 GHz band with a reflection coefficient of -24.9392 dB, which is much lower than the widely accepted standard of -10 dB of the microstrip antennas. This level of impedance matching suggests very low reflection of power and thus radiation efficiency, of utmost importance for dense massive MIMO deployments where mutually coupled losses and mismatch losses may destroy system performance. Furthermore, the obtained operating bandwidth spinning from 24.2 GHz to 28.76 GHz confirms 4.56 GHz enhanced a broad and wide bandwidth behavior definitely suitable for the 5G millimeter wave applications. Such bandwidth provides robustness to the effects of fabrication tolerances and array integration on the frequency shift. In the light of massive MIMO PIFA array design, these results confirm the efficiency of HFSS-optimized geometries in boosting the performance of the array, facilitating reliable transmission of high data rates, improving spectral efficiency, and ensuring the stability of operation across the target 5G frequency range.

5.2.2. VSWR of Single PIFA at 28GHz

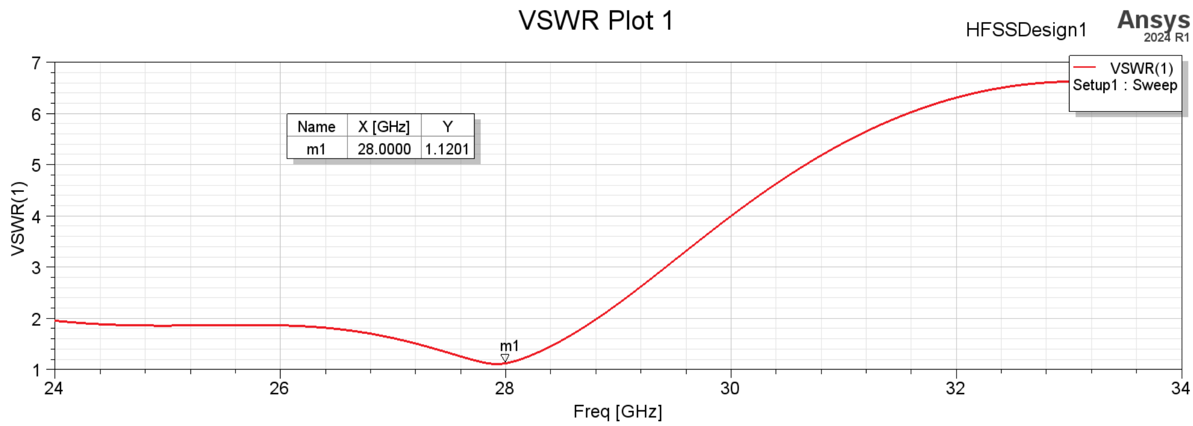

Figure 5.2.3: Single PIFA VSWR at 28GHz

The HFSS simulation shows that the designed single PIFA element has a voltage standing wave ratio at 28 GHz of 1.1 dB, which means that the antenna and the feed line are a perfect impedance match. Since a VSWR value below 3 should be generally considered acceptable for practical antenna operation, the result obtained demonstrates a rather good margin of performance over minimum requirements. This high measurement of matching implies that there is negligible reflected power and efficient power transfer, which is particularly important if the element is replicated in massive MIMO PIFA arrays, in which cumulative mismatch can impact the overall array efficiency. In the case of 5G millimeter wave systems, such low VSWR contributes to enhanced radiation efficiency of 5G millimeter wave systems, stable array behavior, and steady beamforming performance, verifying the validity of the design approach using the HFSS software that contributes to performance improvement in large-scale MIMO antenna information.

5.2.3. Total Gain of Single PIFA at 28GHz

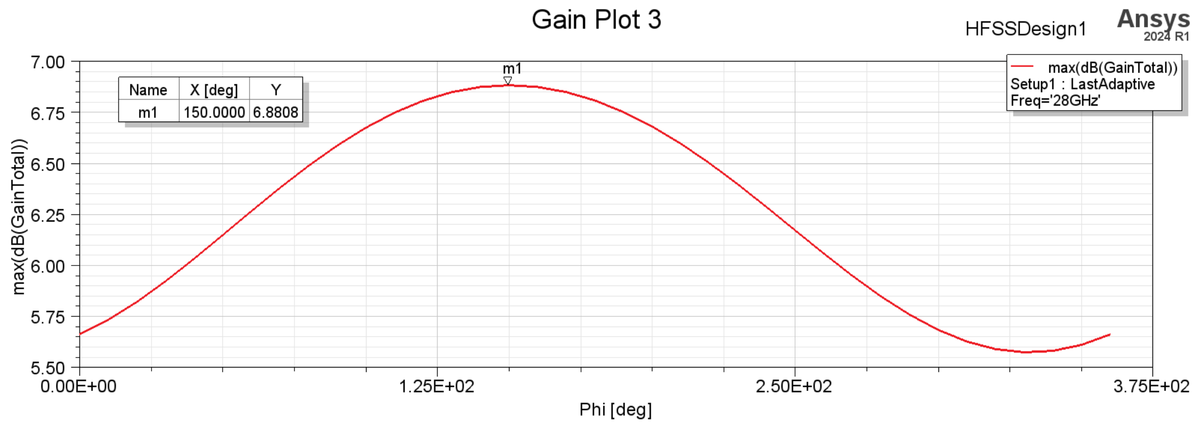

Figure 5.2.4: Total Gain of Single PIFA at 28GHz

Figure 5.3 Total Gain Single PIFA 28 GHz: The simulation result of the single PIFA at 28 GHz is presented, and the total gain is 6.8 dB, which is reasonable for an isolated element but quite limited by natural comparison with the gain levels that can result from the antenna array. The primary lobe of radiation at approximately 10 deg points indicates a somewhat slanted beam similar to that accompanied by the natural radiation behavior of a single element (no beam shaping is applied at the array level). In the case of large-format MIMO PIFA array design, raising the gain to this moderate level emphasizes the need for an efficient combination of several suitably matched elements to develop the high directivity and beam-forming capability needed for 5G millimeter-wave communication. These single elements, organized in large arrays and optimized by HFSS, will provide the interference element construction with many higher arrays' gain and dynamic beam steering functions and be able to offer high-quality coverage and link reliability. Thus, the single element gain measured serves as a reference to verify the design of the element and to highlight the performance improvements reached due to the implementation of a massive MIMO PIFA array interface to 5G systems in the future.

5.2.4. Directivity of Single PIFA at 28GHz

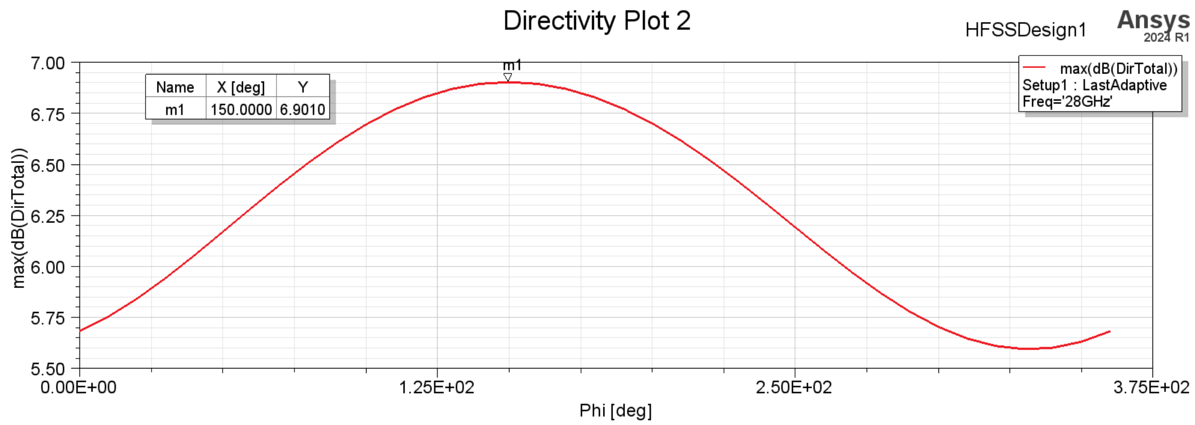

Figure 5.2.5: Directivity of Single PIFA at 28GHz

The simulation results of a single element PIFA resonate at 28 GHz and achieve a total directivity of approximately 6.9 dB, and thus the radiation pattern is slightly focused on the direction of intended propagation. Directivity is a measure of the ability of the antenna to focus radiated RF on the receiver, which is a very important requirement for reliable millimeter-wave 5G links. In this design, the directive gain is found to be greater than the total gain, indicating the excellent radiation efficiency and the effectiveness of the antenna's directional capability. These results indicate a fundamental enhancement of single-element patch antennas at high frequencies, and to mitigate for more directivity, massive MIMO PIFA array configurations need to be developed. When extended to array-based designs and optimized using HFSS, the collective behavior of the multiple radiating elements allows the design of beam steering, higher array directivity, and improved effective gain, compensating for losses in the individual elements. Consequently, the simulation results prove that even though a single patch element delivers acceptable baseline performance, there is substantial improvement of the coverage, link robustness, and spectral efficiency for 5G wireless communication systems by the well-designed massive MIMO PIFA arrays.

5.2.5. Radiation efficiency of single PIFA at 28 GHz

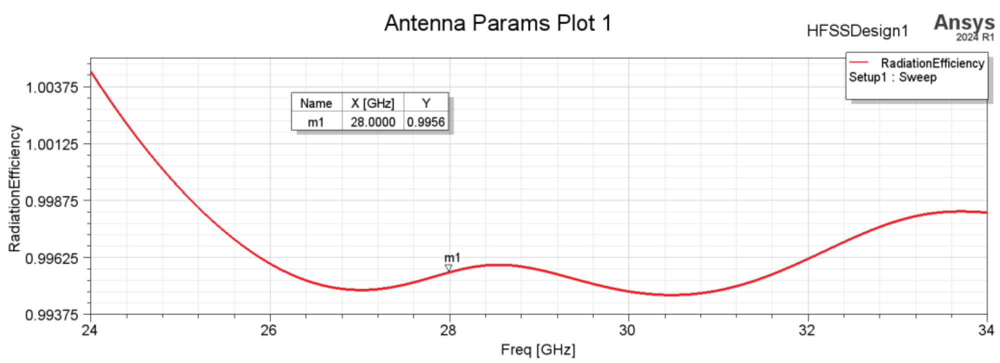

Figure 5.2.6: Radiation efficiency of single PIFA at 28 GHz

The proposed single PIFA was assessed on the frequency range of 24-34 GHz in radiation efficiency. The antenna has a radiation efficiency of 0.9956 (99.56%) at the target resonance frequency 28 GHz, which means that almost all the accepted power is transformed into radiated electromagnetic power. This great efficiency proves that both conductor and dielectric losses should be negligible at the operating frequency, which proves the appropriateness of the chosen substrate and geometry to mm-Wave applications. This is due to the minor variation above unity at lower frequencies, which is caused by numerical approximation and mesh convergence tolerance within the simulation environment. In general, the achieved radiation efficiency confirms the suitability of the proposed PIFA design to the high-frequency 5G communication systems.

5.2.6. 3D Polar Plot of Directivity Single Element PIFA at 28GHz

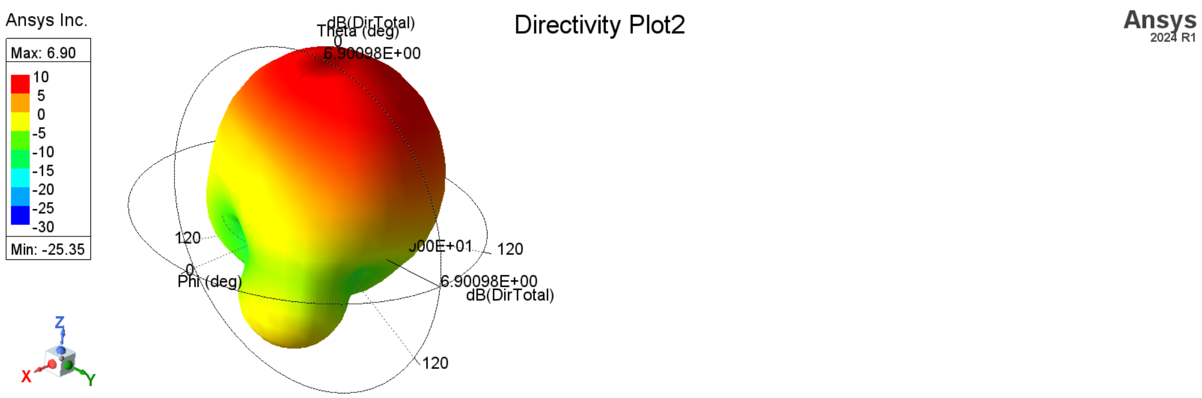

Figure 5.2.7: 3Polar Plot Single Element PIFA at 28GHz

The given 3D polar plot shows spatial distribution of radiated power from the single-element PIFA, which has a clear definition of dominant radiation directions of radiated power and extent of energy spread in 3D space. This radiation characteristic states the fact of the inherently broad and limited radiation beam control of a single radiating element at 28 GHz, which limits the coverage and the directional flexibility under dense 5G environments. When these insights from the simulations are transferred to the design of massive MIMO PIFA arrays, the significance of array configuration, element spacing, and phase control can be recognized. Through multiple PIFA elements in conjunction and optimization in HFSS, the radiation pattern can be reconfigured as a smaller, steerable radiation pattern with a higher directivity and a more desirable spatial selectivity. Thus, the 3D polar analysis not only serves as a validity factor for the baseline performance of the single-element antenna but also offers critical building blocks for improving beamforming capability, interference mitigation, and overall system performance in 5G wireless communication systems through massive MIMO PIFA array designs.

5.2.7. Radiation pattern of Directivity single PIFA

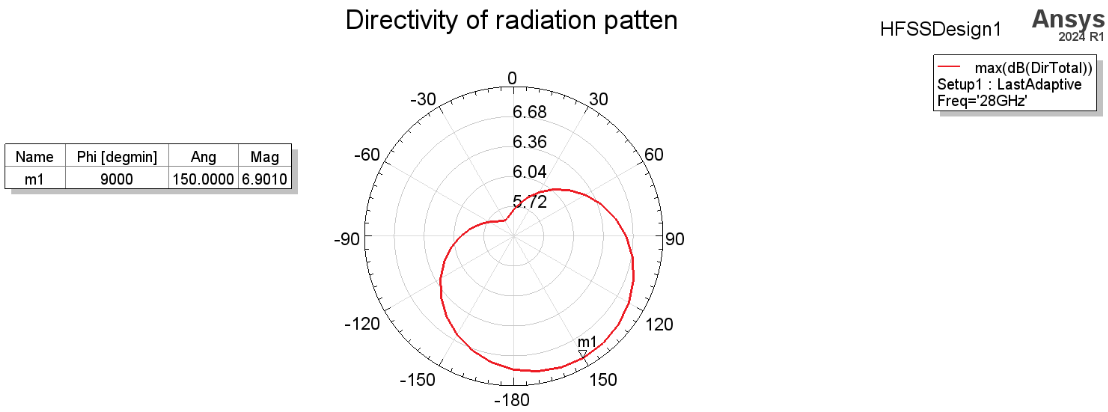

Figure 5.2.8: Radiation pattern of Directivity of Single PIFA Element

The proposed single PIFA was tested to be directed at the frequency of 28 GHz. The highest directivity attained is 6.901 dB, which illustrates a linear value of about 4.9. This means that the antenna emits almost 5x more power in its main direction of radiations than an ideal isotropic radiator. The radiation pattern shows that there is a strong main lobe at about 150º, and the back radiation is suppressed because of the existence of a ground plane. The radiation efficiency is 99.56%, which means that the antenna gain is very close to the value of directivity, which validates there are no substantial losses of power dissipated. The resulting directivity is typical of quarter-wave PIFA behavior as well as confirming the design as appropriate to directional mm-Wave applications.

5.3. Simulation Results of 1x2 PIFA Antenna Array at 28GHz

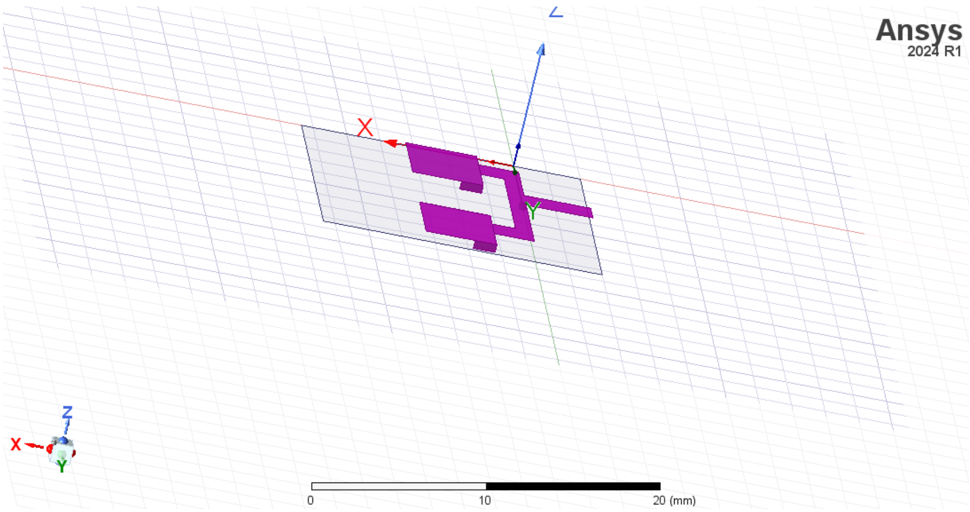

Figure 5.3.1 1x2 PIFA Array structure

5.3.1. Reflection Coefficient and BW of 1x2 PIFA Antenna Array at 28GHz

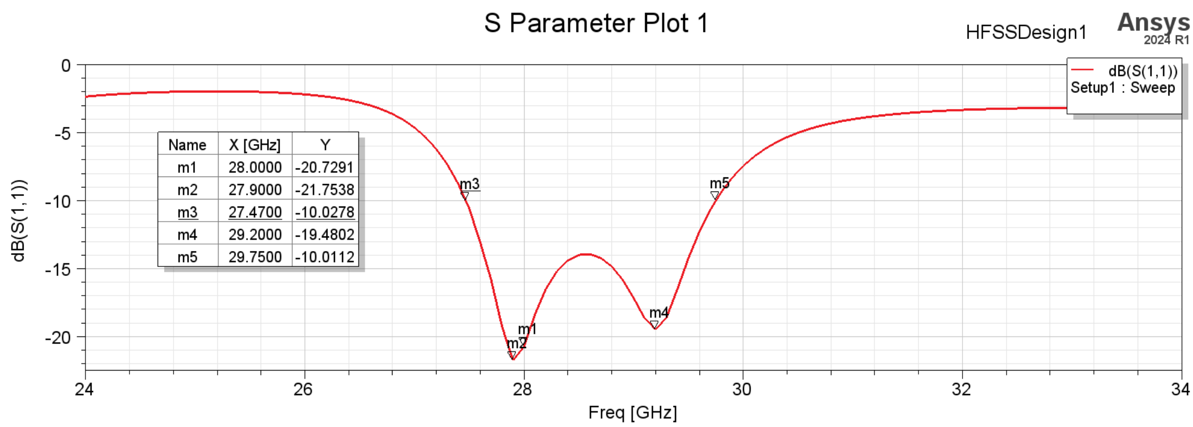

Figure 5.3.2: Reflection Coefficient and Bandwidth of 1x2 PIFA Antenna Array at 28GHz

The simulated reflection coefficient of a 1*2 PIFA array shows a dual-resonance behavior due to the array configuration and coupling between elements within the 24-34 GHz range. which indicates excellent impedance matching of -20.7291 dB, which is 99.2% power delivered to the antenna at the targeted 28 GHz mm-wave region. Below -10 dB is the perfectly accepted threshold for efficient impedance matching for microstrip-based antennas. This result shows that there is a large fraction of the input power that is effectively radiated rather than reflected to the source and which demonstrates the suitability of the array to millimeter-wave operation. The obtained operating band goes from 27.47 GHz to 29.75 GHz and thus achieves a 2.3 GHz bandwidth and fractionally 8.2% sufficiency for high data-rate 5G applications.

5.3.2. VSWR of 1x2 PIFA Antenna Array at 28GHz

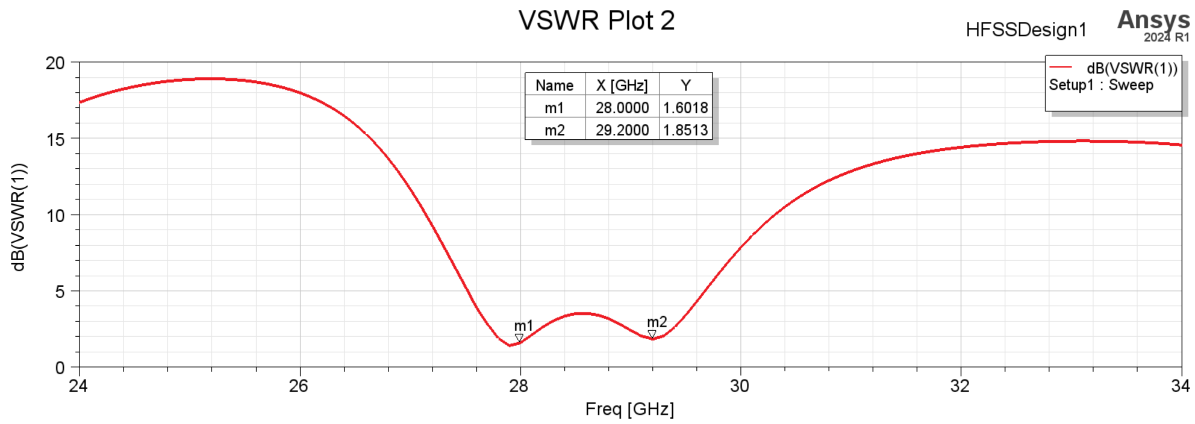

Figure 5.3.3: VSWR of 1x2 PIFA Antenna Array at 28GHz

The VSWR result of the 1x2 array element gives 1.6 dB, which is within the practical antenna operating range of less than 3 dBi. This HFSS simulation finding indicates that a PIFA array could be used to achieve a reasonable level of impedance identical to it, and thus the majority of the power delivered to the radiation could be reported with controllable loss of reflection. This VSWR value is close to the upper acceptable boundary, indicating that the designed element is a significant match for millimeter wave frequencies. When these results are taken in the context of massive MIMO PIFA array design using HFSS, this indicates that array-level optimization is important. By carefully adjusting the geometry, spacing, and feeding networks of array arrangements, improved overall input matching can be achieved, giving reduced effective VSWR and improved and stable performance over the 5G frequency band. Therefore, in the simulation result, it is demonstrated that when using an optimized massive MIMO PIFA array as a 5G wireless communication system, it is possible to get good baseline behavior; much better results on power efficiency, beamforming reliability, and link robustness are achieved.

5.3.3. Total Gain of 1x2 PIFA Antenna Array at 28GHz

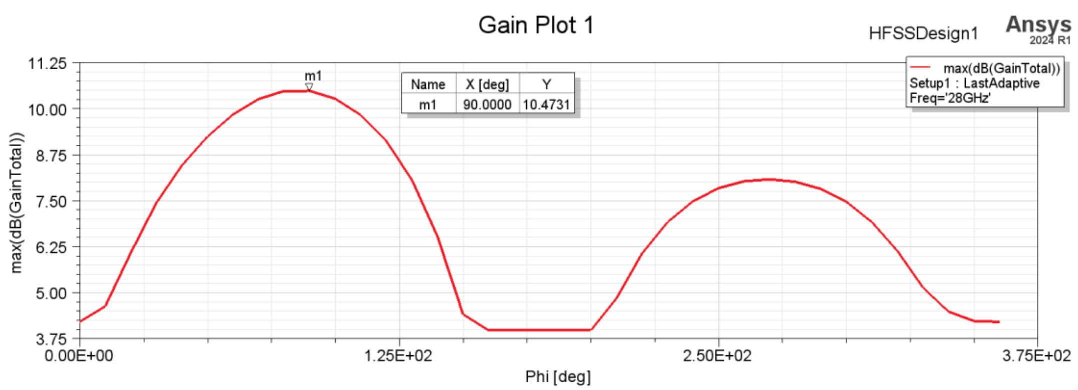

Figure 5.3.4: Total Gain of 1x2 PIFA Antenna Array at 28GHz

The analyzed 1x2 element PIFA array designed to simulate total gain at 28 GHz is 10.47 dBi and has a larger radiation capability than a single element as well as against the much larger gain of antenna array designs. Looking at the radiation pattern, it's visible that the maximum gain is around 10.47 dBi, which indicates the presence of a tilted main lobe instead of a strongly focused beam towards the broadside; this can constrain the effective coverage and link reliability in scenarios using directional 5G millimeter waves. This behavior is a characteristic of the limitations of single radiating elements such as available aperture size and control over beam orientation. When these results are interpreted in the context of massive MIMO PIFA array design using HFSS, they certainly present a reason to consider the need for array-based enhancement. With a combination of a few PIFA elements with controlled spacing and phase, a large overall array gain may be increased with the capability to steer the beam directly to the desired users. Thus, using these simulation results, it can be shown that while using a single patch antenna has acceptable baseline performance, significant gain, coverage, and spatial selectivity improvement for 5G wireless communication systems can be achieved by the carefully optimized massive MIMO PIFA array design.

5.3.4. Directivity of 1x2 PIFA Antenna Array at 28GHz

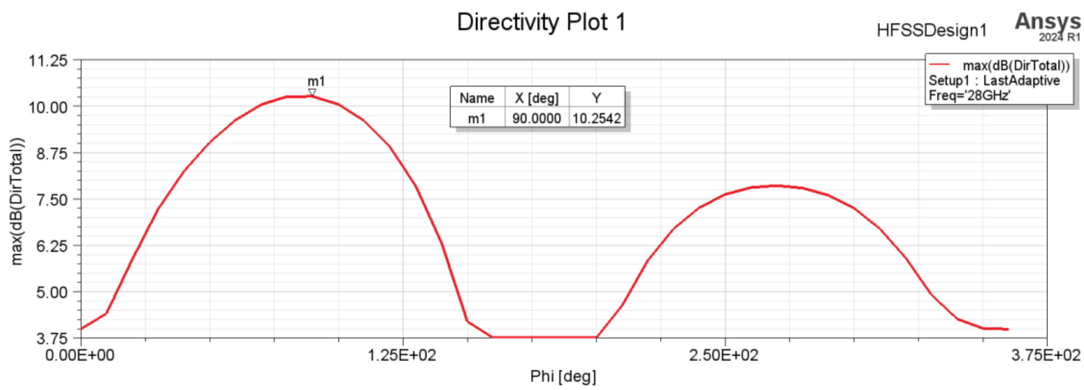

Figure 5.3.5: Directivity of 1x2 PIFA Antenna Array at 28GHz

The analyzed 1x2 element PIFA array designed to simulate total gain at 28 GHz is 10.47 dBi and has a larger radiation capability than a single element as well as a much larger gain than antenna array designs. Looking at the radiation pattern, it's visible that the maximum gain is around 10.47 dBi, which indicates the presence of a tilted main lobe instead of a strongly focused beam towards the broadside; this can constrain the effective coverage and link reliability in scenarios using directional 5G millimeter waves. This behavior is a characteristic of the limitations of single radiating elements such as available aperture size and control over beam orientation. When these results are interpreted in the context of massive MIMO PIFA array design using HFSS, they certainly present a reason to consider the need for array-based enhancement. With a combination of a few PIFA elements with controlled spacing and phase, a large overall array gain may be increased with the capability to steer the beam directly to the desired users. Thus, using these simulation results, it can be shown that while using a single patch antenna has acceptable baseline performance, significant gain, coverage, and spatial selectivity improvement for 5G wireless communication systems can be achieved by the carefully optimized massive MIMO PIFA array design.

5.3.5. 3D Polar Plot of 1x2 PIFA Antenna Array at 28GHz

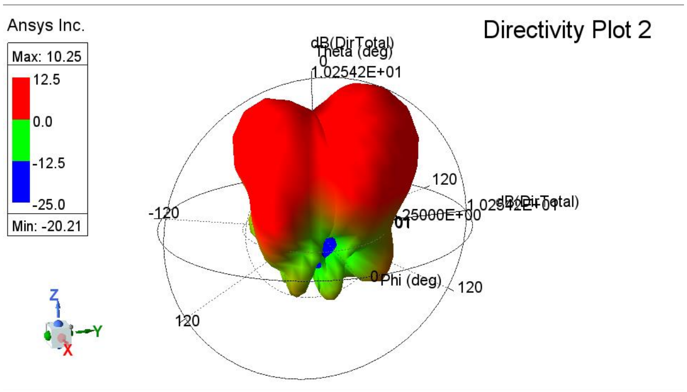

Figure 5.3.6. 3D polar Plot of 1x2 PIFA Antenna Array at 28GHz

The 3D polar plot of the 1x2 PIFA antenna array shows us the distributed 3D space of radiated energy of the 1x2 element of the rectangular patch antenna, and the radiation direction of the radiation distribution of the dominant radiated energy direction and side-lobe characteristics of the patch antenna are clearly identified. This result is associated with the natural limitation that a single radiating element at 28 GHz has a still rather wide beamwidth and limited control of direction. When these simulation insights are extended in the design of large MIMO PIFA arrays, the importance of multi-element integration is seen. By arranging multiple PIFA elements and by optimizing the excitation phase and spacing of these elements with HFSS, the radiation pattern can be changed to narrower (steerable) radiation beams having increased directivity and spatial selectivity. Therefore, the 3D polar radiation analysis not only provides validation of the baseline directional performance of the 1x2 PIFA element antenna but also an important foundation for the purpose of improved beamforming capability, reduction of interference, and overall performance enhancement in 5G wireless communication systems through massive MIMO PIFA array designs.

5.3.6. Radiation pattern of 1x2 PIFA Antenna Array at 28GHz

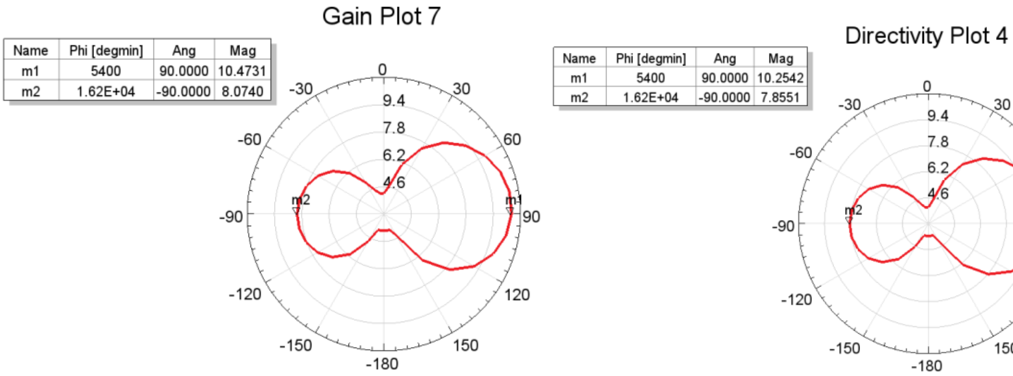

Figure: 5.3.7 Radiation pattern of 1x2 PIFA Antenna Array at 28GHz

The proposed 1x2 PIFA array radiation pattern was simulated, and the result is presented in Figure [Insert Figure Number]. The plot has a typical bidirectional radiation form where the magnitudes of gain reach 10.47 dBi at 90° and 8.07 dBi at 270° (-90°). The array has a peak gain of over 10 dBi, meaning it has a high degree of directivity in the form of the azimuth plane. An experimental front-to-back ratio value of about 2.4 dB suggests that the radiation has almost symmetrical behavior, which proves the effectiveness of the 1x2 element design in focusing the energy to the horizontal axes and keeping the nulls to minimum depth in the main lobes.

5.3.7. Radiation efficiency of 1x2 PIFA array

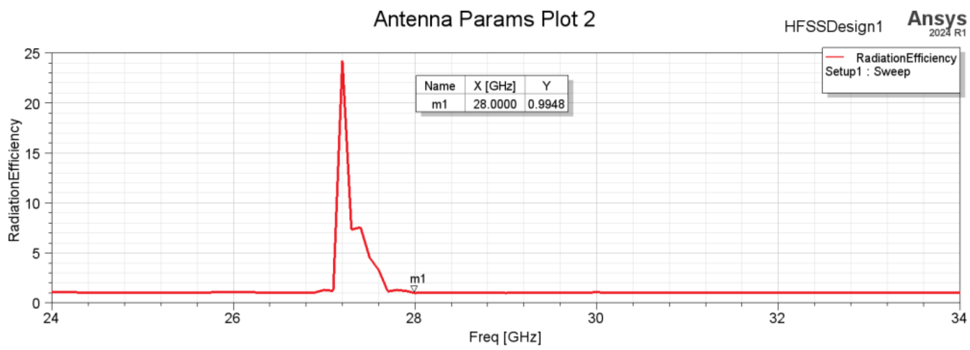

Figure 5.3.8 Radiation efficiency of 1x2 PIFA array

The radiation efficiency results of the 1x2 PIFA antenna array reveal that there is a distinct peak around the operating frequency of the antenna array. The radiation efficiency at the marked point of 28 GHz is approximately 0.9948, which corresponds to approximately 99.48% efficiency with only 0.52 maximum loss occurring to conductor, dielectric, or surface wave loss. This is very efficient and proves that the antenna structure is highly optimized at the desired 28 GHz millimeter-wave band, with low internal losses. This sharpness in the change of efficiency at the levels of 27-27.3 GHz indicates the presence of a high resonance behavior where the antenna switches quickly between lower radiation efficiency and near-ideal performance at the design frequency. In general, the 1x2 PIFA array shows high radiation efficiency at 28 GHz, which proves that the antenna is effective in converting the provided power into radiation and can be successfully used in 5G millimeter-wave communication in the high frequencies.

5.4. 4x4 PIFA MIMO Antenna Array at 28GHz

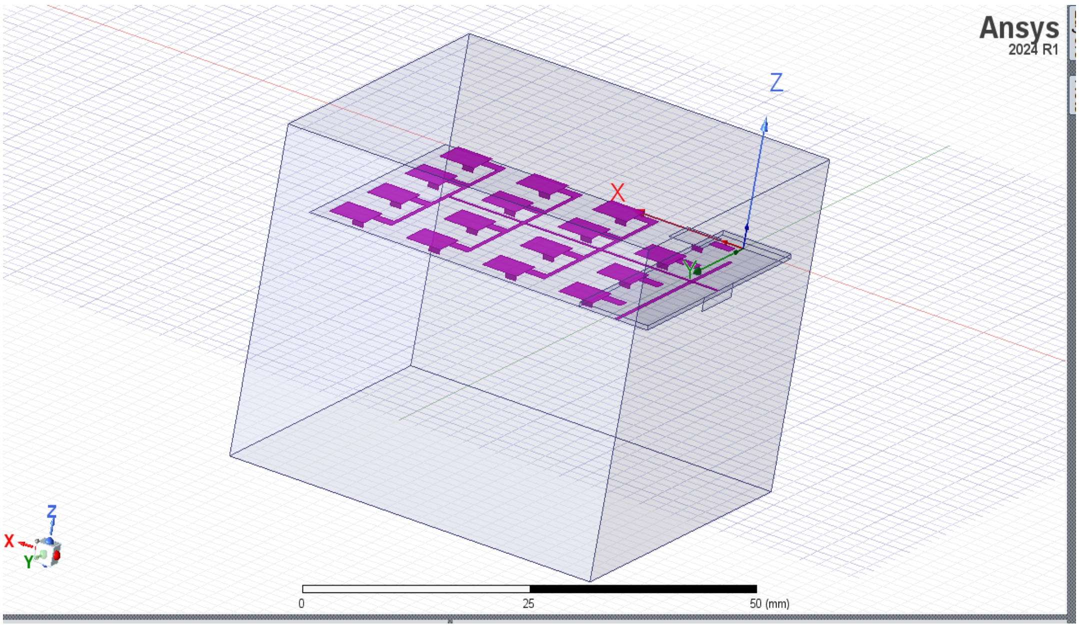

Figure 5.4.1. 4x4 PIFA Antenna Array structure

5.4.1. Reflection Coefficient and BW of 4x4 MIMO PIFA Array at 28GHz

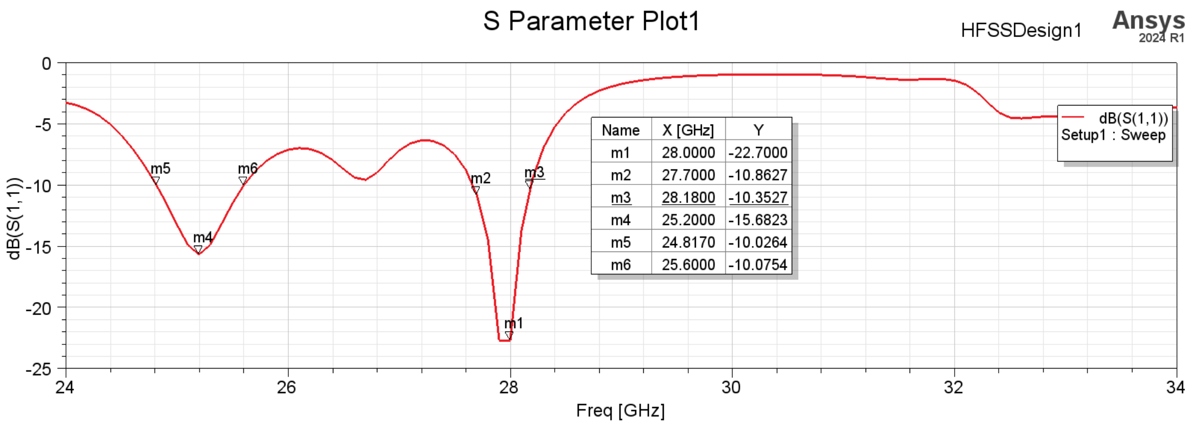

Figure 5.4.2: Reflection Coefficient and BW of 4x4 PIFA Antenna Array at 28GHz

The simulated reflection coefficient (S11) of the proposed 4x4 PIFA array proves that the 24-34 GHz frequency range exhibits impedance matching. The main resonance frequency of 28 GHz is a minimum return loss of -22.7 dB, which is an excellent result of impedance matching. The respective -10 dB impedance bandwidth is between about 27.70 GHz and 28.18 GHz, which determines a bandwidth of around 0.5 GHz and a fractional value of about 1.4%, and the second resonance is at 25.2 GHz with a return loss of -15.68 dB, where the -10 dB bandwidth is 24.8 GHz to 25.60 GHz, which is 0.8 GHz; its fractional bandwidth is about 2.85%, and the sum of these two resonance bands, 0.5 GHz and 0.8 GHz, gives 1.3 GHz. This result confirms that there is sufficient bandwidth to 5G mm-wave bands, and the antenna attains a high impedance that matches at the desired 28 GHz design frequency, besides having an extra lower-frequency resonance with a narrow band response owing to the effect of array coupling and structure. As such, the simulation verifies the effectiveness of optimized massive MIMO arrays, which not only keep the impedance match good but also achieve enhanced radiation efficiency, beamforming capability, and overall system performance, which makes them very suitable for high-capacity 5G wireless communication networks.

5.4.2. VSWR of 4*4 PIFA MIMO Antenna Array at 28 GHz

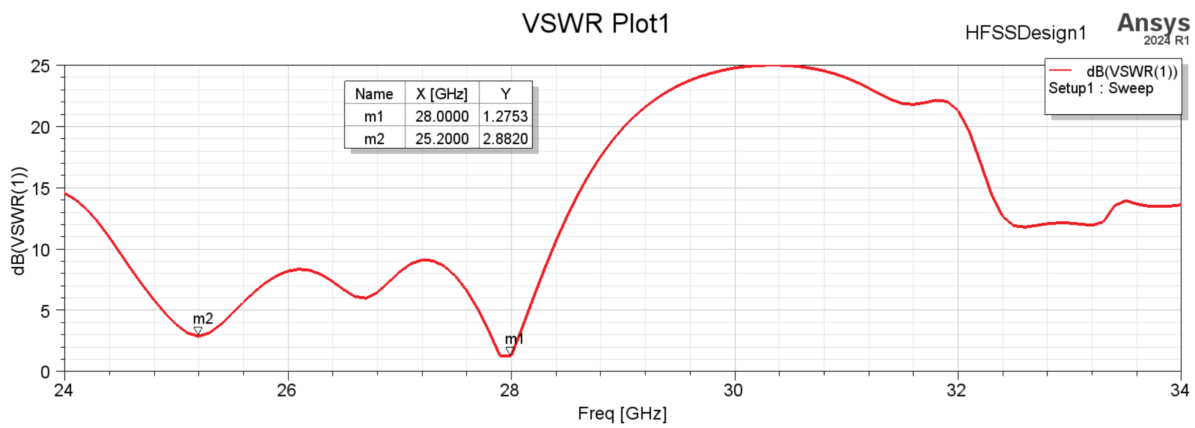

Figure 5.4.3: VSWR of 4x4 PIFA Antenna Array at 28GHz

The simulated voltage standing wave ratio (VSWR) for the 4x4 PIFA MIMO antenna array at 28 GHz is 1.2 dB, which is well within the limit of common methods to be considered as an effective antenna operation of 3 dB. VSWR is a critical characteristic of RF engineering and telecommunications because it quantifies the degree of impedance match between the antenna load and the characteristic impedance of the transmission line or waveguide that directly affects the power transfer efficiency as well as minimized reflections. The low VSWR value means that the designed array has good impedance matching so that most of the input power is radiated efficiently. In the context of massive MIMO PIFA array design with HFSS, this result shows the effectiveness of multi-element optimization of losses of mismatch and improvement of overall radiation. Such matched arrays are one of the keys to achieving improved beamforming, improved system efficiency, and better 5G communication links that experience higher reliability, especially at the millimeter wave frequencies where good impedance control is critical to high-capacity network operation.

5.4.3. Total Gain of 4x4 PIFA MIMO Antenna Array at 28GHz

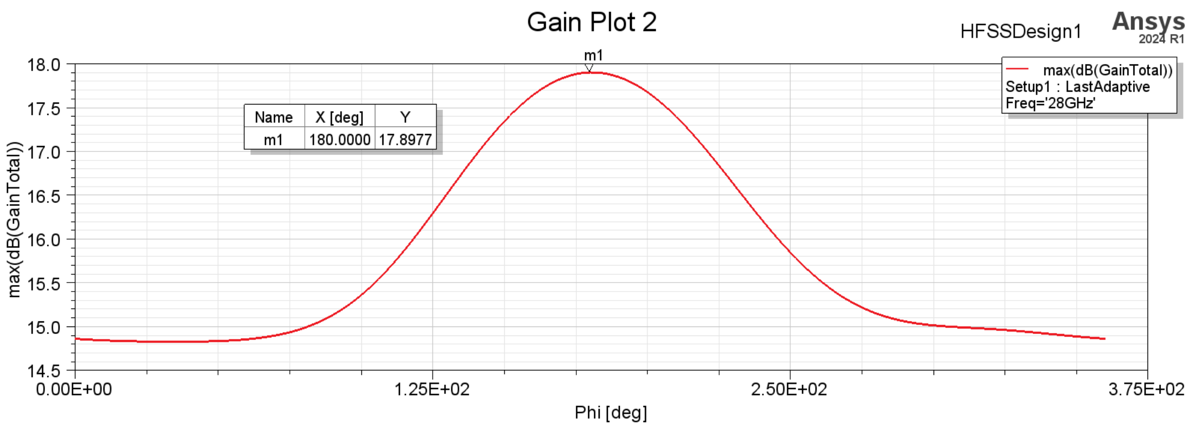

Figure 5.4.4: Total gain of 4x4 PIFA Antenna Array at 28GHz

The simulated total gain of the 4*4 PIFA MIMO antenna array at 28 GHz is 17.89 dBi, which indicates a high gain performance that is crucial for millimeter-wave 5G, where path losses are large. The capacity of the antenna to concentrate the energy in a specific direction, where an isotropic radiator will then radiate the same input power, is the measure of the capacity of the antenna to direct the energy where it is needed and enhance the power of the signals as well as the reliability of the link between the antenna and transmitter. Compared to single-element designs, the large increase in gain for the 4x4 array proves the benefits of multi-element designs such as constructive interference of radiated fields and improved beam directivity. Under MIMO PIFA arrays, optimized in HFSS, the following results demonstrate that the potential exists for making these beams very directional and steerable, which aids in enhancing spectral efficiency, coverage, and interference management. Consequently, the large gain obtained in simulation verifies the suitability of massive MIMO PIFA arrays for the performance requirement of high capacity 5G wireless communication systems.

5.4.4. Directivity of 4x4 PIFA MIMO Antenna Array at 28GHz

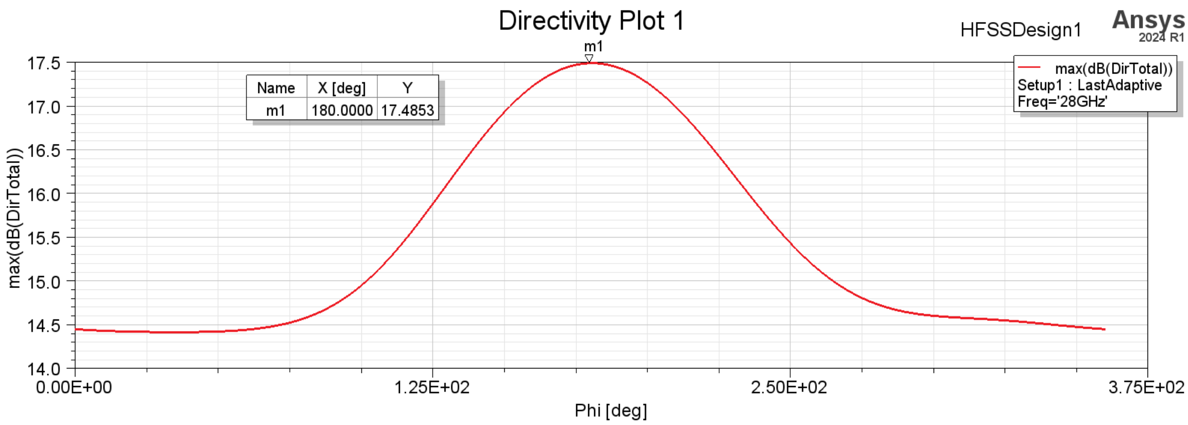

Figure 5.4.5: Directivity of the 4x4 PIFA Antenna Array at 28GHz

The simulated total directivity of the 4*4 PIFA MIMO antenna array at the frequency of 28 GHz is 17.48 dBi, which is a high level of direct gain, indicating a capability of the MIMO antenna array to focus radiated energy towards desired directions. Directive gain is an important antenna measure used for antenna or array design to quantify the efficiencies of power concentration of an antenna or an array at certain directions, which is often critical to enhance the link reliability and reduce the interference signal in 5G dense networks. The array configuration has significantly greater directivity than the single-element antennas due to the constructive combinations of the fields of more than one element and optimal spacing, enabling it to generate higher directional effects like multi-focused beam patterns. These HFSS simulation findings reveal the suitability of the massive MIMO PIFA array to enhance spatial selectivity, accurate beam steering, and massive capacity as well as low-interference 5G communication. Consequently, the high directivity confirms that multi-element PIFA arrays play an important role in obtaining an efficient energy transmission and better performance of the network in millimeter-wave 5G systems.

5.4.5. 3D Polar Plot of 4x4 PIFA MIMO Antenna Array at 28GHz

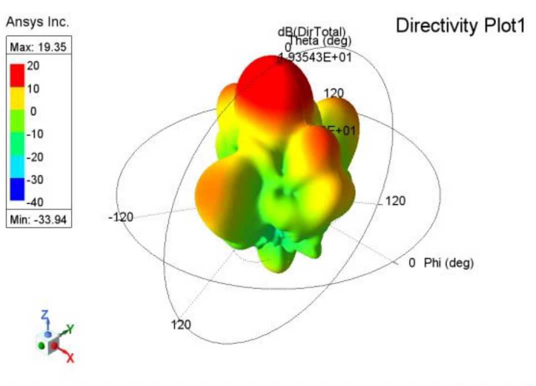

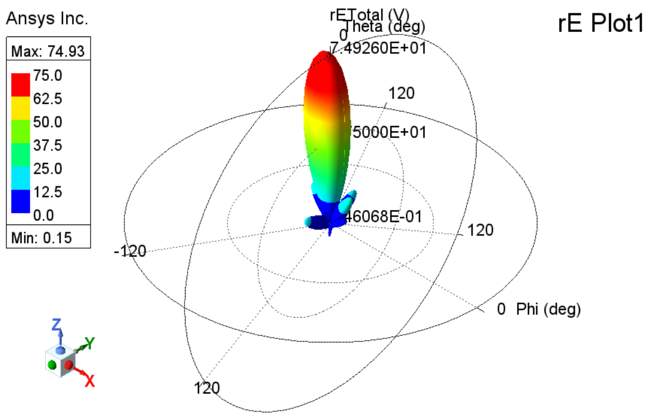

Figure 5.4.6: 3D Polar plot of 4x4 PIFA Antenna Array at 28GHz

The 3D polar plot of the 4x4 PIFA MIMO antenna array at 28 GHz shows an overall visualization of the radiation characteristics of the designed antenna array, showing the directional characteristics, the design gain, and the directivity of the design array in three-dimensional (3D) space. The following plot clearly shows how the array forms the energy in certain directions, showing the improved beam shape and spatial concentration that are attained by the multi-element configuration. The visualization confirms that the array not only delivers high gain and directivity but also has well-defined radiation lobes, which could be used in millimeter-wave-based 5G applications where the precise steering of energy and interference it could generate are of prime importance. These results show that compared with single-element designs, the massive MIMO array enables better control of beam patterns; namely, it permits effective beamforming, link improvements, and higher spectral efficiency. Overall, the 3D polar analysis has validated the benefits of using optimized PIFA arrays in HFSS, highlighting their importance to developing high-performance 5G wireless communication systems with increased directional radiation, energy concentration, and spatial selectivity.

5.4.6. Radiation pattern of the 4X4 massive MIMO PIFA array

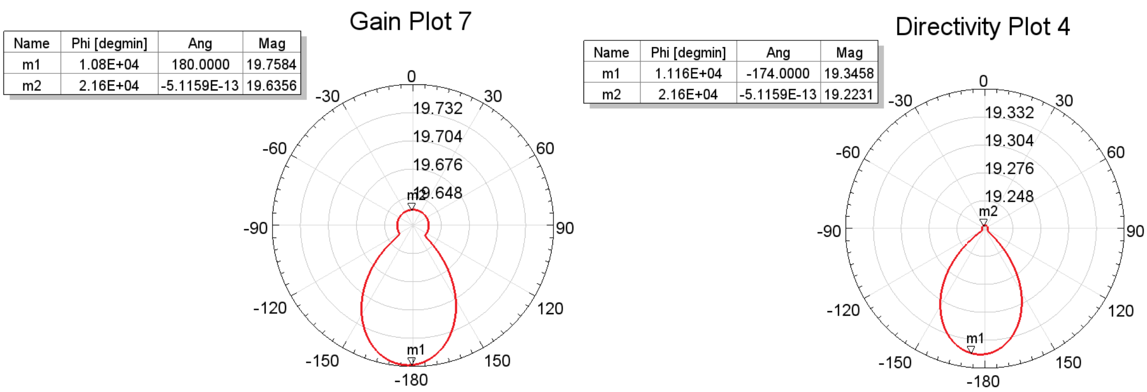

Figure 5.3.7 radiation pattern of the 4X4 massive MIMO PIFA array

The radiation pattern of the 4X4 PIFA array exhibits a directional pattern with the main lobe and the side radiation being rather weak. The highest gain is at 180°, where the peak gain is 19.76 dBi, which means that the antenna array is successful in concentrating most of its radiated power in this direction. This large gain can largely be explained by the positive interaction between radiation of the 16 elements making up the array that contributes to the total directivity. A secondary radiation level of about 19.64 dBi is observed at about 0°, though slightly less than the main lobe, and this proves that the main direction of the radiation is at 180°. A relatively small beam width and few side lobes are also characteristics of the polar plot, indicating that the antenna array used in 5G systems is specific to arrays at high frequency. The general trend suggests that the enhancement of a 4x4 array has a high directivity and gain; thus, it can be used in a narrow band of applications where a high level of directivity and enhanced link efficiency is needed in high-frequency wireless communication. Again, the directivity of the radiation pattern of the 4x4 PIFA array has a high-gain performance and a peak directivity at the -174° angular position with 19.35 dBi. This strong directivity affirms the ability of the 4x4 element structure to focus electromagnetic energy into a reduced spatial space. The curved, rounded shape of the main lobe supports the functional stability of the design and implies the practical control of the extraneous radiation lobes, which is vital to high-frequency millimeter-wave communication systems.

5.4.7. 4x4 massive MIMO PIFA Array Envelope Correlation Coefficient (ECC)

Table 5.1 4x4 massive MIMO PIFA Array Envelope Correlation Coefficient (ECC)

Data Table 1 HFSSDesign1 Ansys 2024 R1

	Freq [GHz]	CorrelationCoefficient MIMO Calculation 1
1	28.000000	0.001221

The result of the Envelope Correlation Coefficient (ECC) of the proposed 4x4 array of antennas at 28 GHz is 0.001221, which shows very low correlation between the antenna elements. The values of ECC in the MIMO antenna systems can be considered good at values below 0.5, whereas the values below 0.01 are very good as far as diversities are concerned. The value of ECC obtained is thus much less than the recommended value, which proves that the isolations and mutual couplings are very low among the antenna elements. This low correlation makes sure that the radiation patterns of the elements are independent enough, and this enhances diversity of signals, capacity of channels, and general performance of the MIMO system. The suggested antenna array is therefore very appropriate to a millimeter-wave 28 GHz communication system, where effective spatial diversity and high-data-rate transmission are mandatory.

5.5. 4x5 Massive MIMO PIFA Array at 28GHz

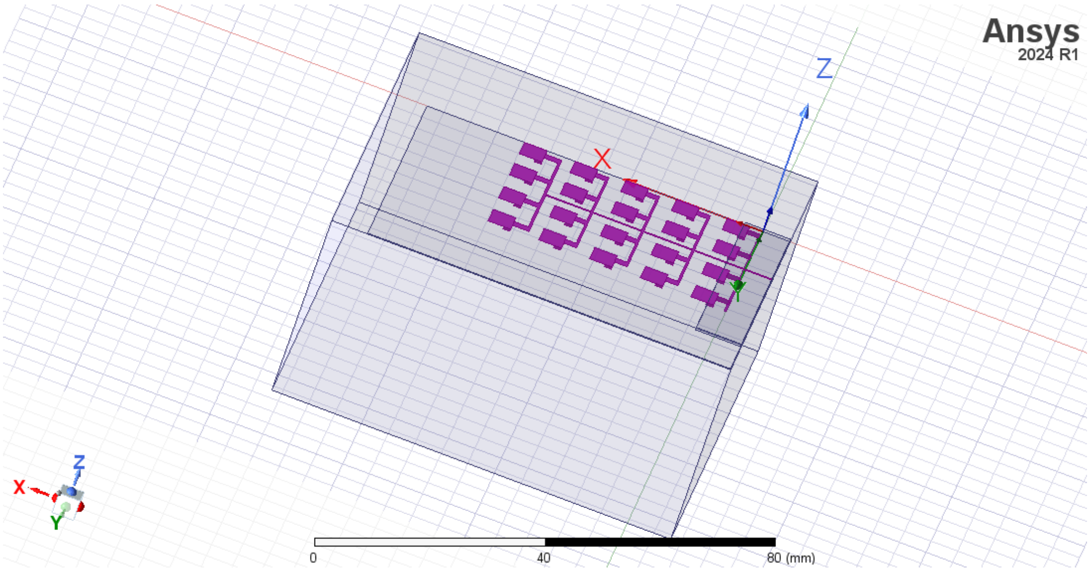

Figure 5.5.1. 4x5 Massive MIMO PIFA Array at 28GHz

5.5.1. Reflection Coefficient and BW of 4x5 PIFA MIMO Array at 28GHz

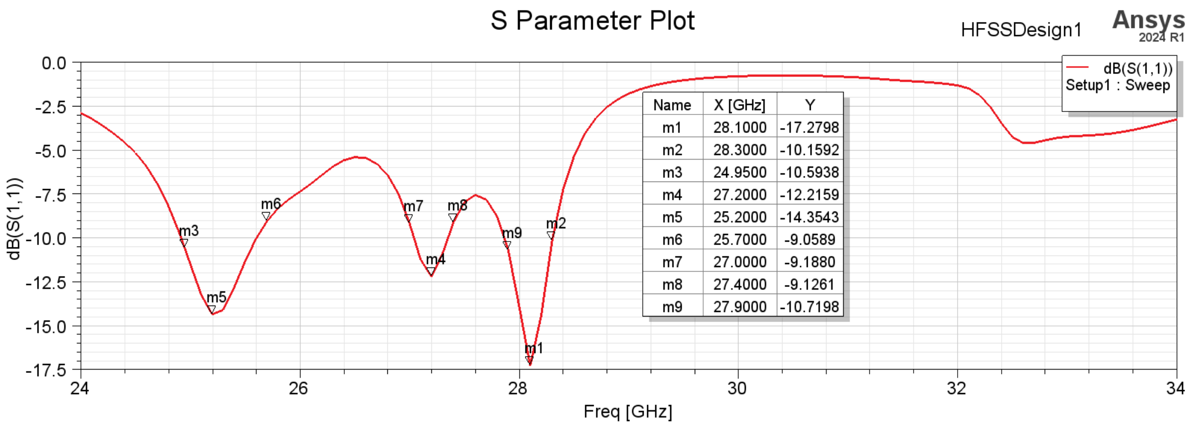

Figure 5.5.2: Reflection Coefficient and BW of 4x5 PIFA MIMO Array at 28GHz

The proposed 4×5 massive MIMO PIFA array of the simulated S_{11} result at the main resonance frequency of 28.1 GHz has a reflection coefficient of -17.27 dB. This implies that it has a reflection coefficient value of approximately 1.87% of the input power, and the remainder of about 98.13% is sent to the antenna, which is very high, and thus, the power transfer at the target frequency is efficient. The -10 dB bandwidth of impedance is around 24.9 GHz to 28.3 GHz with a bandwidth of around 3.4 GHz, the fractional bandwidth is about 12%, which is quite wide considering a PIFA-based millimeter-wave array and indicates that the structure should be able to operate at broadband frequencies. Other resonant dips at 25.2 GHz (–14.35

dB) and 27.2 GHz (–12.21 dB) are good signs of multi-resonant behavior, probably added by the array coupling and PIFA geometry, which is useful in broadening the impedance bandwidth. The array shows good matching at about 28 GHz, good delivered power efficiency, and a versatile fractional bandwidth that is applicable in 28 GHz band millimeter-wave communication systems. In general, the acquired S11 results of the designed 4x5 PIFA massive MIMO array can offer efficient power delivery, low reflection loss, and sufficient bandwidth to support high-capacity millimeter-wave wireless communication applications of 5G.

5.5.2. VSWR of 4*5 Massive MIMO PIFA Array at 28GHz

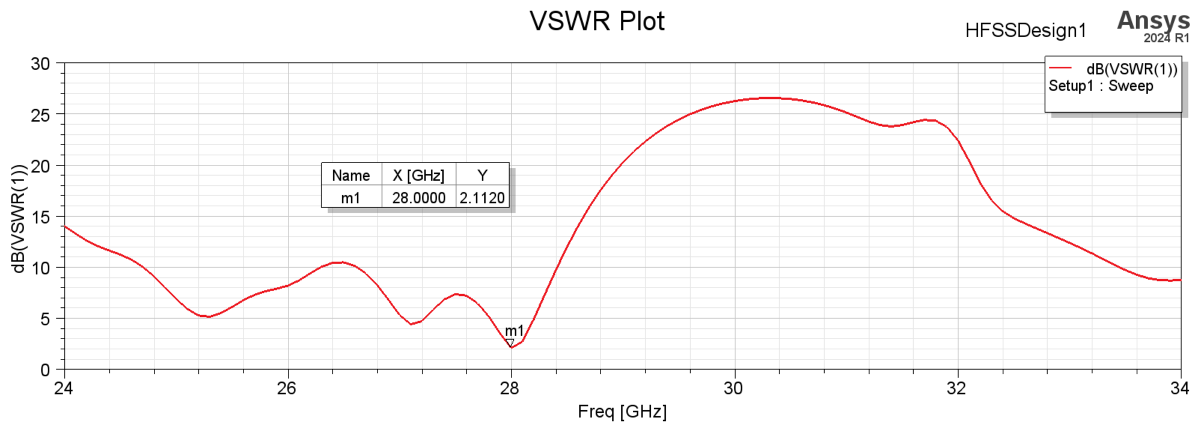

*Figure 5.5.3: VSWR of 4*5 PIFA MIMO Antenna Array at 28GHz*

The result of the designed antenna at 28 GHz in terms of simulated voltage standing wave ratio is 2.1 dB, which is well below the generally acceptable 3 dB range. This proves acceptable incident power is efficiently transferred to the antenna, and there is a small amount of reflection against the source. VSWR is one of the important metrics in RF and microwave engineering, indicating a good impedance match between the load and the characteristic impedance of the transmission medium, and lower values indicate better matching and less standing-wave formation. In the framework of the design of a massive MIMO PIFA array based on HFSS with 5G wireless systems, it is crucial that such a desirable VSWR at the element level be achieved, which would increase the overall array efficiency, ensure consistency of input impedance across the operating band, and reduce the losses caused by mismatch at high concentrations of arrays. In turn, the achieved VSWR performance can support the operation of millimeter waves reliably, the transmission of wideband signals, and enhance the capacity of systems and the accuracy of beamforming in 5G massive MIMO deployments.

5.5.3. Total Gain of 4x5 PIFA MIMO Antenna Array at 28GHz

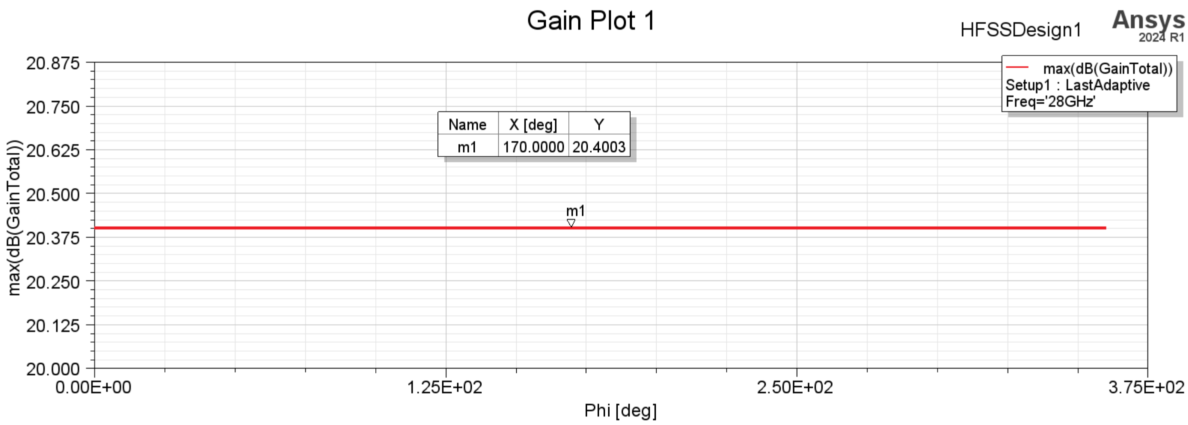

Figure 5.5.4: Total Gain of 4x5 PIFA MIMO Antenna Array at 28GHz

The simulated result validates that the developed antenna presents a total gain of 20.4 dB at 28 GHz with a high directional radiation efficiency that is highly desirable in the millimeter-wave 5G uses. Antenna gain is a measure of the intensity of the radiated radiation in a given direction compared to the intensity it would have emitted in all directions given the same accepted power. Such high gain is necessary at 28 GHz, where free-space path loss is an issue, to guarantee coverage, enhance link reliability, and transmit high-data-rate data. With the HFSS massive MIMO PIFA array design, this high gain is indicative of good optimization of the elements, as well as positive field summation in the array. It is the outcome of the experiment that the selected array layout and electromagnetic tuning can drastically enhance the beam directivity and energy concentration, which enhances beamforming strength, boosts spectral efficiency, and makes 5G wireless communication systems with high reliability work.

5.5.4. Directivity of 4x5 Massive MIMO PIFA Array at 28GHz

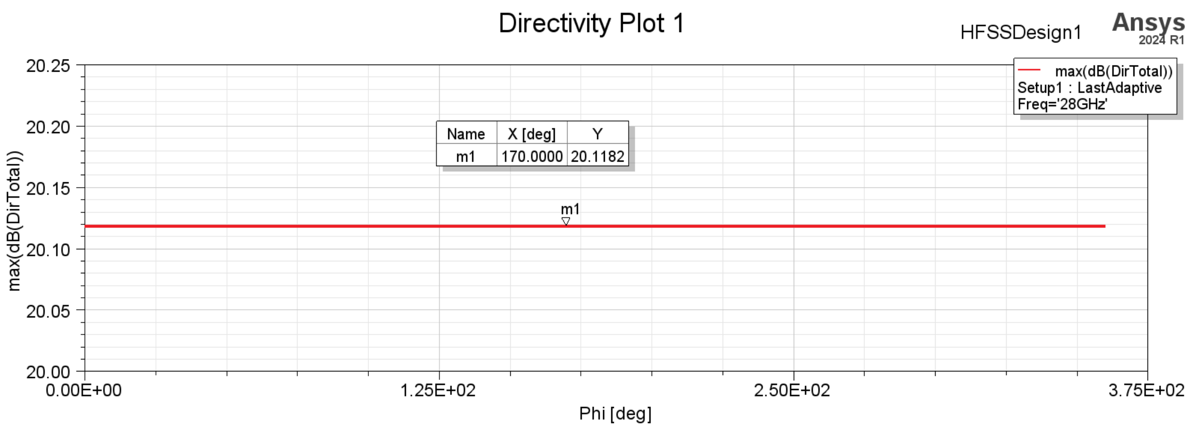

Figure 5.5.5: Directivity of 4x5 Massive MIMO PIFA Array at 28GHz

The simulation data shows that the 4x5 PIFA antenna array has a total directivity of 20.1 dB at 28 GHz, which represents a good capability of focusing the radiated energy, which is directed in the desired direction. The directivity of an antenna is the measurement of the ability of an array to concentrate power into a desired direction relative to an ideal isotropic radiator, and the greater the value, the better the spatial selectivity. Very high directivity is needed at millimeter-wave frequencies, such as 28 GHz; high directivity is essential to compensate for increased propagation losses and to support reliable directional links. Compared to the massive MIMO PIFA array design with respect to HFSS, such a degree of directivity confirms that both geometries and the spacing between the elements used as well as the excitation are well optimized to allow beams to be steered precisely as well as unwanted radiations to be minimized. Consequently, the increased directivity is associated with high beamforming accuracy, high signal-to-interference ratios, and capacity of the system, which are all vital performance requirements of 5G wireless communication systems.

5.5.5. 3D Polar Plot of Directivity 4x5 Massive MIMO PIFA Array at 28GHz

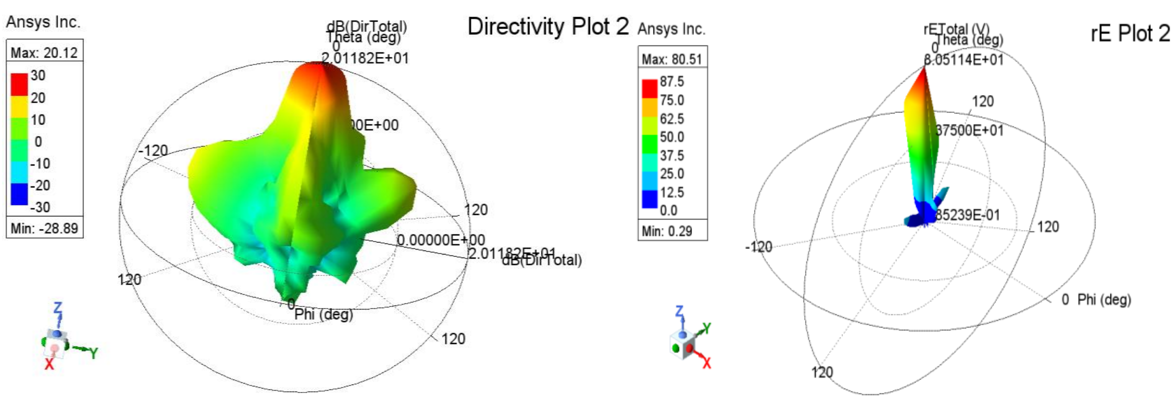

Figure 5.5.6: 3D Polar Plot of 4x5 Massive MIMO PIFA Array at 28GHz.

The three-dimensional radiation pattern of the proposed 4×5 PIFA array depicts the spacing distribution of directivity of the operating frequency of 28 GHz. It is seen that the highest directivity is about 20.12 dB, which implies a very directive radiation property to be used in mm-Wave massive MIMO applications. This value of directivity is high enough to verify the fact that the antenna array is successful in focusing radiated power in the desired direction instead of diffusing it in every direction. This action is likely to be seen in a 4x5 array set up where the constructive interference of the individual PIFA elements improves the main beam and reduces radiation in unwanted directions. This is evident in the fact that the dominant lobe is well aligned with the broadside direction, indicating that the geometry of the array and the separation between the elements are set to the optimal value to obtain coherent radiation at the design frequency. And also, the simulated three-dimensional far-field radiated pattern of the total electric field (rE Total) shows a very directional radiated pattern with a main predominant lobe in the broadside direction. The maximum magnitude of the electric field is reached around 80.51 V/m, whereas at the back the radiation is strongly suppressed, and that speaks for an enhanced front-to-back ratio. Minor side lobes are observed, which are apparently due to the limiting effects of array dimensions and spacing. The overall radiation behavior is consistent with constructive interference between the 4x5 PIFA elements, which leads to the improvement in the directivity suitable for mm-Wave 5G applications. In spherical coordinates the far-field characteristics of the radiation are expressed in terms of the following angle measures: elevation angle (θ), taking values in the perpendicular direction to the z-axis and measured from the positive direction of the z-axis; and azimuth angle (φ), taking values in the plane x-y and measured from the positive direction of the x-axis. However, these angular parameters specify the distribution of radiated electromagnetic fields in space.

5.5.6. Radiation pattern of 4x5 Massive MIMO PIFA Array

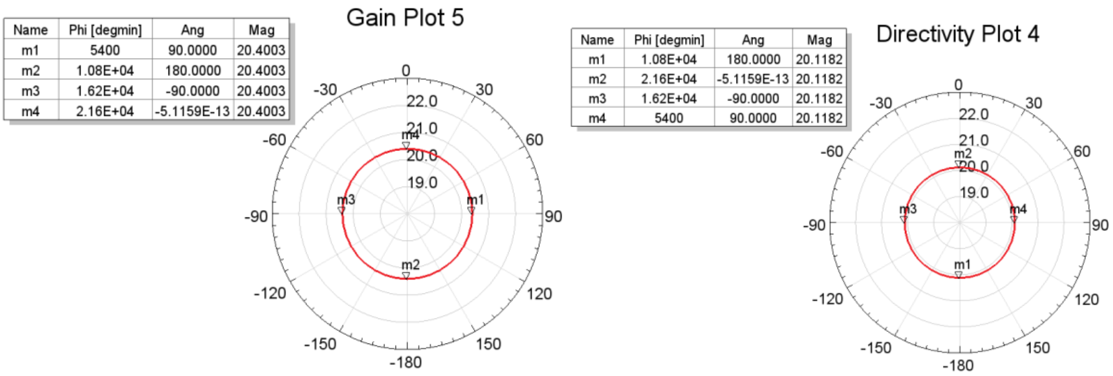

Figure 5.5.7. Radiation pattern of 4x5 Massive MIMO PIFA Array

The radiation of the proposed 4×5 planar inverted-F antenna (PIFA) array shows the stable and almost omnidirectional behavior along the azimuth plane, which is shown in the polar gain plot. The peak gain of the antenna is 20.4 dBi; this value is nearly the same at various angularities (90 0, 180 0, and -90 0) and shows that the gain does not change much when the antenna is operated around the radiation plane. The pattern is almost circular, which indicates an equal allocation of radiation, which is desirable in wireless communication systems, and needs to have a wide angle. This kind of radiation behavior guarantees that the signal that is transmitted is able to make good functional contact with the user in other spatial directions without notable loss in signal strength. The high gain level of the array is largely due to the constructive interaction of multiple radiating elements, and this elevates the effective aperture, and radiation efficiency is enhanced. This consistent and steady radiation behavior confirms that the proposed 4×5 PIFA array offers great coverage in space and signal strength is strong and is highly applicable in 28 GHz millimeter-wave 5G massive MIMO communication systems, where good connectivity and large-scale user coverage are critical.

5.5.7. Envelope Correlation Coefficient (ECC) of 4x5 PIFA Array

Table 5.1 Envelope Correlation Coefficient (ECC) of 4x5 PIFA Array

Data Table 1 HFSSDesign1 Ansys 2024 R1

	Freq [GHz]	CorrelationCoefficient MIMO Calculation 1
1	28.000000	0.003134

As the simulation result data table of MIMO metrics, the Envelope Correlation Coefficient (ECC) of the proposed 4x5 PIFA MIMO antenna array at the 28 GHz center frequency is 0.003134. The ECC is a quantitative measure of the degree of correlation between the radiation patterns of the elements of a MIMO system, which goes to quantify the degree to which the elements can be used independently. Mathematically, ECC may be calculated based on the far-field radiation patterns or may be estimated based on S-parameters; a number lower than 0.5 usually represents acceptability, and a number lower than 0.1 a good diversity result. ECC values are regarded as excellent at advanced 5G and massive MIMO applications with 0.01 or less. The value of ECC that was obtained is 0.003134, which is very low, and the ECC approaches zero, and it is an indication that the antenna elements in the 4×5 array have very uncorrelated radiation properties. This means that there is low mutual coupling between the elements and that there is high pattern diversity between the elements. Thus, the suggested design will guarantee high spatial multiplexing capacity, channel capacity, and diversity gain, as well as stable transmission of signals in mm-Wave communication systems of 28 GHz. The extremely small ECC value then justifies the appropriateness of the proposed array in high-performance 5G massive MIMO applications.

5.5.8. Diversity Gain (DG) of 4x5 Massive MIMO PIFA Array at 28 GHz

Table 5.2. Diversity Gain (DG) of 4x5 Massive MIMO PIFA Array at 28 GHz

Data Table 2 HFSSDesign1 Ansys 2024 R1

	Freq [GHz]	DiversityGain MIMO Calculation 1
1	28.000000	9.999951

The diversity gains in the proposed 4x5 MIMO antenna system remain within a very close margin of the theoretical maximum diversity gains of 10 dB, with an actual value of 10 dB at the center of the operating frequency band of the 28 GHz antenna. This near-ideal performance of the DG is directly due to the very low envelope correlation coefficient between the antenna elements, which makes it clear that the received signals are subjected to very independent fading channels. The high diversity of the antenna is ascertained by the minor variations in DG at the higher frequencies that are inconsequential and do not have any adverse effect on the overall work of the system.

5.5.9. Total Active Reflection Coefficient (TARC) of 4x5 MIMO PIFA Array

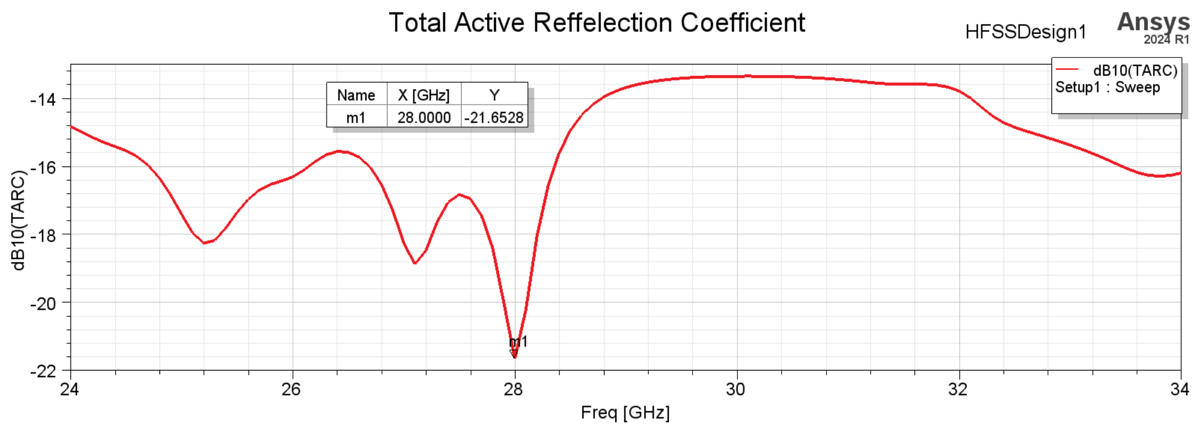

Figure 5.5.8: Total Active Reflection Coefficient (TARC) of 4x5 PIFA Array

Total Active Reflection Coefficient (TARC) is a parameter used to describe the performance of a multi-port MIMO antenna in the event that all the ports are excited considering mutual coupling and phase interaction among the elements. TARC is a more realistic measure of array performance as measured in active MIMO mode compared to the more traditional S11 parameter, which is based on a singular assessment of a single port under matched terminations.

Based on the presented result, the minimum TARC is found at 28 GHz with the value of -21.65 dB, and this shows an excellent match of the active impedance at the design frequency. A value of TARC that is less than -10 dB is enough to ensure that most of the power entering the circuit is actually radiated instead of bouncing back to the source, and the -21.65 dB obtained shows that there is very low active reflection and high compatibility with the multi-port at 28 GHz. The existence of other moderate dips in the lower frequencies (25-27 GHz) implies a multi-resonant response due to element interaction and array factor effects. In general, the performance of the 4×5 PIFA array proves that the TARC array has strong active matching properties and small reflection during multi-port excitation and thus will be highly applicable in 28 GHz massive MIMO 5G systems when simultaneous multi-element action is needed.

5.5.10. Channel Capacity Loss (CCL) of 4x5 PIFA Array

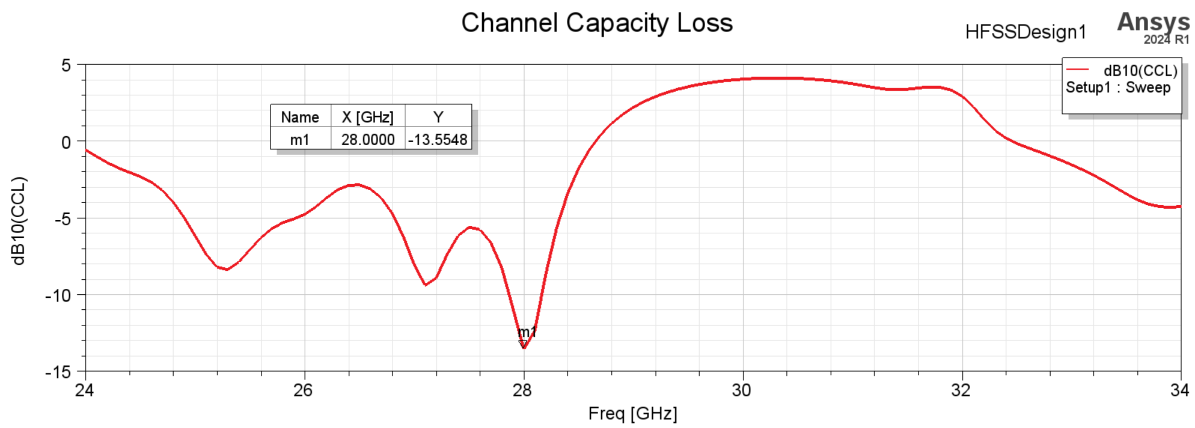

Figure 5.5.9: Channel Capacity Loss (CCL) of 4x5 PIFA Array

Mutual coupling and correlation between antenna elements are accompanied by a decrease in the theoretical MIMO channel capacity, which is quantified by the channel capacity loss (CCL); lower values indicate a higher preservation of spectral efficiency. The proposed 4×5 MIMO antenna has a very low CCL over the operating frequency range due to the minimum of only approximately −13.55 dB at 28 GHz, or a linear CCL of only approximately 0.044 bits/s/Hz. The antenna elements keep information loss to a minimum, and the MIMO capacity is almost optimal, as this extraordinarily low-capacity loss verifies. The almost perfect diversity gains and extremely low ECC correspond to the CCL behavior in question, which proves the potential of the antenna design to provide 5G with high data rates and reliable communication.

5.6. Performance Comparisons of the designed PIFA Array at 28 GHz

Table 5.3. Performance Comparisons of the designed PIFA Array antenna at 28GHz

Designed Works	Frequency	Gain	Directivity	Reflection Coefficient	VSWR	Substrate	Bandwidth
Single PIFA	28 GHz	6.8dBi	6.9dBi	-24.93 dB	1.1 dB	Duroid	4.56GHz
1×2 PIFA Array	28 GHz	10.47dBi	10.25 dBi	−20.7 dB	1.6 dB	Duroid	2.28 GHz
4×4 PIFA Array	28 GHz	17.8dBi	17.48 dBi	−22.7 dB	1.27 dB	Duroid	1.3 GHz
4×5 PIFA Array	**28 GHz**	**20.4dBi**	**20.1dBi**	**-18.3dB**	**2 dB**	**Duroid**	**3.4 GHz**

The obtained simulation outcome of the designed PIFA structures at 28 GHz shows that performance is improved by a clear increase as the size of the arrays increases. The single PIFA has a 6.8 dBi gain, directivity of 6.9 dB, reflection coefficient of -24.93 dB, VSWR of 1.1 dB, and a bandwidth of 4.56 GHz, which shows that it has excellent impedance matching and frequency coverage. Gain and directivity grow to 10.47 dBi and 10.25 dBi, respectively, with expansion to a 1x2 array with a reflection coefficient (-20.7 dB) and VSWR at 1.6 still being very good, although bandwidth decreases (2.28 GHz) because of inter-element coupling. The 4 x 4 array has a further gain of 17.8 dBi and directivity of 17.48 dBi and excellent matching, −22.7 dB, and VSWR 1.27 with a bandwidth of 1.3 GHz. Whereas the 4 x 5 array achieves the highest gain of 20.4 dBi, directivity of 20.15 dBi, VSWR of 2 dB, and bandwidth of 3.4 GHz. These findings indicate that gain and directivity are greatly enhanced, but impedance matching and bandwidth are minimally affected by increasing array size, demonstrating the performance of the proposed PIFA arrays on Duroid substrates as high-performance 28 GHz 5G mm-Wave applications.

5.7. Performance Comparisons of the previous MIMO Antenna with the designed work at only mm-Wave 28GHz

Table 5.4. Performance Comparisons of Previous Massive MIMO Antenna vs proposed antenna at only mm-Wave bands.

Ref	**Year**	**Frequency**	**Array configuration**	**Dimension in mm**		**Gain**	**Directivity**	**Reflection Coefficient**	**VSWR**	**ECC**	**TARC**	**BW**	**Application**
				Over all	**Patch**								
[14]	2025	28GHz	1×8 MSA	80x68	3.6x2.6	15.5dB	N/A	-40dB	N/A	0.00010	N/A	2GHz	5G
[16]	2017	28 GHz	2 x 1 MIMO PIFA	N/A	5x5	8.6dB	9 dB	-17.46 dB	1.2 dB	<0.3	N/A	1.02GHz	5G Dual Band
		37GHz				9.3dB	10 dB	-32.54 dB	1.2 dB	N/A	N/A	1.3GHz	
[18]	2022	60GHz	Single PIFA	3.5x1.6	1.5x0.7	6.2dB	10.34dB	-46.1 dB	1.01 dB	-	-	3.8GHz	cellular V-band
			1×4 PIFA	28.6x3	1.4x1	6.6dB	12.51dB	-48.02 dB	1.03 dB	N/A	N/A	3.2GHz	
			4×4 PIFA	26x26.2	1.5x1.2	12.1dB	15.12dB	-47.23 dB	1.18 dB	N/A	N/A	2.6GHz	
[20]	2023	28GHz	2×1 PIFA	9x10.3	4.2x3.3	9.4dB	9.47dB	-25 dB	1.03dB		N/A	1.43GHz	5G wireless comm
[21]	2021	28 GHz	2 elements slotted PIFA	55x110	3.4x2.3	8 dB	N/A	-25 dB	N/A	N/A	N/A	N/A	5G mobile comm
Proposed	**2026**	28 GHz	Single PIFA	7.414x5.4	4.2x5.1	6.8 dBi	6.9 dBi	-24.93 dB	1.1 dB	-	-	4.56GHz	**5G Base Station & Mobile comm**
		28 GHz	1x2 PIFA	7.414 x 11.4	4.2x5.1	10.4dBi	10.25i	-20.72 dB	1.6 dB	0.00160	-12.8	2.28GHz	
		28 GHz	4x4 PIFA	25.414 x 23.4	4.2x5.1	17.8dBi	17.48 dBi	-22.7 dB	1.27 dB	0.001221	-22.7	1.3GHz	
		28GHZ	**4×5 PIFA**	**31.414 x 23.4**	**4.2x5.1**	**20.4dBi**	**20.1 dBi**	**-18.75dB**	**2 dB**	**0.003134**	**-21.65**	**3.4 GHz**	

This comparative study of previous antenna designs versus the proposed 2026 massive MIMO PIFA array is an HFSS-based investigation into the achievements of the 5G applications based on the performance metrics. Previous designs, 2016-2025, had differing gain values of 3-15.5 dBi, directivity of 5-15.2 dBi, and reflection coefficients of -10 dB to -40 dB, with bandwidths of 100MHz to 3 GHz based on the possibilities of simultaneously high gain, narrow-beam control, and extended-band operation. These designs were physically large or simply did not have full performance data, especially in regard to TARC, ECC, DG, and CCL integration with an array. Conversely, the proposed 4×5 massive MIMO PIFA array is designed with a high gain of 20.4 dBi with directivity of 20.1 dBi in a small 31.414 x 23.4 mm area whilst having a reflection coefficient of -18.62 dB and VSWR of 2 with a bandwidth of 3.4 GHz. These findings show that it has better impedance matching, small power transmission, and directional radiation than the previous designs, making HFSS-optimized multi-element PIFA arrays effective to improve spectral efficiency, beamforming, and overall operation in millimeter-wave communication systems of 5G.

CHAPTER SIX

CONCLUSIONS, THESIS CONTRIBUTIONS, AND FUTURE RECOMMENDATIONS

6.1.Conclusions

This thesis has provided the HFSS-based study of single-element and array-based PIFA antennas at 28 GHz in 5G millimeter-wave applications. It began with a well-matched single PIFA element, and in a systematic process, as the array is progressive in terms of 1×2 to 4×5 massive MIMO arrays, the gains, directivity, impedance matching, and beamforming improvements are significant. Simulation findings affirm that both single and small-array PIFA designs offer reasonable baseline performance but are by definition constrained in being able to overcome serious path loss and directional needs at millimeter-wave frequencies. On the other hand, the proposed 4×5 massive MIMO PIFA array is an optimal solution with high performance, high gain, bandwidth, and directivity; decent reflection coefficient and VSWR; small physical size; and high bandwidth, as it will be used in practical 5G applications. The comparative analysis with the existing literature also helps to confirm that the proposed design is able to provide high gain-to-size efficiency without using sophisticated meta-surfaces or overly large apertures, high gain, directivity, and bandwidth in comparison with the current literature. In general, the paper confirms the fact that optimized massive MIMO PIFA arrays can be a strong and scalable solution to high capacity and reliable 5G wireless communication systems.

6.2.Thesis Contributions

The primary value of the work is the systematic design, optimization, and comparative analysis of compact massive MIMO arrays of PIFA antennas at 28 GHz in HFSS. The thesis offers a straightforward design approach that correlates single-element performance with large-scale array performance, with consideration of the influence of the geometry of the elements, the separation between elements, and element-to-element coupling on the important antenna performance. The proposed massive MIMO 4×5 PIFA array has high gain, directivity, and bandwidth in a much smaller footprint than most of the designs reported before. An elaborate performance comparison framework is also added to the work, comparing the proposed antenna to the state-of-the-art MIMO and metasurface-based solutions in the same frequency band. Besides that, the research provides explicit information regarding the change of impedance matching, VSWR, radiation patterns, and 3D polar characteristics with array scales, which will be of practical use to the researchers and engineers who are planning small-scale antenna arrays in millimeter wave 5G systems.

6.3.Future Recommendations

This research can be furthered in a number of constructive ways in the future. It is suggested that the proposed massive MIMO PIFA arrays can be fabricated and tested experimentally to confirm the simulated values and investigate the effects of fabrication on the real world, i.e., fabrication tolerances, connector losses, environmental effects, etc. An additional performance increase might be attained with the inclusion of sophisticated beamforming networks, reconfigurable feeding systems, or variable elements to allow adaptive beam steering and spectrum and bandwidth utilization. Further research into mutual coupling reduction methodologies, e.g., decoupling structures or electromagnetic bandgap materials, can be done to enhance the efficiency of arrays in ultra-dense arrangements. It would further be desirable to design supporting dual-band or multi-band operation in other 5G and beyond-5G millimeter-wave bands to make it more useful. Lastly, it is advisable to conduct system-level testing of the proposed antenna in a realistic 5G network environment to assess user mobility and multi-user MIMO performance to completely measure its effect on capacity, coverage, and energy efficiency in the next-generation wireless communication environment.

REFERENCE

[1] L. Wakrim, A. El Yassini, A. Khabba, S. Ibnyaich, A. Zeroual, and M. M. Hassani, "Dual Band PIFA MIMO Antenna Design with High Isolation for Mobile and Wireless Applications by Using the Genetics Algorithms and Non-uniform Overlapping Method," *Wirel. Pers. Commun.*, vol. 125, no. 2, pp. 1145–1161, Jul. 2022, doi: 10.1007/s11277-022-09593-2.

[2] R. Kumari, A. K. Jha, A. Sachan, A. Kishan, and M. Jain, *Design and Analysis of Pattern Reconfigurable MIMO Antenna Using PIFA Structure*, vol. 721 LNEE. Springer Singapore, 2021. doi: 10.1007/978-981-15-9938-5_56.

[3] A. Srivastava, *Advances in Smart Communication and Imaging Systems*. 2020.

[4] Anon, "Communication terminals," *Electr. Commun.*, vol. 65, no. 1, pp. 73–79, 1991, doi: 10.1038/scientificamerican0972-130.

[5] S. M. Gaber, R. A. Kareem, and A. A. Ibrahim, "High isolation quad ports MIMO antenna loaded with FSS for 5G communication," *Sci. Rep.*, vol. 15, no. 1, pp. 1–17, 2025, doi: 10.1038/s41598-025-05616-7.

[6] N. M and D. R. N, "A comprehensive review on recent advances in frequency selective surface-based gain and isolation enhancement for multi input multi output (MIMO) antennas," *Discov. Electron.*, vol. 2, no. 1, Dec. 2025, doi: 10.1007/s44291-025-00146-y.

[7] "4 citation-319773573."

[8] M. Kamran Ishfaq, T. Abdul Rahman, H. T. Chattha, and M. Khalily, "A Novel Millimeter Wave Linear PIFA Array Antenna for 5G Next Generation Wireless Communication System," *1st ICRIL-International Conf. Innov. Sci. Technol. (lICIST 2015)*, no. April, pp. 664–668, 2015.

[9] S. Padmanathan *et al.*, "Compact Multiband Reconfigurable MIMO Antenna for Sub-6GHz 5G Mobile Terminal," *IEEE Access*, vol. 10, pp. 60241–60252, 2022, doi: 10.1109/ACCESS.2022.3180048.

[10] M. A. Al-Tarifi, M. S. Sharawi, and A. Shamim, "Massive MIMO antenna system for 5G base stations with directive ports and switched beamsteering capabilities," *IET Microwaves, Antennas Propag.*, vol. 12, no. 10, pp. 1709–1718, Aug. 2018, doi:

10.1049/iet-map.2018.0005.

[11] A. A. Nikam and R. B. Patil, "Design and development of multiband PIFA antenna for vehicular LTE/5G and V2X communication," *Eurasip J. Wirel. Commun. Netw.*, vol. 2023, no. 1, 2023, doi: 10.1186/s13638-023-02306-8.

[12] V. Jamali, A. M. Tulino, G. Fischer, M. Ralf, and R. Schober, "Scalable and Energy-Efficient Millimeter Massive MIMO Architectures : Reflect-Array and Transmit-Array Antennas".

[13] Q. U. A. Nadeem, A. Kammoun, M. Debbah, and M. S. Alouini, "Design of 5G Full Dimension Massive MIMO Systems," in *IEEE Transactions on Communications*, Institute of Electrical and Electronics Engineers Inc., Feb. 2018, pp. 726–740. doi: 10.1109/TCOMM.2017.2762685.

[14] N. Alsaab *et al.*, "High-Performance Series-Fed Array Multiple-Input Multiple-Output Antenna for Millimeter-Wave 5G Networks," *Sensors (Basel).*, vol. 25, no. 4, Feb. 2025, doi: 10.3390/s25041036.

[15] C. C. By, "18 Element Massive MIMO / Diversity 5G Smartphones," vol. 2, no. April, pp. 533–545, 2021.

[16] A. Rachakonda, P. Bang, and J. Mudiganti, "A compact dual band MIMO PIFA for 5G applications," *IOP Conf. Ser. Mater. Sci. Eng.*, vol. 263, no. 5, 2017, doi: 10.1088/1757-899X/263/5/052034.

[17] K. Kundu, A. Dubey, A. Dhama, and N. N. Pathak, "Planar inverted F Antenna, PIFA array in 5G applications," *J. Phys. Conf. Ser.*, vol. 2062, no. 1, 2021, doi: 10.1088/1742-6596/2062/1/012002.

[18] T. Watro Wata, "Design and Performance Analysis of PIFA Microstrip Antenna Array at mmWave for MIMO Cellular Radio Communication."

[19] M. M. Fakharian, "A massive MIMO frame antenna with frequency agility and polarization diversity for LTE and 5G applications," *Int. J. RF Microw. Comput. Eng.*, vol. 31, no. 10, Oct. 2021, doi: 10.1002/mmce.22823.

[20] S. E. Didi *et al.*, "New microstrip patch antenna array design at 28 GHz millimeter-wave for fifth-generation application," *Int. J. Electr. Comput. Eng.*, vol. 13, no. 4, pp. 4184–4193, 2023, doi: 10.11591/ijece.v13i4.pp4184-4193.

[21] T. Padmapriya and S. V. Manikanthan, “Implementation of dual-band Planar Inverted F- Antenna (PIFA) using machine learning (ML) for 5G mobile applications,” no. Ml, 2021, doi: 10.4108/eai.7-6-2021.2308603.

[22] I. N. Taban, A. H. Khidhir, and A. A. Naser, “Design and Optimization of Planar Inverted F Antenna (PIFA) for Wireless Applications,” *Al-Nahrain J. Sci.*, vol. 26, no. 1, pp. 27–30, 2023, doi: 10.22401/ANJS.26.1.05.

[23] M. A. Saeed and A. O. Nwajana, “Design of a Rectangular Linear Microstrip Patch Antenna Array for 5G Communication,” *IEEE Int. Symp. Phased Array Syst. Technol.*, no. July, pp. 25–27, 2024, doi: 10.1109/ARRAY58370.2024.10880409.

[24] S. K. Ezzulddin, S. O. Hasan, and M. M. Ameen, “Optimization of rectangular microstrip antenna patch parameters to operate with high radiation performances for 5G applications,” *AIP Conf. Proc.*, vol. 2386, no. January, 2022, doi: 10.1063/5.0066800.

[25] X. Yin, W. Ren, Z. Xue, and W. Li, “Metamaterial-Based Wide-Angle Scanning Circularly Polarized Phased Array With Stable Gain,” *IEEE Open J. Antennas Propag.*, vol. 6, no. 2, pp. 594–602, 2025, doi: 10.1109/OJAP.2025.3541235.

[26] M. Fernández, C. Vázquez, and S. Ver Hoeye, “Dual-Mode, Dual-Polarization Fully-Woven Textile Antenna for Simultaneous Wireless Information and Power Transfer Applications in the 2.4 GHz Band,” *IEEE Open J. Antennas Propag.*, vol. 6, no. 2, pp. 603–612, 2025, doi: 10.1109/OJAP.2025.3541420.

[27] L. Zhang *et al.*, “A Dual-Port Dual-Wideband Dual-Sense Circularly Polarized DRA With a Novel Feeding Mechanism,” *IEEE Open J. Antennas Propag.*, vol. 6, no. 1, pp. 229–234, 2025, doi: 10.1109/OJAP.2024.3491222.

[28] X. Guan, Y. He, Z. Xue, W. Ren, and W. Li, “Design an Omnidirectional Circularly-Polarized Antenna for Azimuth Wide-Angle Scanning Array,” *IEEE Open J. Antennas Propag.*, vol. 5, no. 6, pp. 1629–1638, 2024, doi: 10.1109/OJAP.2024.3426651.

[29] Z. Thu Thu Lin and H. Myo Tun, “Design and Fabrication of a Planar Inverted-F Antenna (PIFA) for LEO Satellite Application,” *Am. J. Electromagn. Appl.*, vol. 8, no. 1, p. 28, 2020, doi: 10.11648/j.ajea.20200801.14.

[30] A. Jafargholi, M. Safaei, R. Fleury, and R. Tafazolli, “Low-Profile ESPAR Using Metamaterial-Inspired Structure,” *IEEE Open J. Antennas Propag.*, vol. 5, no. 6, pp. 1612–1622, 2024, doi: 10.1109/OJAP.2024.3426608.

[31] D. EL NABAOUI *et al.*, "Multiband Planar Inverted F Antenna (PIFA) for ISM, WLAN and WiMAX Applications," 2019, doi: 10.4108/eai.24-4-2019.2284080.

[32] E. Rhee, "Miniaturized PIFA for 5G communication networks," *Appl. Sci.*, vol. 10, no. 4, 2020, doi: 10.3390/app10041326.

[33] K. Nadali, N. Kumar Maurya, P. Mcevoy, and M. J. Ammann, "A Dual-Band Dual-Polarized Antenna for Harvesting in Cellular and Digital Terrestrial Television Bands," *IEEE Open J. Antennas Propag.*, vol. 5, no. 6, pp. 1489–1498, 2024, doi: 10.1109/OJAP.2024.3407050.

[34] F. Positano, L. Santamaria, R. Staraj, and L. Lizzi, "Compact Omnidirectional Circularly Polarized Antenna via Alford Loop and Wire-Patch Structure Combination," *IEEE Open J. Antennas Propag.*, vol. 5, no. 2, pp. 277–285, 2023, doi: 10.1109/OJAP.2023.3340975.

[35] U. Myrzakhan, F. A. Ghaffar, M. Vaseem, and A. Shamim, "Additively-Manufactured, Magnetically Controlled, Frequency and Polarization Reconfigurable Phased Array Antenna," *IEEE Open J. Antennas Propag.*, vol. 6, no. 1, pp. 264–273, 2025, doi: 10.1109/OJAP.2024.3496296.

[36] C. Zhao and D. Shen, "Low-RCS High-Gain Broadband Substrate-Integrated Waveguide Antenna Based on Elliptical Polarisation Conversion Metasurface," *IET Microwaves, Antennas Propag.*, vol. 19, no. 1, Jan. 2025, doi: 10.1049/mia2.70016.

[37] S. Kumaravel and M. Karthikeyan, "Circularly polarized dual-band resonance in a miniaturized implantable antenna using combined hexagonal and rhombic patches," *Sci. Rep.*, vol. 15, no. 1, pp. 1–12, 2025, doi: 10.1038/s41598-025-86882-3.

[38] R. Y. Khattak, Q. Z. Ahmed, S. Shoaib, P. I. Lazaridis, and T. T. Alade, "Recent Advances in Antennas for Biotelemetry and Healthcare Applications," *IEEE Open J. Antennas Propag.*, vol. 5, no. 6, pp. 1499–1522, 2024, doi: 10.1109/OJAP.2024.3462289.

[39] M. Mahabub Alam *et al.*, "Design and Analysis of Triple-Band SIW Antenna for K-Band and Ka-Band Applications," in *International Exchange and Innovation Conference on Engineering and Sciences*, Kyushu University, 2024, pp. 760–766. doi: 10.5109/7323346.

[40] S. O. Zakariyya, V. O. Omole, B. O. Sadiq, R. A. Alao, J. A. Adesina, and E. Obi,

"Design of an Improved Microstrip Antenna Operating at a Frequency Band of 28 GHz," 2024.

[41] A. Feeding, "A Novel Topology of a 3 × 3 Series Phased Array Antenna with Aperture-Coupled Feeding," 2024.

[42] "32 citation-398712663."

[43] M. K. Taher Al-Nuaimi and Y. He, "RCS reduction of a microstrip antennas using cross polarization conversion metasurface," *2019 IEEE Int. Symp. Antennas Propag. Usn. Radio Sci. Meet. APSURSI 2019 - Proc.*, pp. 1907–1908, 2019, doi: 10.1109/APUSNCURSINRSM.2019.8888587.

[44] Z. Huang, Q. Zhang, F. Han, H. Wang, and S. Chen, "High Gain and Broadband Metalens Antenna for Terahertz Communication".

[45] A. A. Hasan *et al.*, "On Modeling Antennas Using MoM-Based Algorithms : Wire-Grid versus Surface Triangulation," 2023.

[46] B. C, A. S. Arun, M. G. R. S, P. M. S, and S. G. A, "Enhancing gain and bandwidth in a multiband microstrip patch antenna through L-slot and partial ground plane integration," *Sci. Rep.*, vol. 15, no. 1, pp. 2–13, 2025, doi: 10.1038/s41598-025-13947-8.

[47] Daria Coman, Maria Sîrbu-Drăgan, Simona Halunga, and Diana Brînaru, "Design and Analysis of Antennas and Antenna System for 5G Technology," pp. 0–19, 2025, doi: 10.20944/preprints202502.0413.v1.

[48] M. Boudjerda *et al.*, "Design and Optimization of Miniaturized Microstrip Patch Antennas Using a Genetic Algorithm," *Electron.*, vol. 11, no. 14, pp. 1–14, 2022, doi: 10.3390/electronics11142123.

[49] R. Arora, A. Kumar, S. Khan, and S. Arya, "Finite Element Modeling and Design of Rectangular Patch Antenna with Different Feeding Techniques," *Open J. Antennas Propag.*, vol. 01, no. 02, pp. 11–17, 2013, doi: 10.4236/ojapr.2013.12004.

[50] D. Rano, M. A. Chaudhary, and M. S. Hashmi, "A New Model to Determine Effective Permittivity and Resonant Frequency of Patch Antenna Covered with Multiple Dielectric Layers," *IEEE Access*, vol. 8, pp. 34418–34430, 2020, doi: 10.1109/ACCESS.2020.2974912.

[51] R. Maged, A. S. A. El-Hameed, M. M. Mabrook, and T. M. Said, "Enhanced performance of microstrip antenna fabricated on a composite dielectric substrate coupled with multiple dielectric superstrates," *Opt. Quantum Electron.*, vol. 56, no. 5, pp. 1–18, 2024, doi: 10.1007/s11082-024-06487-4.

[52] S. Kumar, S. K. Palaniswamy, H. C. Choi, and K. W. Kim, "Compact Dual Circularly-Polarized Quad-Element MIMO/Diversity Antenna for Sub-6 GHz Communication Systems," *Sensors*, vol. 22, no. 24, pp. 1–12, 2022, doi: 10.3390/s22249827.

[53] I. Matching, "Impedance Matching," 2025.

[54] X. Y. Liu, Z. T. Wu, Y. Fan, and E. M. Tentzeris, "A Miniaturized CSRR Loaded Wide-Beamwidth Circularly Polarized Implantable Antenna for Subcutaneous Real-Time Glucose Monitoring," *IEEE Antennas Wirel. Propag. Lett.*, vol. 16, pp. 577–580, 2017, doi: 10.1109/LAWP.2016.2590477.

[55] R. A. Santos, N. M. L. Sousa, I. Bianchi, M. Sharma, R. A. Penchel, and D. C. Nascimento, "Dual-Polarized Microstrip Patch Antenna With Enhanced Bandwidth and Gain Using Mode Perturbation and λ/4 Resonator Coupling," *IEEE Open J. Antennas Propag.*, vol. PP, p. 1, 2025, doi: 10.1109/OJAP.2025.3631572.

[56] L. J. Foged, F. Mioc, B. Bencivenga, M. Sabbadini, and E. Di Giampaolo, "Infinite ground plane antenna characterization from limited groundplane measurements," *2010 IEEE Int. Symp. Antennas Propag. CNC-USNC/URSI Radio Sci. Meet. - Lead. Wave, AP-S/URSI 2010*, no. 1, pp. 25–28, 2010, doi: 10.1109/APS.2010.5561891.

[57] R. Kalsi and A. Nothofer, "Cavity Model for a Patch Antenna Embedded with a Hybrid Ground Plane," pp. 1–9, 2024, [Online]. Available: http://arxiv.org/abs/2410.03028

[58] Y. Antonenko, Y. Antonenko, D. Shtoda, A. Gribovsky, V. Katrich, and S. Berdnik, "Research of a Microstrip Antenna Array Excited by a Planar Waveguide with a quasi-TEM Mode," *Proc. Int. Semin. Direct Inverse Probl. Electromagn. Acoust. Wave Theory, DIPED*, vol. 2023-Septe, pp. 90–94, 2023, doi: 10.1109/DIPED59408.2023.10269460.

[59] "47 citation-379697222."

[60] Y. Ahmed, "Antenna Arrays," *Signals Commun. Technol.*, vol. Part F1285, pp. 99–131, 2023, doi: 10.1007/978-981-99-2917-7_6.

[61] M. F. Ahmed, M. H. Kabir, and A. Z. M. T. Islam, "Impact of Feed Point Position on

Patch Antenna's Return Loss and Bandwidth for UWB Applications," *J. Multidiscip. Appl. Nat. Sci.*, vol. 4, no. 1, pp. 30–38, 2024, doi: 10.47352/jmans.2774-3047.158.

[62] A. Abrardo, A. Toccafondi, and M. Di Renzo, "Design of Reconfigurable Intelligent Surfaces by Using S-Parameter Multiport Network Theory - Optimization and Full-Wave Validation," *IEEE Trans. Wirel. Commun.*, vol. 23, no. 11, pp. 17084–17102, 2024, doi: 10.1109/TWC.2024.3450722.

[63] R. Li *et al.*, "Impedance Bandwidth Enhancement Using Capacitor-Controlled Series Resonance in an Antenna's Feeding Structure," *J. Electromagn. Eng. Sci.*, vol. 24, no. 2, pp. 129–137, 2024, doi: 10.26866/jees.2024.2.r.212.

[64] M. A. Haque *et al.*, "High-isolation dual-band MIMO antenna for next-generation 5G wireless networks at 28/38 GHz with machine learning-based gain prediction," *Sci. Rep.*, vol. 15, no. 1, Dec. 2025, doi: 10.1038/s41598-025-02646-z.

[65] J. J. Degnan and B. J. Klein, "Optical Antenna Gain 2:Receiving Antennas Errata," *Appl. Opt.*, vol. 13, no. 12, p. 2762, 1974, doi: 10.1364/ao.13.002762.

[66] M. AboEl-Hassan, A. E. Farahat, and K. F. A. Hussein, "Gain enhancement wideband CPW antenna based on artificial magnetic conductor," *Sci. Rep.*, vol. 15, no. 1, pp. 1–27, 2025, doi: 10.1038/s41598-025-89622-9.

[67] P. Y. Qin, Y. J. Guo, and C. H. Liang, "Effect of antenna polarization diversity on MIMO system capacity," *IEEE Antennas Wirel. Propag. Lett.*, vol. 9, no. 2, pp. 1092–1095, 2010, doi: 10.1109/LAWP.2010.2093116.

[68] N. Ganeshwaran, J. K. Jeyaprakash, M. G. N. Alsath, and V. Sathyanarayanan, "Design of a Dual-Band Circular Implantable Antenna for Biomedical Applications," *IEEE Antennas Wirel. Propag. Lett.*, vol. 19, no. 1, pp. 119–123, Jan. 2020, doi: 10.1109/LAWP.2019.2955140.

[69] N. Communications and S. M. Radha, "applied sciences A Compact , Low-Profile , Broadband Quasi-Isotropic Antenna for," 2024.

[70] J. G, I. Singh, and D. K. Choudhary, "Gain and isolation improvement techniques for MIMO antenna: A compendious survey," *Results Eng.*, vol. 25, no. February, p. 104482, 2025, doi: 10.1016/j.rineng.2025.104482.

[71] P. Sharma, R. N. Tiwari, P. Singh, P. Kumar, and B. K. Kanaujia, "and Applications," 2022.

APPENDIX

High Frequency Structural Simulator (HFSS).

Ansys High Frequency Structure Simulator is an electromagnetic field solver based on the full-wave finite element method capable of simulation of any three-dimensional (3D) structure. HFSS is a connector/waveguide simulator. Parametric sweeps, structure optimization, and so on are done on-chip, with the help of on-chip components, including antennas. The HFSS method relies on a three-dimensional finite element model (FEM). That is a frequency domain method (solutions are computed at every frequency independently).

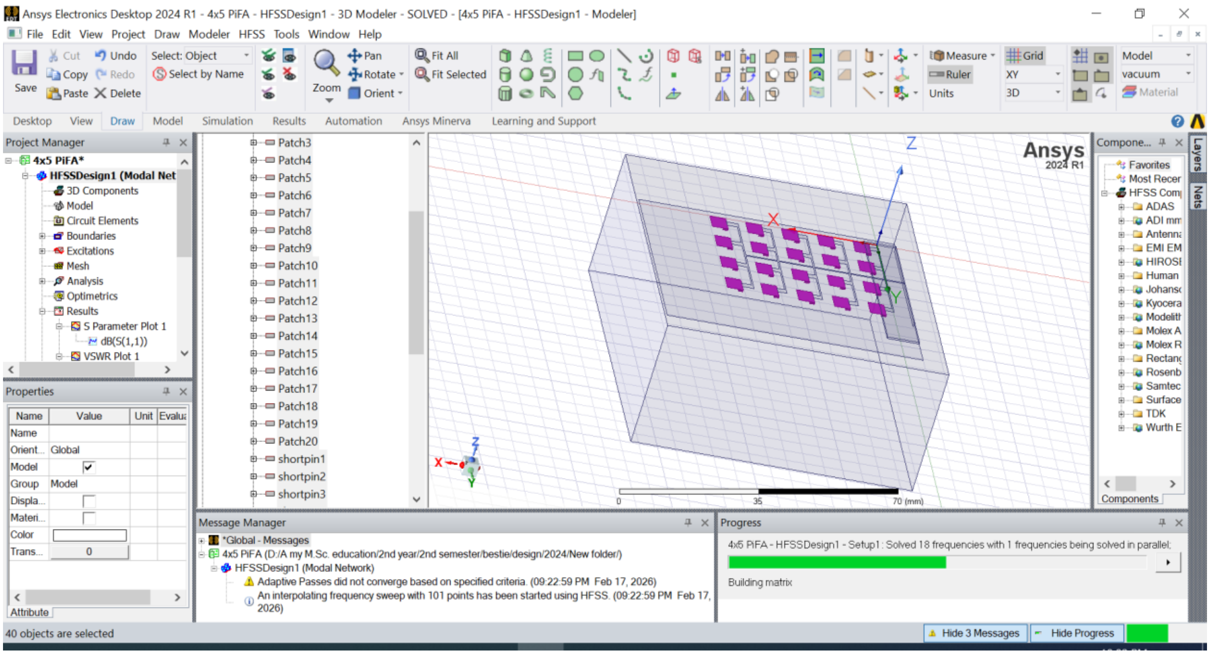

Appendix figure: Ansys 2024 HFSS Tools Software.

Adaptive Analysis Process

An adaptive analysis is a solution process whereby the mesh is refined at every iteration where the error is high, making the solution more accurate. The criteria that govern mesh refinement are defined in the process of an adaptive field solution. With adaptive refinement, a number of problems can be solved.

HFSS produces a primary mesh.

HFSS calculates electromagnetic fields within the structure, which occur in the event of solution frequency excitation using the starting mesh. (Only run a frequency sweep when performing an adaptive solution is required on the solution frequency.) HFSS approximates the areas of the challenging field where the exact solution is highly erroneous as per the existing finite element solution. They are tetrahedral refined regions. Another solution is produced by HFSS with the refined mesh. HFSS resolves the error, and the iterative process (solve, error, analysis, refine) is repeated until convergence is reached or the requested number of adaptive passes is reached. When frequency sweep is done, the HFSS resolves the issue at the remaining frequency points without refining the mesh any further.

Advantage and Disadvantage of HFSS.

Advantage

- A large problem can be solved
- Arbitrary objects can be simulated.
- Automatic mesh refinements
- Extremely versatile
- These are a big number of excitations, boundaries,
- Easy to learn and easy to use
- Optimization procedure
- User-defined plots
- Essentially helpful in simulating periodic structures.

Disadvantage

- Very large matrix takes long time to simulate.
- Any volumes should be discretized.
- A huge volume device, is long-lasting to simulate.